DEVELOPMENTAL DYNAMICS 238:2975–3015, 2009

RESEARCH ARTICLE

Normal Table of Postembryonic Zebrafish Development: Staging by Externally Visible Anatomy of the Living Fish

David M. Parichy,* Michael R. Elizondo, Margaret G. Mills, Tiffany N. Gordon, and Raymond E. Engeszer

The zebrafish is a premier model organism yet lacks a system for assigning postembryonic fish to developmental stages. To provide such a staging series, we describe postembryonic changes in several traits that are visible under brightfield illumination or through vital staining and epiflourescent illumination. These include the swim bladder, median and pelvic fins, pigment pattern, scale formation, larval fin fold, and skeleton. We further identify milestones for placing postembryonic fish into discrete stages. We relate these milestones to changes in size and age and show that size is a better indicator of developmental progress than is age. We also examine how relationships between size and developmental progress vary with temperature and density, and we document the effects of histological processing on size. To facilitate postembryonic staging, we provide images of reference individuals that have attained specific developmental milestones and are of defined sizes. Finally, we provide guidelines for reporting stages that provide information on both discrete and continuous changes in growth and development. *Developmental Dynamics 238:2975–3015, 2009.* © 2009 Wiley-Liss, Inc.

Key words: *Danio rerio*; zebrafish; normal stages; skeleton; swim bladder; flexion; pigment pattern; fin; fin fold

Accepted 29 August 2009

INTRODUCTION

An essential tool for any model organism is a normal table of development for assigning individuals to particular stages of the life cycle (Hopwood, 2007). Only with such a staging series can experiments be repeated and results compared across laboratories. Over the past 30 years, the zebrafish *Danio rerio* has become an important vertebrate for a variety of studies, encompassing genetics, development, physiology, behavior, and evolution. An excellent normal table of zebrafish development is available for embryonic stages (Kimmel et al., 1995), which greatly elaborated on an earlier series (Hisaoka and Battle, 1958). Nevertheless, an adequate staging series for postembryonic development is still lacking.

A postembryonic staging system is needed because changes occur in a variety of traits during this period in zebrafish and in other organisms. In the zebrafish for example, postembryonic development entails the appearance of median adult fins and pelvic fins, increasing stratification and complexity of skin, continued skeletal development, loss of the larval fin fold, and marked changes in the gut, kidneys, and gonads, as well as the peripheral and central nervous systems. There have been some descriptions of such changes, either for the whole organism (Schilling, 2002), or focusing on particular traits (Kirschbaum, 1975; Milos and Dingle, 1978; Cubbage and Mabee, 1996; Schilling and Kimmel, 1997; Iovine and Johnson, 2000; Ledent, 2002; Sapede et al., 2002; Bird and Mabee, 2003; Parichy and Turner, 2003; Webb and Shirey, 2003; Sire and Akimenko, 2004; Elizondo et al., 2005; Goldsmith et al., 2006; Robertson et al., 2007; Harris et al., 2008; Patterson et al., 2008).

Here, we analyze zebrafish postembryonic development with the goal of providing a generally useful system for assigning fish to stages after

Department of Biology, University of Washington, Seattle, Washington
Grant sponsor: NIH, National Institute of Child Health and Human Development; Grant number: R03 HD050201.
***Correspondence to: David M. Parichy, Department of Biology, Box 351800, University of Washington, Seattle WA 91895. E-mail: dparichy@u.washington.edu**

DOI 10.1002/dvdy.22113
Published online 6 November 2009 in Wiley InterScience (www.interscience.wiley.com).

embryogenesis. We relate changes in several traits to size and age, and we show that size is a more useful indicator of developmental progress than is age. We further identify several developmental milestones, and we examine how the sizes at which such milestones are achieved varies with temperature and density. We also provide images of reference individuals. Finally, we suggest conventions for reporting stages of postembryonic zebrafish that account for both qualitative and quantitative changes in size and developmental state. Our goal in this study is not to provide extensive details on internal anatomical changes, but to provide a means to easily and rapidly assign stages to individual larvae. The staging systems we propose should facilitate detailed anatomical and developmental analyses of this important but still neglected period of development.

LIFE HISTORY STAGE DEFINITIONS

There have long been debates over how to define the broad life history stages of teleosts (Balon, 1999; Hensel, 1999; Kovac and Copp, 1999; Webb, 1999a; Urho, 2002; Snyder et al., 2004). In the context of this study, we use the following definitions and considerations:

Embryo

Classically, offspring are considered embryos until they hatch or are born. While hatching has profound ecological and behavioral consequences, it nevertheless occurs over a wide range of times (e.g., 48–72 hours postfertilization [hpf]) and developmental morphologies in zebrafish and many other organisms. Thus, we follow Kimmel et al. (1995) in defining an arbitrary end to the embryonic period, specifically by the attainment of the *protruding mouth stage* (~72 hpf at 28.5°C).

Larva

An individual that is no longer an embryo but has yet to become a juvenile.

Juvenile

The state at which most adult characteristics have been acquired in the absence of sexual maturity. Here defined by the attainment of a complete pattern of scales (squamation) and complete loss of the larval fin fold.

Adult

Defined by the production of viable gametes and the appearance of secondary sexual characteristics in fish that are in breeding condition.

Metamorphosis

Most fishes are considered to undergo a metamorphosis in which a larval morphology is transformed into that of a juvenile or adult (Webb, 1999b; Power et al., 2008). Metamorphosis includes the loss of some larval features (e.g., fin fold), remodeling of others (e.g., gut, nervous system), and the acquisition of new adult features (e.g., scales), and these processes can be under hormonal control, as in amphibians (Brown and Cai, 2007). While zebrafish undergo a period of metamorphic remodeling, in the absence of experimental data to reveal the onset and cessation of such changes, we do not here define this period explicitly. We do, however, refer to metamorphosis of the pigment pattern (Parichy and Turner, 2003; Kelsh and Parichy, 2008).

Postembryonic Development

Broadly, this can be defined as any period after embryogenesis; includes extensive growth, as well as patterning and morphogenesis during the development and maintenance of the adult form. Many such changes in zebrafish postembryonic development are likely to be identical or homologous to later organogenesis, as well as fetal and neonatal development of mammals.

QUALITATIVE AND QUANTITATIVE ANATOMICAL TRAITS

To evaluate developmental progress of postembryonic zebrafish requires identifying traits that undergo sufficient changes during this period as to be potentially diagnostic for the attainment of defined development states. Zebrafish larvae have a variety of such traits that are visible at relatively low magnification under a stereomicroscope with brightfield transmitted or incident illumination. These include qualitative characteristics (e.g., caudal fin shape), as well as continuous and meristic quantitative traits (e.g., body height and fin ray counts, respectively). Table 1 and Figure 1 provide criteria for evaluating or measuring such traits.

In addition to traits visible in brightfield, fluorescent vital dyes make it possible to assess development for some other traits, including the skeleton and the lateral line sensory system. For example, calcein reveals skeletal ossification (Du et al., 2001), which occurs largely during postembryonic development (Fig. 2; Cubbage and Mabee, 1996; Bird and Mabee, 2003; Elizondo et al., 2005). Features revealed by vital stains thus complement features visible with brightfield illumination.

DEVELOPMENT RATE

Time since fertilization is a convenient surrogate for developmental stages of embryos reared at standard temperature and in standard media, although even under these conditions individuals exhibit developmental variability and named stages based on distinct morphological criteria are to be preferred (Kimmel et al., 1995). As development proceeds in posthatching, free-feeding larvae, genetic and environmental factors and their interactions contribute increasingly to growth and development rate variation. For example, Figure 3 shows extensive variation in growth rates of larvae reared individually. These observations suggest that days postfertilization (dpf) is not adequate for staging.

In zebrafish and other fishes, standard length (SL; defined in Table 1 and Fig. 1) is used sometimes as a proxy for developmental stage (Cubbage and Mabee, 1996; Fuiman et al., 1998; Bird and Mabee, 2003; Campinho et al., 2004). To compare the utility of SL and dpf as indicators of developmental progress, we fitted models relating each to several traits of the larvae shown in Figure 3. Comparing coefficients of determination

TABLE 1. Trait Descriptions

Standard length[a] (SL)	Distance[b] from the snout[c] to the caudal peduncle.[d] In pre-flexion larvae that do not have a caudal peduncle, distance from the snout to the posterior tip of the notochord.[e]
Snout–vent length (SVL)	Distance from snout to posterior margin of the vent.[f]
Snout–operculum length	Distance from snout to most posterior point of operculum.
Height at nape	Distance from ventral to dorsal, immediately posterior of head, perpendicular to the axis defined by standard length.
Height at anterior of anal fin (HAA)	Distance from ventral to dorsal, defined ventrally by the confluence of the anterior margin of the anal fin, the posterior of the peritoneal cavity and the ventral margin of the myotomes; perpendicular to the axis defined by standard length. In older larvae, ventral margin defined by the ventral point of the myotomes at the insertion of the anteriormost anal fin ray.
Eye diameter	Distance at the longest axis of the eye (as determined by specimen orientation).
Flexion angle (FL°)	Angle measure between a horizontal line drawn along the anterior notochord (or vertebral column) and a line drawn down the center of the upturned caudal portion of the notochord (or vertebral column). Examined with transmitted light.
Swim bladder (SB) lobes	Divided into anterior and posterior lobes; scored as number of lobes present (0, 1, 2)
Swim bladder anterior (aSB) lobe diameter	Distance describing longest axis of the anterior (second-forming) swim bladder lobe.
Swim bladder lobe angle (SB°)	Angle measure between lines drawn to indicate the longest axis of each swim bladder lobe.
Median fin fold	Simple median fin fold that develops in embryos and persists in whole or in part until the juvenile stage; here divided into major and minor lobes.
Fin bud appearance	For pelvic fins, noted as the first observance of the fin buds from the abdomen. For dorsal or anal fins, noted as the first observable condensation of mesenchyme as a bulge where the fin will form.
Fin ray appearance	Noted as the first observance of bony lepidotrichia comprising one or more fin segments.
Fin ray number	Count of fin rays present at distal tips of caudal, dorsal, anal, or pelvic fins. Fused rays were counted separately. Examined with transmitted light.
Fin ray segments	Number of fin ray segments in the longest fin ray of the caudal, dorsal, anal, or pelvic fins. Counted from base of fin to tip, with any partial ray segments included in the count. Examined with transmitted light.
Metamorphic melanophore pattern	Qualitative scores of metamorphic melanophore pattern (0–5; see text)

[a]SL is distinct from total length, which is measured to the distal tip of the caudal fin. Total length can be confounded by fin damage and is not recommended for staging purposes.
[b]All distances are minimum straight line.
[c]Most anterior point of the head excluding the lower jaw.
[d]Posteriormost region of body where caudal fin rays insert.
[e]Equivalent to "notochord length" of Bird and Mabee (2003).
[f]Urogenital opening or anus.

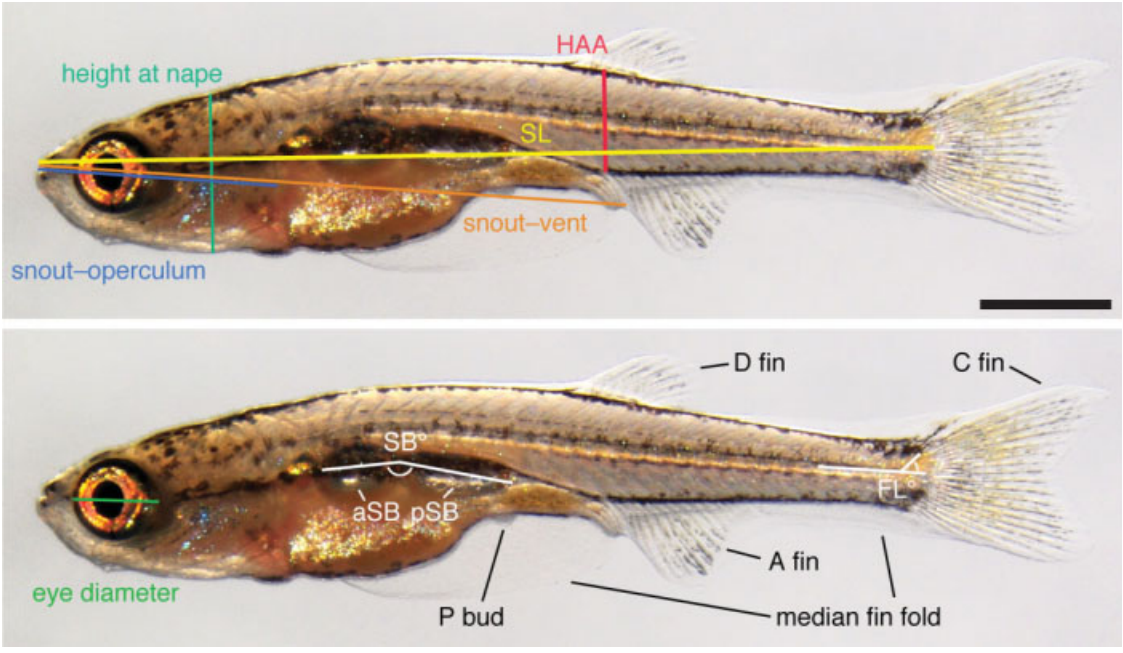

Fig. 1. Traits of postembryonic zebrafish that are potentially useful for staging. SL, standard length; HAA, height at anterior of anal fin; FL°, flexion angle of notochord; aSB, swim bladder anterior lobe; pSB, swim bladder posterior lobe. Fins: A, anal; C, caudal; D, dorsal; P, pelvic. Scale bar = 1 mm.

Fig. 2. External features of developing larvae and internal ossification of the same individuals revealed by calcein staining. Larvae are not to scale.

(R^2) across 13 traits (Table 2) showed that dpf explains significantly less developmental variance than SL (paired Wilcoxon sign-rank test: $P < 0.0005$; median R^2: dpf = 0.73, SL = 0.94). These findings suggest that SL is to be preferred over dpf as an indicator of developmental progress in zebrafish.

MEASUREMENTS OF LARVAL SIZE

Different measures of size are typically highly correlated, although allometric changes during development can modify these relationships. We examined how SL scales with other size measures (Table 1; Fig. 1). Among these, snout–vent length and snout–operculum length are parallel to SL. Because it can be useful to describe larval size along the dorsal–ventral axis, we also examined correlations with height at nape and height at the anterior margin of the anal fin (HAA). Figure 4 shows that all measures of size are highly correlated with SL (and with one another), despite moderate departures from linearity at some size ranges (e.g., HAA).

A generally useful measure of size should be robust to measurement error, and this requires landmarks to be easily identified, and measurements themselves to be large enough to perform at typical magnifications. Considering these issues together, we recommend SL for anterior–posterior measurements and HAA (when HAA > 0.5 mm) for dorsal–ventral measurements. The regressions provided in Table 3 relate SL and HAA to other quantitative measures of size.

DEVELOPMENT OF SELECTED TRAITS

In addition to larval size, several other traits also suggest themselves as indicators of developmental progress. Here, we briefly review postembryonic changes in several of these. As statistical analyses indicate high correlations between SL and developmental progress (Table 2), we refer to changes below relative to SL, as typically observed. Image panels in figures below provide SL for the individuals shown. These values are provided for ease of reference and, because of individual variability, should not be interpreted as either precise stages or as population mean SLs, which are provided after this section.

Head Shape

Whereas the embryonic head is somewhat square with a ventrally located mouth, during early postembryonic development the mouth moves increasing dorsal and anterior (Fig. 5; 4.8 mm SL). Meanwhile, the head becomes more triangular with a protruding anterior. Changes in mouth position have been described previously during the hatching period

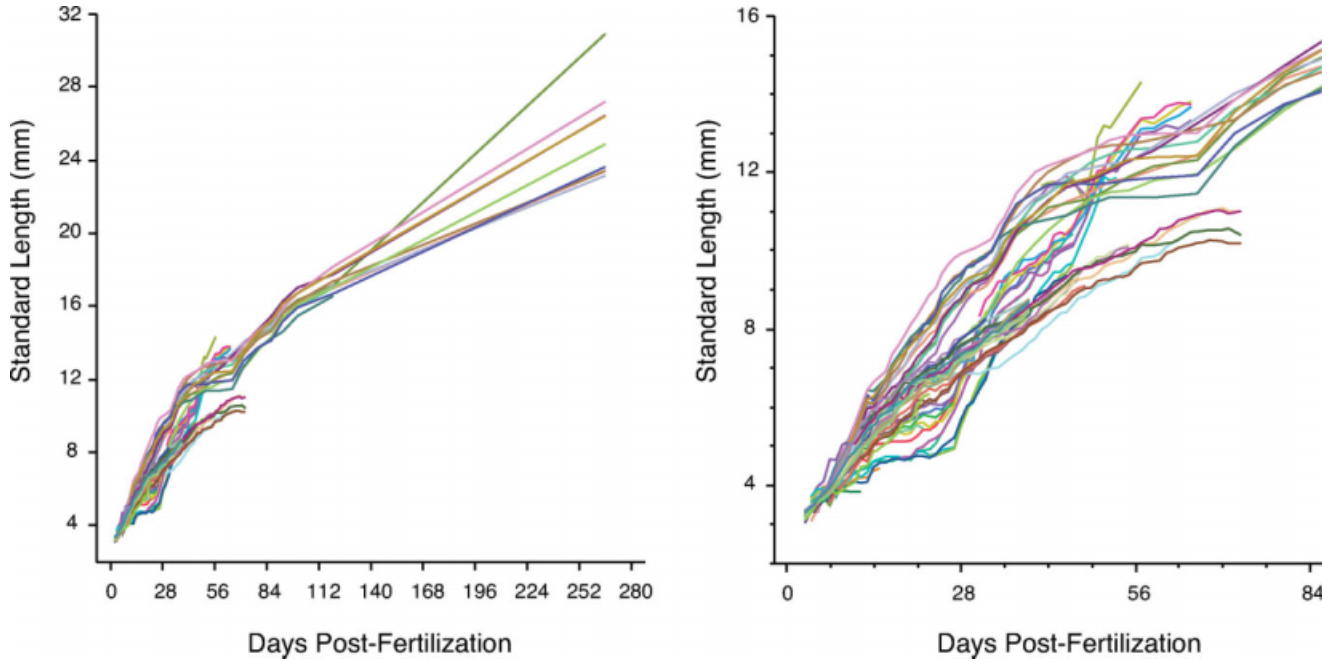

Fig. 3. Growth varies markedly among larvae. Each trajectory shows consecutive standard length (SL) for single fish reared individually (N = 54) in three different batches. Left, trajectories between 3 and 280 days postfertilization (dpf). Right, same trajectories expanded to show 3–84 dpf. For more details, see Growth and Environmental Effects Section below.

(Schilling and Kimmel, 1997). Head dimensions subsequently grow relatively linearly to one another as measured by depth at nape, snout–operculum distance, and eye diameter (data not shown). Notably, prolonged anesthesia can produce swellings over the otherwise smooth dorsal surface of the head.

Progressive ossification of cranial skeletal elements is shown in Figure 6. To quantify this progress, we identified bones or complexes of bones that are readily seen and scored in either lateral view or ventral view. Quantitative analyses of such developmental units indicated relatively ordered developmental progressions (Fig. 7), with the onset of laterally visible changes occurring as early as ~4.6 mm SL (dorso-orbital complex and hyomandibula) and as late as ~6.0 mm SL (supraoccipital). From ventrally, we observed clear transitions at ~4.8 mm SL (hypohyals ventral) and at ~5.3 mm SL (basihyal) and additional changes are observable into later development (e.g., notochord extension complex and length of the urohyal).

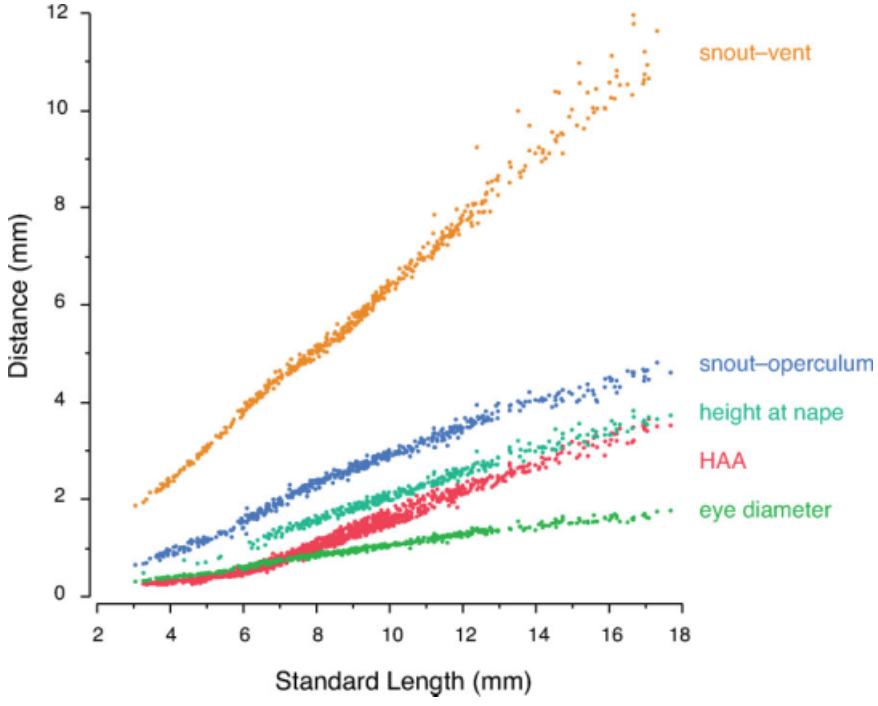

Fig. 4. Size measurements are highly correlated. Shown are relationships for several easily measured characters relative to standard length (SL) for larvae examined repeatedly through development. Relationships for snout–operculum length vs. SL, and eye diameter vs. SL, are slightly curvilinear, whereas the relationship of height at anterior of anal fin (HAA) vs. SL is curvilinear at small sizes (probably owing to the failure of small larvae to lay flat), but is reasonably linear at larger sizes. Larvae used for size measurements are the same individuals for which growth trajectories are shown in Figure 3.

TABLE 2. Predictive Abilities of dpf and SL for Several Developmental Traits[a]

Trait	Modeling type	dpf R^2	SL R^2
FL°	Continuous	0.81	0.97
Melanophore pattern	Ordinal	0.29	0.57
SB lobes	Ordinal	0.64	0.86
SB°	Continuous	0.64	0.81
A rays	Continuous	0.76	0.95
A segments	Continuous	0.77	0.95
C rays	Continuous	0.83	0.89
C segments	Continuous	0.86	0.97
D rays	Continuous	0.73	0.90
D segments	Continuous	0.78	0.96
P bud	Nominal	0.70	0.94
P rays	Continuous	0.70	0.93
P segments	Continuous	0.63	0.95

[a]Models were fitted with smoothing splines for continuous traits and maximum likelihood-based logistic regressions for ordinal and nominal traits. dpf, days postfertilization; SL, standard length; FL°, flexion angle of notochord. SB, swim bladder. Fins: A, anal; C, caudal; D, dorsal; P, pelvic.

TABLE 3. Prediction of SL and HAA From Other Quantitative Measures and Estimation of Initial Sizes After Histological Processing[a]

Dependent	Predictor	Regression	R^2
SL	HAA[b]	SL = (3.56 x HAA) + 4.40	0.98
	SVL	SL = (1.48 x SVL) + 0.55	0.99
	Nose–operculum[c]	SL = (3.29 x nose–operculum) + 0.73	0.98
	Eye diameter[c]	SL = (9.49 x eye diameter) + 0.22	0.98
	Depth at nape	SL = (4.12 x depth at nape) + 1.62	0.99
	C segments	SL = (0.58 x C segments) + 4.62	0.93
	SL post-fixation	$SL = (1.00 \times SL_{post\text{-}fix}) + 0.29$	1.00
	SL post-ISH	$SL = (1.42 \times SL_{post\text{-}ISH}) + 0.46$	0.99
	HAA post-fixation	$SL = (4.05 \times HAA_{post\text{-}fix}) + 3.71$	0.99
	HAA post-ISH	$SL = (5.20 \times HAA_{post\text{-}ISH}) + 3.38$	0.94
HAA	HAA post-fixation	$HAA = (1.02 \times HAA_{post\text{-}fix}) + 0.00$	1.00
	HAA post-ISH	$HAA = (1.36 \times HAA_{post\text{-}ISH}) - 0.18$	0.98

[a]All regressions $P < 0.0001$. SL, standard length; HAA, height at anterior of anal fin; SVL, snout–vent length; ISH, in situ hybridization.
[b]Regressions for HAA only consider values of HAA > 0.5 mm, owing to non-linearity at lesser values; this regression includes measurements ($n = 1769$) from individually reared larvae and batch-reared fish across temperatures (see text for details).
[c]The regressions have moderate departures from linearity near ~5.5 mm SL and >15 mm SL.

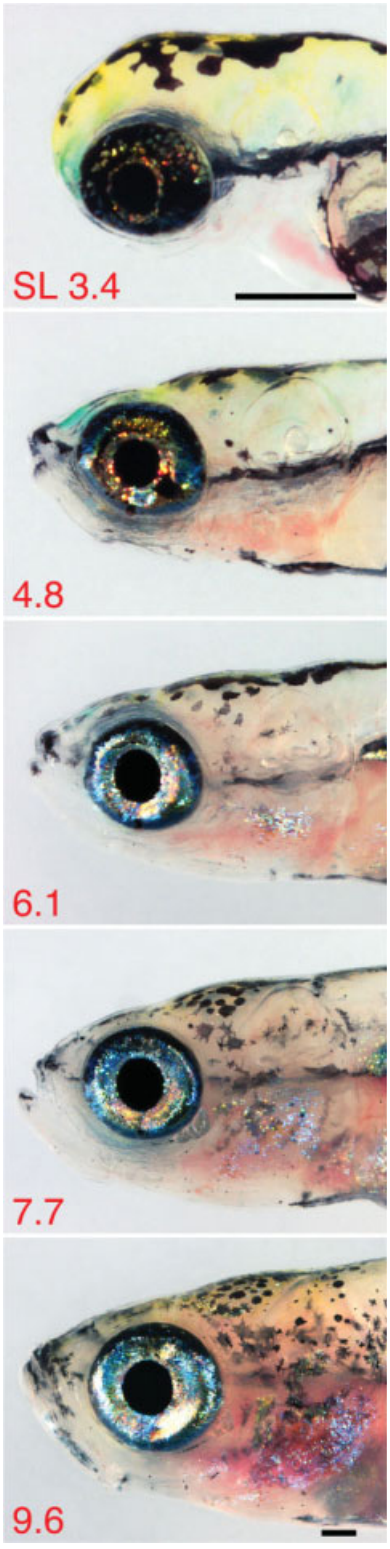

Fig. 5. Head development. Marked shape change occurs during the embryo–larval transition, with additional more subtle changes during later development. Standard length (SL) of individuals shown is in red at the lower left of each panel. Images shown are at decreasing magnifications. Scale bars = 3.4 and 9.6, 250 μm.

Notochord Flexion

During the early larval period, the posterior notochord bends dorsally in a process termed flexion, which is easily seen with transmitted light (Figs. 8, 9). This process begins at ~4.5 mm SL and is completed by ~6.5 mm SL, with a final flexion angle of ~45°.

Swim Bladder

Several changes in the swim bladder (or "gas bladder") are visible during embryonic and postembryonic development (Figs. 9, 10; Robertson et al., 2007). Swim bladder inflation and "float-up" occur by ~3.7 mm SL, shortly after hatching. At this time, a single, *posterior swim bladder lobe* is

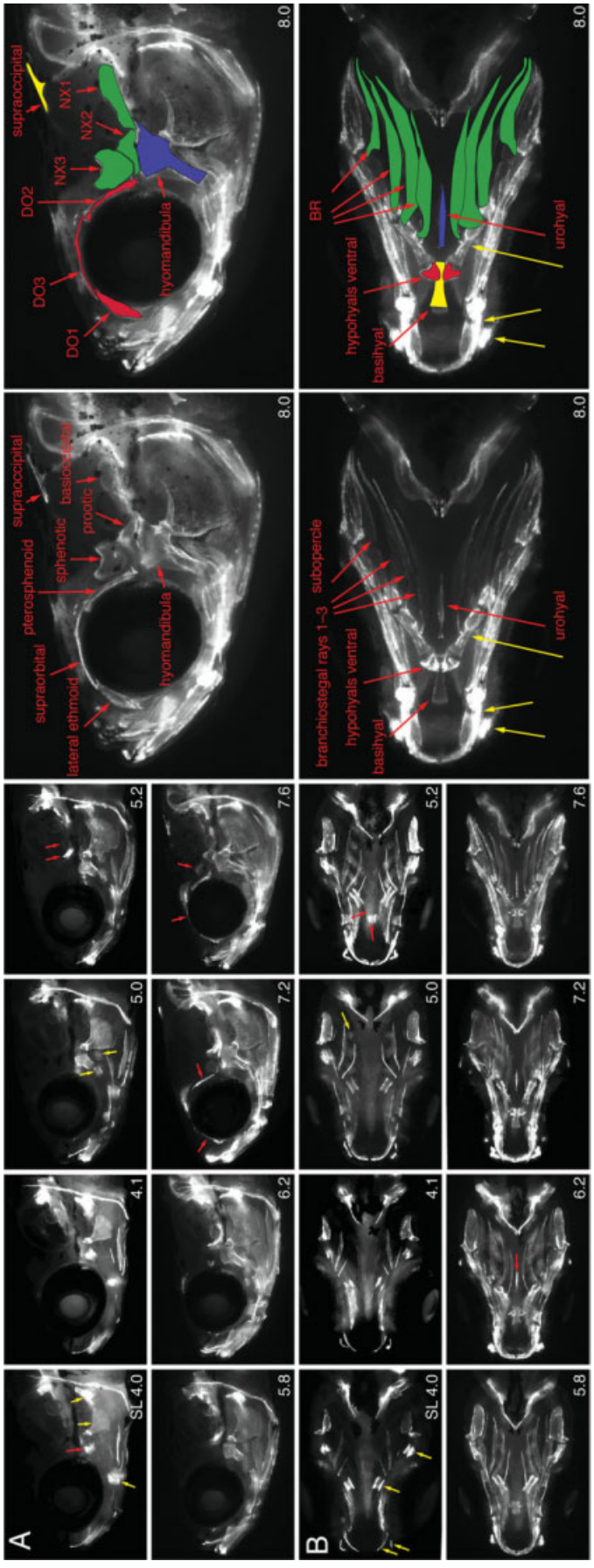

Fig. 6. Ossification of craniofacial skeleton revealed by calcein staining. Lateral and ventral views are of the same individuals; different individuals are shown across stages (standard length [SL] in lower right of each panel). All images are projections that flatten multiple focal planes. Selected skeletal elements are indicated with arrows (annotations are provided left to right in each panel unless otherwise noted; red arrow and regular type below = scored quantitatively; yellow arrow and italic type below = additional bones not scored). Overlays indicate skeletal units scored in Figure 7. **A**: 4.0, *quadrate*, hyomandibula, *opercle*, *ceratobranchial 5*; 5.0, *ceratobranchial 2*, *ceratobranchial 3*; 5.2, prootic, basioccipital; 7.2, lateral ethmoid, pterosphenoid; 7.8, supraorbital, sphenotic; 8.0, red overlay = dorso-orbital complex [DO1, lateral ethmoid; DO2, pterosphenoid, DO3, supraorbital], green overlay = notochord extension complex [NX1, basioccipital; NX2, prootic; NX3, sphenotic]; blue overlay = hyomandibula; yellow overlay = supraoccipital. **B**: 4.0, *dentary*, *infraorbital*, *ceratohyal*, *hyomandibula* (scored for lateral view); 5.0, *ceratobranchial 4*; 5.2, ventral hypohyals, basihyal; 6.2, urohyal; 8.0, *infraorbital 1*, *dentary*, *ceratohyal*, yellow overlay = basihyal, red overlay = ventral hypohyals, green overlay = branchiostegal ray complex [BR, branchiostegal rays], blue overlay = urohyal.

apparent. A second, *anterior swim bladder lobe* appears at ~6.0 mm SL, initially as a small bulge immediately anterodorsal to the posterior lobe. During this time, the posterior lobe lengthens and ultimately changes from a relatively symmetrical oval to bending ventrally at its posterior. This bending is evident in the reduced angle between the major (i.e., longest) axes of the anterior and posterior lobes. During later development (>8.5 mm SL), the swim bladder is partially obscured by the adult primary ventral melanophore stripe (see below).

Median Fins

The caudal fin is first to develop. A condensation of mesenchyme is evident ventral to the posteriormost region of the notochord shortly after flexion initiates; the first fin rays (lepidotrichia) appear shortly thereafter, typically by ~4.9 mm SL (Figs. 11, 12). Once the first fin ray segments have formed, there is a relatively linear increase in segment number for the longest of the fin rays (Fig. 12). During the early period after rays appear, the fin is slightly longer dorsally than ventrally (Fig. 11, 5.6 mm SL, 5.9 mm SL). Gradually, the dorsal and ventral regions become similar in length (Fig. 11, 6.0 mm SL) and dorsal and ventral lobes begin to emerge (Fig. 11, 6.4 mm SL; Fig. 13). Rays within these lobes have more segments than rays within the intervening cleft (Goldsmith et al., 2006).

Caudal fin ray development also is revealed by calcein staining, and the greater internal resolution allows distinguishing between fin rays ventral and dorsal to the notochord axis (Figs. 14, 15). We term these rays *subnotochordal* and *supranotochordal*, respectively. Whereas subnotochordal rays begin to develop ~4.9 mm SL, supranotochordal rays appear considerably later, >6.0 mm SL. Calcein staining also shows progressive ossification for bones at the base of the fin ("hypural complex"), between 5.2 and 6.5 mm SL.

The anal fin is the second to develop. Condensed mesenchyme is apparent within the fin fold (see below) posterior to the anus (Fig. 16, 5.4 mm SL). This mesenchyme will

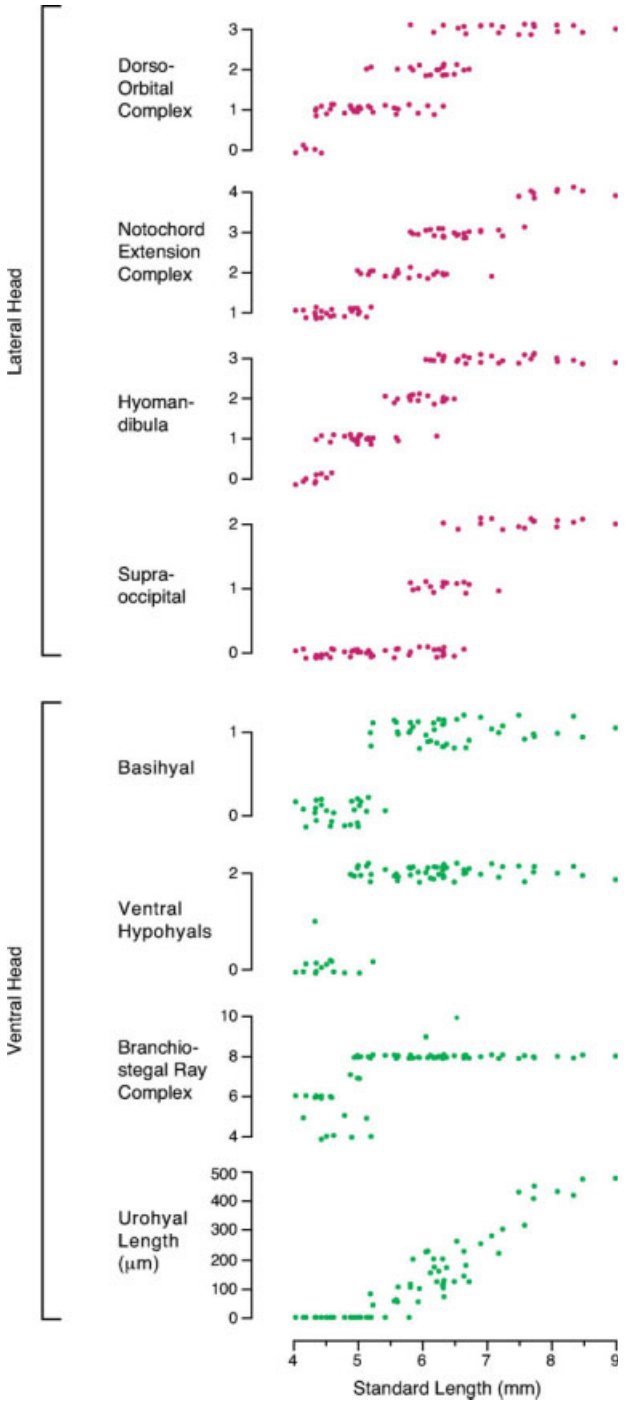

Fig. 7. Ossification progress by standard length (SL). Shown are scores for defined lateral and ventral units of the craniofacial skeleton revealed by calcein staining. All scores are jittered vertically for clarity, except for length of the proximal branchiostegal ray (bottom). Each point represents the value for an individual fish of the indicated SL. Scoring was based on the following criteria, with 0 always indicating an absence of staining; the onset of calcein staining for individual bones is indicated by "+" in the following, when more qualitative descriptions are not given: *dorso-orbital complex*, 1 = lateral ethmoid+, 2 = pterosphenoid+, 3 = supraorbital+; *notochord extension complex*, 1 = basioccipital+, 2 = prootic+, 3 = sphenotic+ (begins to extend medial-dorsally into a single rounded end), 4 = sphenotic++ (staining widens into two rounded ends); *hyomandibula*, 1 = staining in narrow ring, 2 = expansion of staining into dorsal process of bone, 3 = expansion of staining into ventral process and widening of dorsal process; *supraoccipital*, 1 = first appearance, 2 = posterior elongation and lateral curvature; *basihyal*, 1 = first appearance; *ventral hypohyals*, 1 = first bone ossified, 2 = second bone ossified; *branchiostegal ray complex*, scores indicate number of bones stained (paired branchiostegal rays plus paired subopercles; while generally there are only three pairs of branchiostegal rays, some individuals exhibit four pairs; Cubbage and Mabee 1996); *urohyal*, anterior–posterior length of stained region, with no staining = 0.

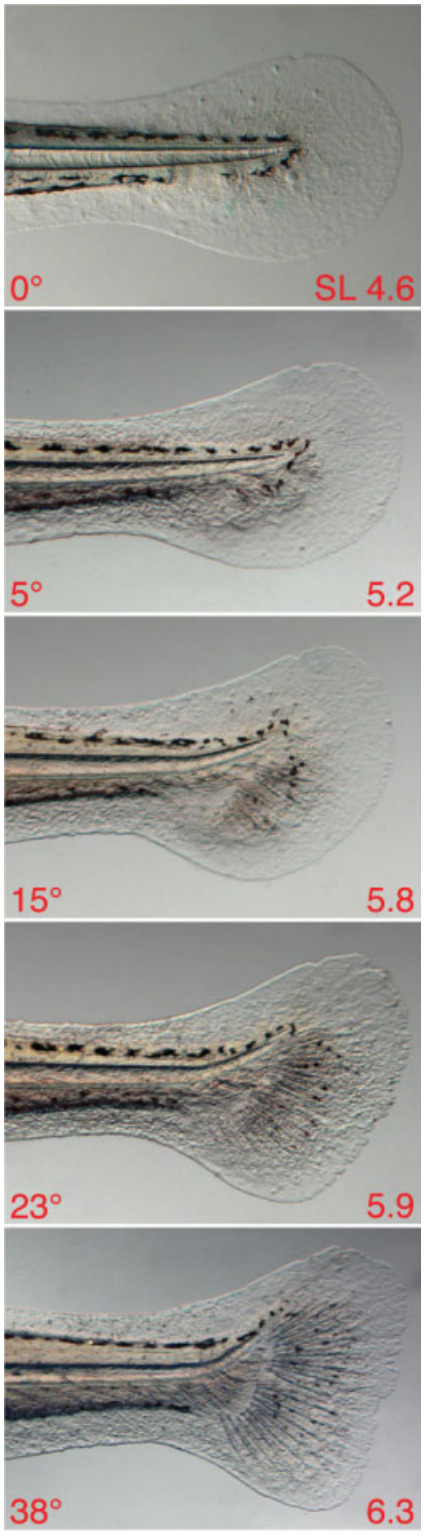

Fig. 8. Notochord flexion in a single individual. In each panel, degrees of flexion are shown at the lower left and corresponding standard length (SL) at the lower right. As the notochord bends, the rate of SL increase drops briefly (e.g., 15–23°).

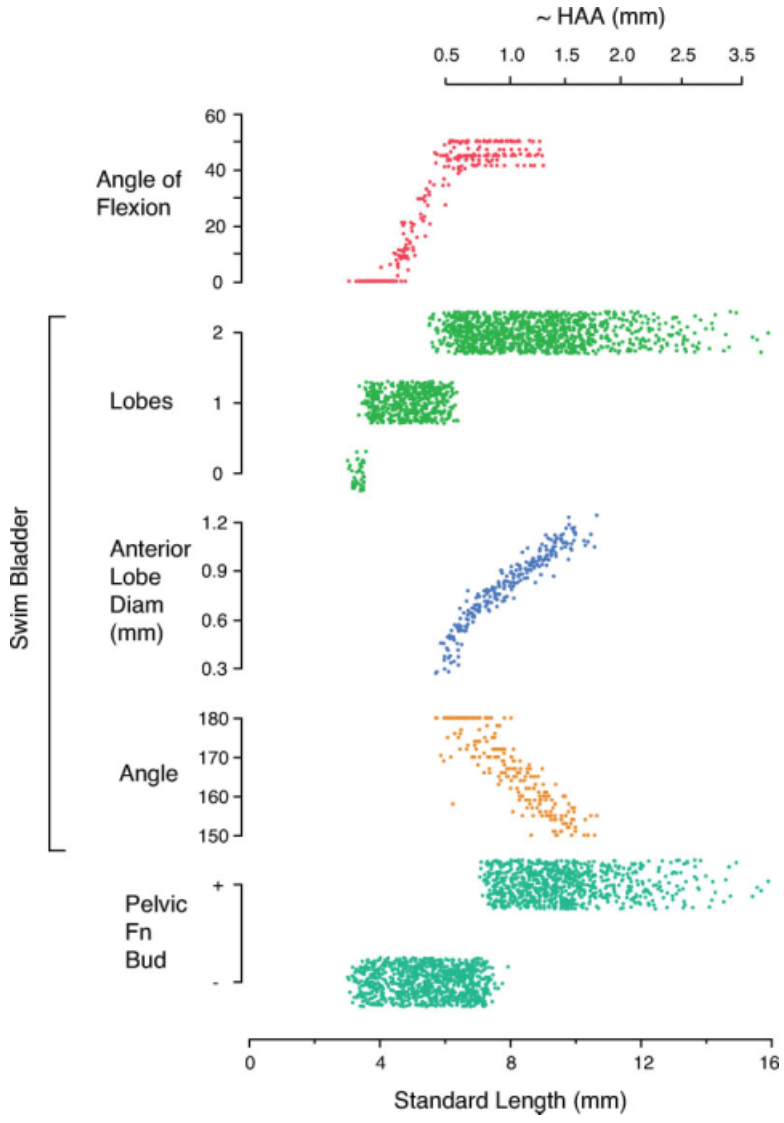

Fig. 9. Relationships between standard length (SL) and notochord angle of flexion, swim bladder characteristics, and pelvic fin bud appearance in larvae examined repeatedly through development. Shown above is approximate height at anterior of anal fin (HAA) relative to SL as predicted in Figure 4 and Table 3. The meristic traits, swim bladder lobes and pelvic fin buds, are jittered for clarity of presentation.

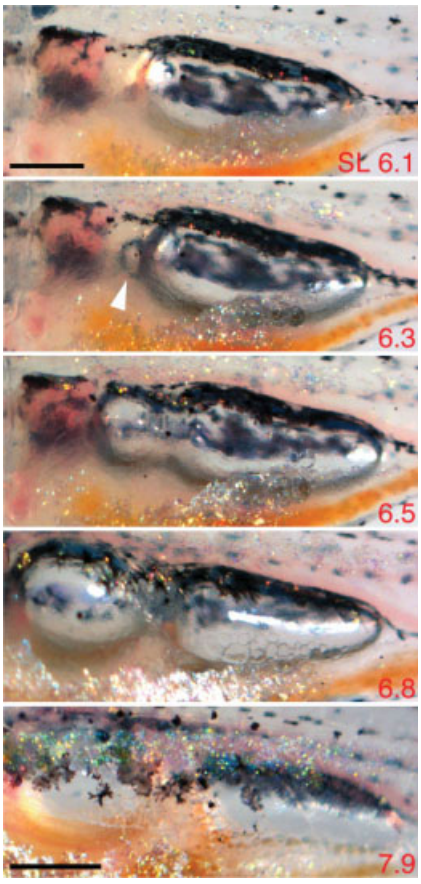

Fig. 10. Changes in swim bladder morphology. Shown is a single individual, viewed from ventrolaterally (standard length [SL] at lower right of each panel). Larvae initially have a single, posterior swim bladder lobe. A second, anterior lobe appears as a bud adjacent to the posterior lobe, then inflates within a short period of time. Images shown are at decreasing magnifications. Scale bars = 6.1 and 7.9, 250 μm.

generate the radial bones at the fin base. Lepidotrichia become apparent at ~6.3 mm SL, with bones of several rays appearing simultaneously. All rays develop by ~8.5 mm SL and ray segment addition proceeds relatively linearly through ~11.0 mm SL (Figs. 12, 17). Calcein staining more clearly reveals radial ossification, which begins typically ~7.0 mm SL (after the first caudal ray segments have already ossified; Figs. 15, 18).

The dorsal fin develops slightly later than the anal fin, first evident by condensed mesenchyme visible within the dorsal fin fold (Fig. 16, 5.7 mm SL). Lepidotrichia appear at ~6.5 mm SL (Fig. 12), although individuals vary in the precise timing of ossification (e.g., Fig. 16, 6.7 mm SL). As for the other fins, ray segment addition proceeds relatively linearly (Figs. 12, 17). Calcein staining reveals fin ray segment ossification as early as 5.8 mm SL, and the onset of radial ossification considerably later, at ~7.2 mm SL (Figs. 15, 19).

Vertebral Ossification and Pleural Ribs

Calcein staining reveals an anterior-to-posterior sequence of vertebral ossification (Fig. 14). The number of terminal (posterior) centra that have ossified provides an additional measure of developmental progress between 4.5 and 6.5 mm SL (Figs. 14, 20). Likewise, development of the pleural ribs occurs anteriorly to posteriorly beginning ~5.8 mm SL (Figs. 20, 21).

Pelvic Fins

The paired pelvic fins buds are apparent as rounded protuberances from the ventrolateral body wall, ventral to the posteriormost region of the posterior swim bladder lobe (Fig. 22, 7.5 mm SL). After the out-growing bud has become longer than it is wide, the first rays become apparent in the proximal region (Fig. 22, 8.8 mm SL). Maximum fin ray number is achieved

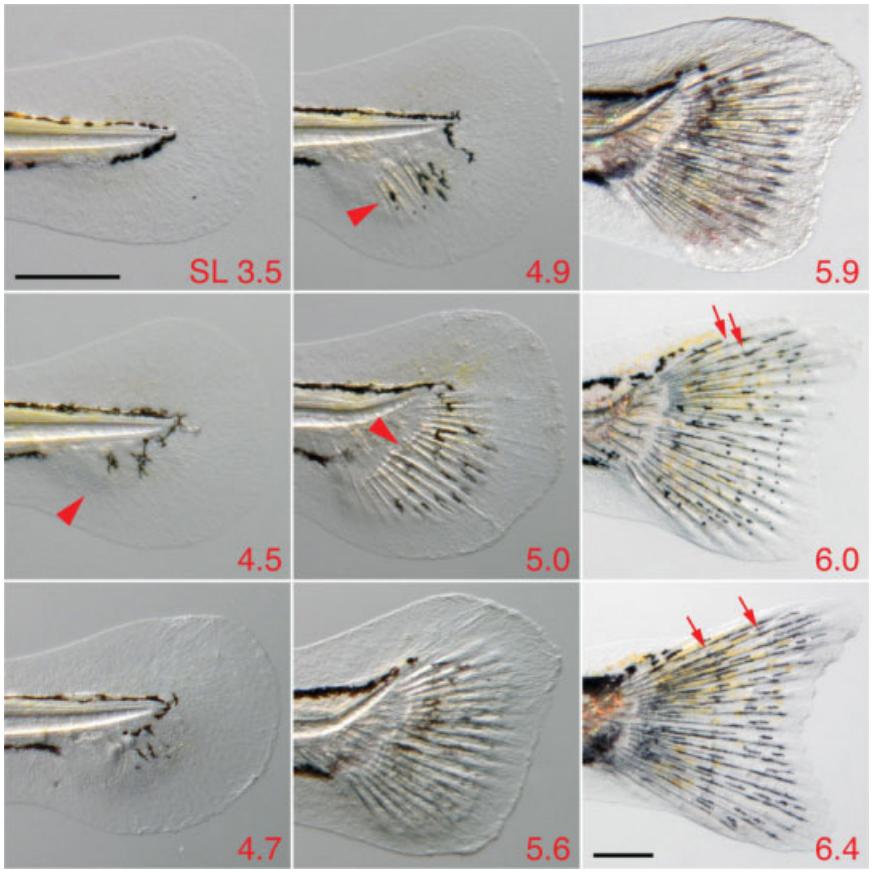

Fig. 11. Early caudal fin development. Shown are multiple individuals with corresponding standard length (SL) in the lower right of each panel. Arrowheads: 4.5, mesenchymal condensation at base of prospective fin; 4.9, fully formed caudal fin ray first segments; 5.0, division between future dorsal and ventral fin rays (also apparent at 4.9). Arrows: 6.0, joints between first and second segments of indicated rays. 6.4, joints between first, second, and third segments of indicated ray. Images shown are at decreasing magnifications. Scale bars = 3.5 and 6.4, 250 μm.

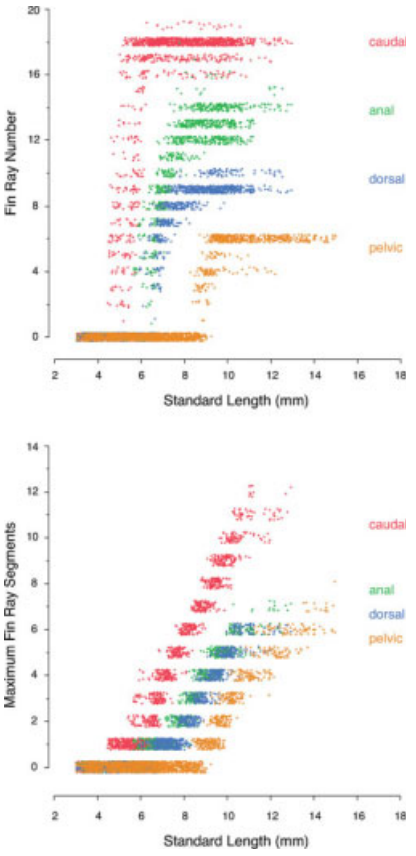

Fig. 12. Relationships between fin characteristics and standard length in larvae examined repeatedly through development. Above, number of fin rays observed in each of the indicated fins. Below, number of fin ray segments in the longest ray within each fin. All values are meristic and jittered for clarity. Pectoral fins were not scored.

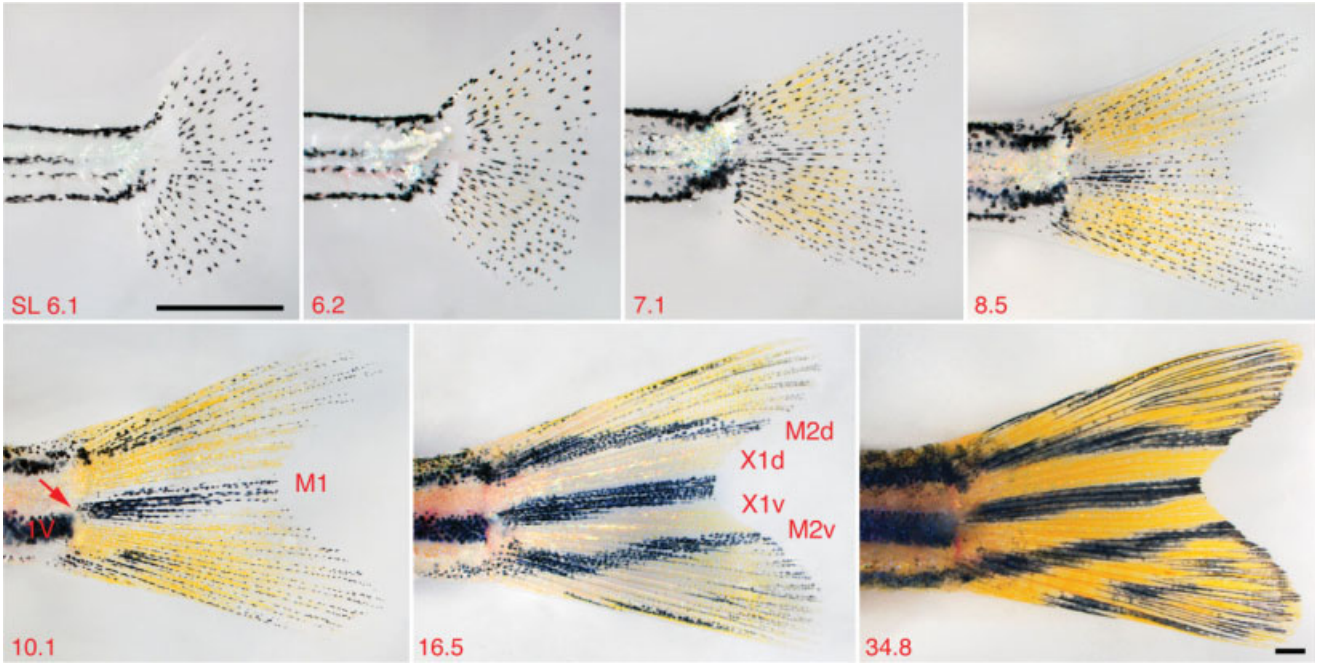

Fig. 13. Late caudal fin development and pigment pattern formation. Shown is a single individual (standard length [SL] at lower left of each panel). An initially rounded fin gradually develops a middle cleft with longer lobes dorsally and ventrally. Emergence of the fin pigment pattern proceeds from an initially uniform field of melanophores, to the development of interspersed xanthophores, and subsequent segregation into the definitive adult stripes (see text for details). Arrow in 10.1: transiently disjunct melanophore stripes on body and fin. 1V, adult ventral primary melanophore on body. M1, first arising caudal fin melanophore stripe; M2d, M2v, second arising dorsal and ventral caudal fin melanophore stripes; X1d, X1v, first arising caudal fin xanthophore interstripes. Images shown are at decreasing magnifications. Scale bars = 6.1 and 34.8, 0.5 mm.

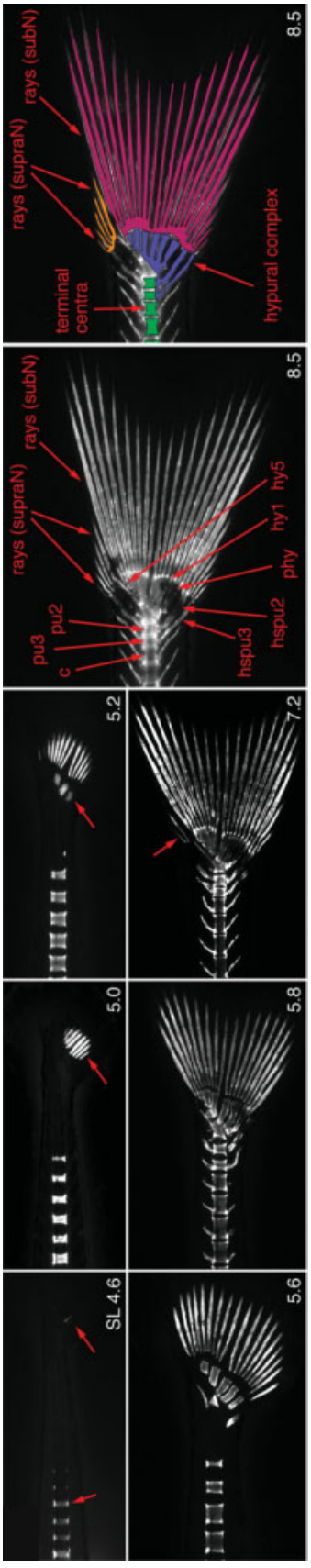

Fig. 14. Ossification progress of caudal complex revealed by calcein staining. Shown are multiple individuals (standard length [SL] in lower right of each panel). Annotations for arrows are provided left to right for each panel; overlays are units scored in Figure 15. 4.6, posteriormost ossified centrum, first ossifying ray segment; 5.0, first segments of multiple ossified fin rays; 5.2, hypurals; 7.2, supranotochordal fin rays; 8.5, c = centra, pu = preural, hspu = hemal spines from preural, phy = parahypural, hy = hypural, green overlay = terminal centra complex [6 posterior centra and both preural (pu) 2 and 3 of the vertebral column]; blue overlay = hypural complex [hypurals (hy) 1–5, parahypural (phy), and the hemal spines (hspu) originating from pu2 and pu3], orange overlay = supranotochordal rays [dorsal procurrent rays appearing dorsal to the notochord], pink overlay = subnotochordal rays [including the principal caudal rays of the dorsal and ventral lobes and the ventral procurrent rays that are supported by hspu2, hspu3, and phy]. Terminal centra counts (shown in Fig. 20) are best performed posterior-to-anterior with hspu2 and hspu3 serving as landmarks for their corresponding centra; staining for these hemal spines occurs before staining of centra. At earlier stages, the terminal somite boundaries can be used to identify segments corresponding to pu2 and pu3.

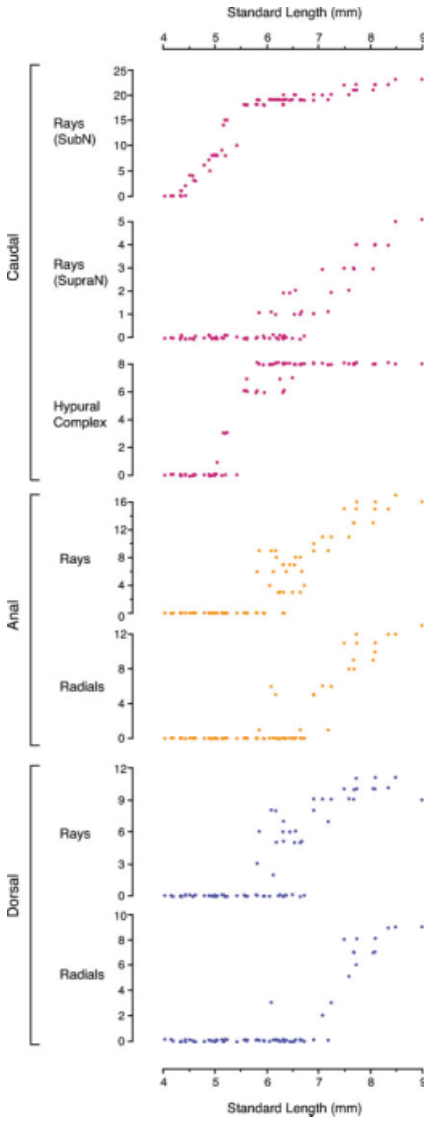

Fig. 15. Ossification progress for median fins by standard length (SL). All scores are jittered vertically for clarity. Scoring was based on the following criteria: *caudal fin rays* (subnotochordal and supranotochordal), simple counts; *hypural complex*, count of total bones stained (see Figure 14 legend); *dorsal and anal fin rays and radials*, simple counts.

by 10–12 mm SL (Figs. 12, 20). Note that much of pectoral fin development occurs during embryogenesis and is described by Kimmel et al. (1995); we do not include data on these fins through postembryonic development because of their reduced diagnostic value as well as the greater difficulty of examining these fins as compared with pectoral and median fins at these stages.

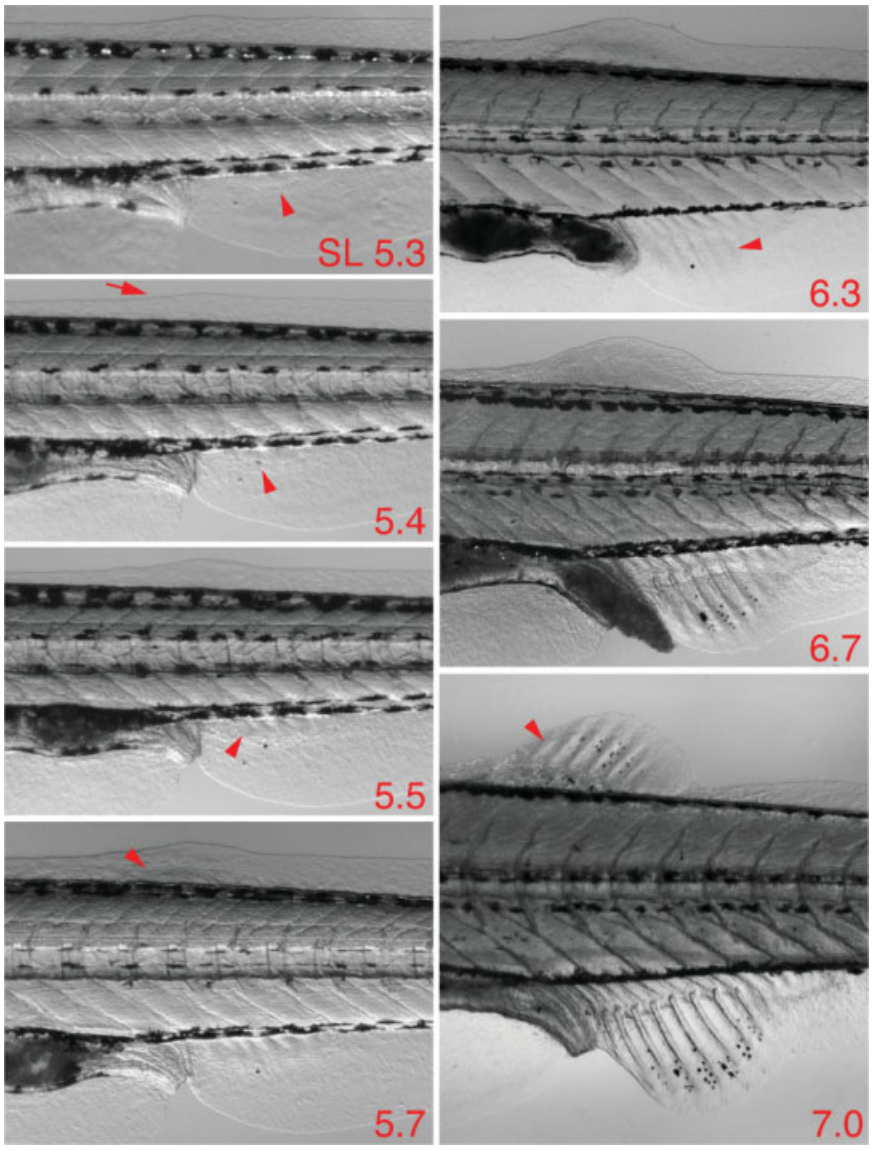

Fig. 16. Early dorsal and anal fin development. Shown is a single individual (standard length [SL] at lower right of each panel). Arrowheads: 5.2, anal fin condensation; 5.4, melanophore (arrow, bulge in fin fold presages dorsal fin condensation); 5.5, condensing anal fin radials; 5.7, dorsal fin condensation; 6.3, anal fin rays; 7.0, dorsal fin rays. Images shown are at decreasing magnifications. Scale bars = 5.3 and 7.0, 250 μm. [Color figure can be viewed in the online issue, which is available at www.interscience.wiley.com.]

Median Fin Fold

The median fin fold is easily seen with transmitted light (Fig. 23), although it is susceptible to damage during handling. We define two fin fold regions. The *major lobe* arises dorsally at the anteroposterior level of the yolk extension and ventrally at the posterior margin of the vent; it extends out from the posterior trunk and postanal tail, and surrounds the posterior tail tip. The *minor lobe* lies ventrally between the yolk sac and anterior of the vent, and extends out from beneath the yolk extension.

Both major and minor lobes are present at ~3.2 mm SL and before hatching, with a slight constriction in the major lobe just anterior to the tail tip. Both lobes then expand away from the body, with the minor lobe becoming increasingly rounded (Fig. 23, 4.2 mm SL). The major lobe bulges further out from the body at the mesenchymal condensation where dorsal fin development initiates (Fig. 23, 5.6 mm SL). Shortly thereafter, the major lobe begins to be resorbed; an early indication being a notch immediately posterior to the dorsal fin (Fig. 23, 6.4 mm SL). Major lobe resorption progresses from anterior to posterior, occurring relatively simultaneously both anterior to the dorsal fin, and posterior to the dorsal fin and the anal fin. Remnants of the major lobe cover approximately the posterior two-thirds of the tail by ~7.4 mm SL and only approximately one-third of the tail by ~8.3 mm SL.

Resorption of the minor lobe is not evident until pelvic fin rays appear, and is noted first as an indentation at the level of the pelvic fin, followed by resorption anteriorly and then posteriorly (Fig. 22). The minor lobe is almost lost by ~10 mm SL, shortly before pelvic fin rays develop second segments; only at the anterior margin of the vent does a small fold of epidermis persist.

Squamation

Development of scales begins posteriorly over the lateral surfaces of the tail at ~8.1 mm SL and proceeds from this location toward the anterior (Sire et al., 1997; Sire and Akimenko, 2004). Scales are visible as subtle ridges in the tail skin when viewed with transmitted illumination (Fig. 24, 9.6 mm SL), but subsequently become more distinctive (Fig. 24, 9.9 mm SL). Simultaneously, subtle condensations of mesenchyme are observable over the dorsum anterior to the anal fin, followed shortly thereafter by overt scale formation (Fig. 24, 12.0 mm SL).

Pigment Pattern: Body

The pattern of *embryonic/early larval melanophores* consists of stripes along the dorsal and ventral edges of the myotomes, at the horizontal myoseptum, and lining the dorsal and ventral surfaces of the yolk sac (Kelsh et al., 2009). Transformation to the adult melanophore pattern begins at ~6 mm SL with the appearance of a few *metamorphic melanophores* over the dorsal and ventral myotomes (Fig. 25) (Johnson et al., 1995; Parichy and Turner, 2003). The number of

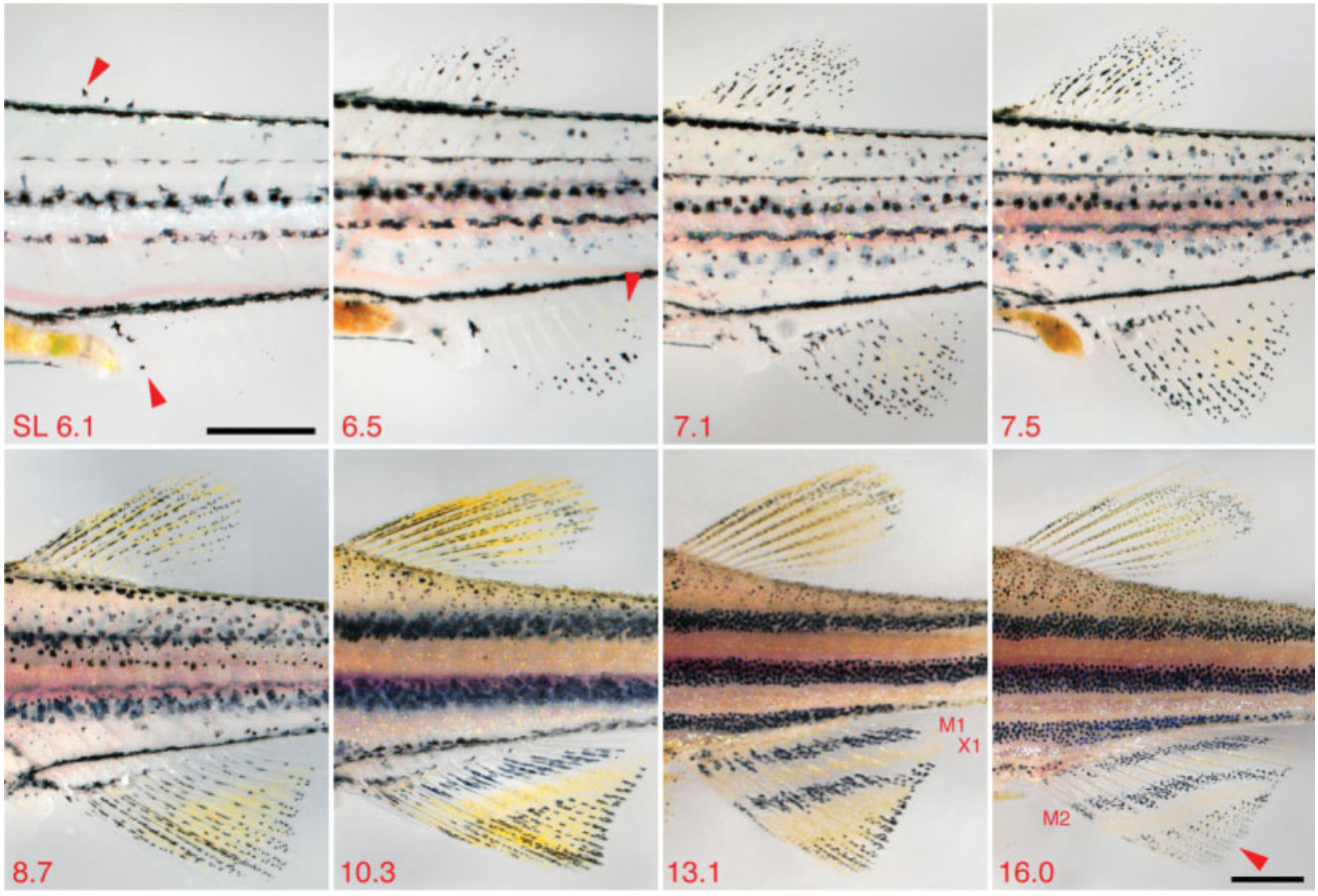

Fig. 17. Late dorsal and anal fin development and pigment pattern formation. A single individual is shown at multiple sizes (standard length [SL] at lower left of each panel). Arrowheads: 6.1, first melanophores in dorsal and anal fins; 6.5, xanthophore appearance in anal fin; 16.0, intermingled melanophores and xanthophores persist distally in anal fin. M1, M2, first and second anal fin melanophore stripes; X1, first anal fin xanthophore interstripe. Images shown are at decreasing magnifications. Scale bars = 6.1, 250 μm; 16.0, 500 μm.

dispersed metamorphic melanophores increases through ~9 mm SL when the first two *primary stripes* (1D, 1V) of the adult begin to be discernible, arising at an angle ~5° offset from the horizontal myoseptum. These stripes become more distinct as dispersed melanophores migrate to them, and additional melanophores differentiate within them. Embryonic/early larval melanophores along the horizontal myoseptum are lost or migrate to join the primary stripes. As the primary stripes become more distinct, the first *interstripe* region becomes increasingly distinct as well. By ~12 mm SL, the primary stripes are complete. The first *secondary stripe* (2V) has been added ventrally by ~14 mm SL, and another secondary stripe (2D) arises dorsally by ~16 mm SL (Fig. 26). Additional secondary stripes are added as the fish continues to grow.

The dorsum of the larva becomes covered with metamorphic melanophores as well. These are dispersed but organize as scales develop (Fig. 26, 10.7 mm SL). Scales exhibit single rows of melanophores at their distal edges initially (Fig. 26, 15.4 mm SL), with additional rows arising during later development.

Iridescent iridophores also contribute to the adult body pigment pattern. In the embryonic/early larval pigment pattern, iridophores occur within the melanophore stripes and covering the swim bladder (Kimmel et al., 1995; Kelsh et al., 2009). Additional metamorphic iridophores develop over the ventral half of myotomes near the swim bladder (Fig. 27A, 5.0 mm SL), marking the first interstripe. Subsequently, these cells are found further anteriorly and posteriorly and a second patch of iridophores arises (Fig. 27C, 5.7 mm SL) at the posterior tail, above the site of notochord flexion. Thereafter, a faint but continuous line of iridophores extends from just posterior to the head to the base of the caudal fin, and becomes progressively more distinctive (Fig. 27B).

Yellow xanthophores are best observed on a white background with incident illumination. They are found initially in association with iridophores and become widely distributed between melanophore stripes (Maderspacher and Nusslein-Volhard, 2003; Quigley et al., 2005). Owing to the difficulty of visualizing xanthophores, we do not describe their development in detail here.

Pigment Pattern: Fins

The pigment pattern of the caudal fin forms concomitant with fin outgrowth. A gap in the embryonic/early larval melanophore stripe along the ventral myotomes is evident where the caudal fin condensation of mesenchyme will appear (Fig. 11, 3.5 mm

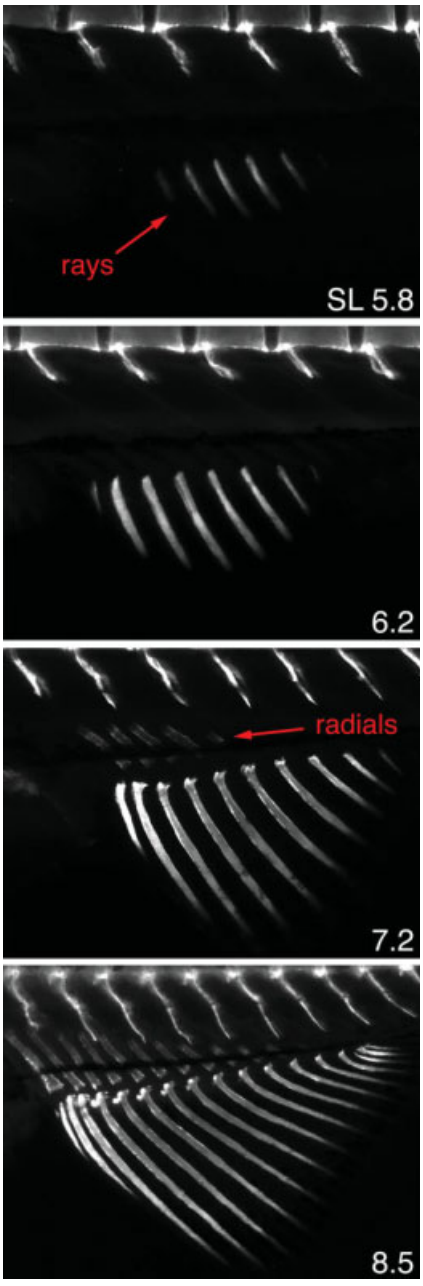

Fig. 18. Calcein staining reveals anal fin ray and radial ossification. Multiple individuals are shown (standard length [SL] at lower right).

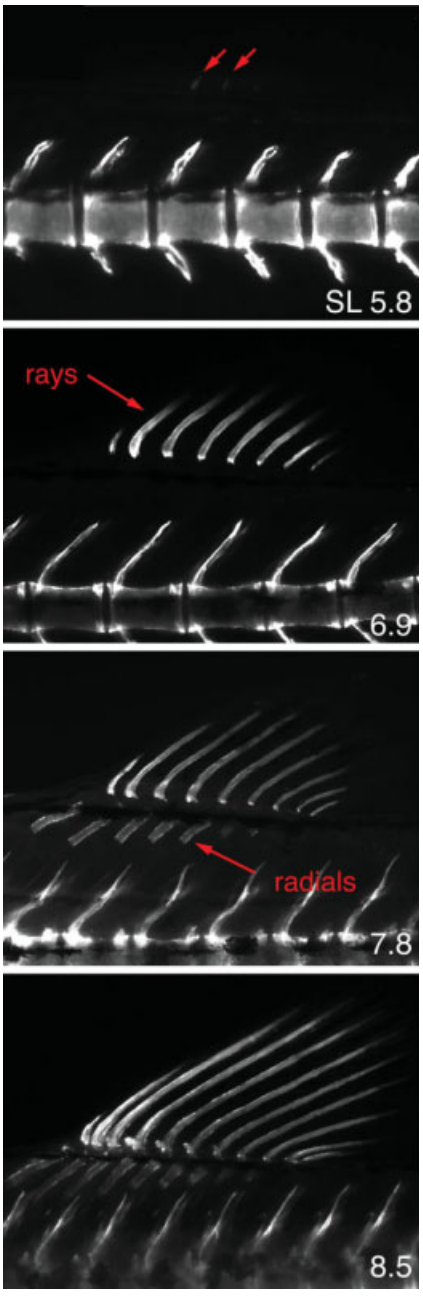

Fig. 19. Calcein staining reveals dorsal fin ray and radial ossification. Multiple individuals are shown (standard length [SL] at lower right). 5.8, arrows show initial ossification of rays.

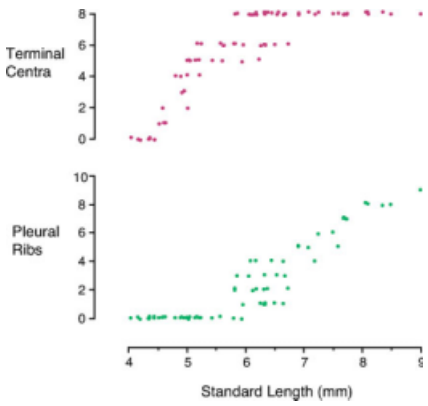

Fig. 20. Quantification of terminal centra and pleural rib ossification. Both are simple counts (see also legend of Fig. 14).

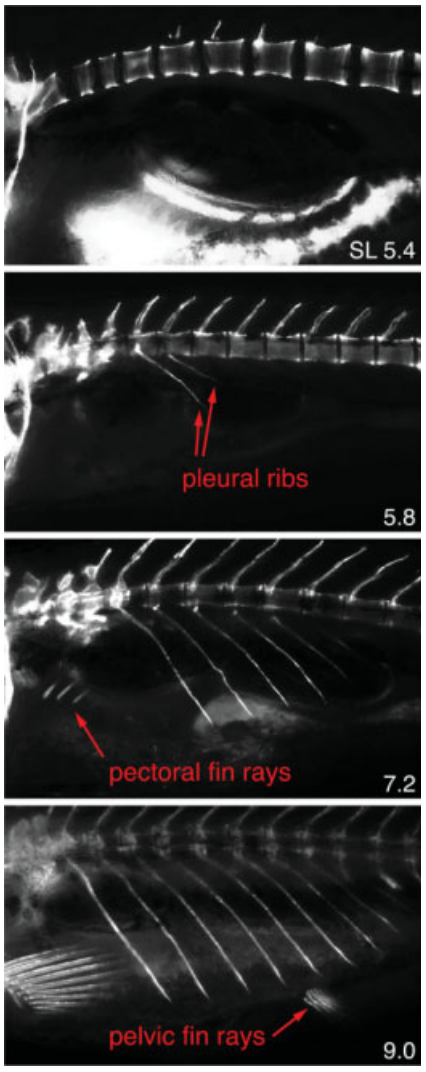

Fig. 21. Ossification of pleural ribs and pelvic fin rays revealed by calcein staining. Multiple individuals (standard length [SL] at lower right).

SL). As this condensation becomes more pronounced, a few melanophores occur over this region (Fig. 11, 4.5 mm SL) and, subsequently, additional melanophores cover the developing fin rays (Fig. 11, 5.6 mm SL). Faint xanthophores are seen shortly after melanophores with the two cell types initially interspersed (Fig. 13, 6.2 mm SL). Gradually xanthophores become more distinctive near the base of the dorsal and ventral lobes and melanophores are increasingly absent from these regions. At the base of the fin, melanophores become concentrated next to the posteriormost region of body stripe 1V, and this zone will develop the first caudal fin melanophore stripe (M1), flanked by the

first caudal fin xanthophore interstripe regions (X1d, X1v). Additional melanophore stripes develop adjacent to body stripes 1D and 2V with intervening xanthophore stripes, and iridophores appear within the xanthophore stripes. M1 becomes transiently offset from 1V (e.g., Fig. 13, 10.1 mm SL), although body and fin stripes later appear relatively continuous.

During anal fin development, a few melanophores are often observed over the early mesenchymal condensation (Fig. 16, 5.4 mm SL) and additional melanophores appear as the fin rays develop (Fig. 16, 6.7 mm SL; Fig. 17). With fin outgrowth, melanophores are present initially in the distal region. Xanthophores first arise in the posterior region of the fin and subsequently are found more widely and intermingled with melanophores. Gradually, a melanophore stripe (M1) near the base of the fin becomes distinctive, as well as a xanthophore stripe more distally (X1). As the fin grows additional stripes form, with interspersed melanophores and xanthophores persisting at the distal tip.

The dorsal fin exhibits melanophores as the first rays develop (Figs. 16, 17). Xanthophores appear shortly thereafter. In contrast to the caudal and anal fins, melanophores and xanthophores remain largely intermingled and stripes do not form.

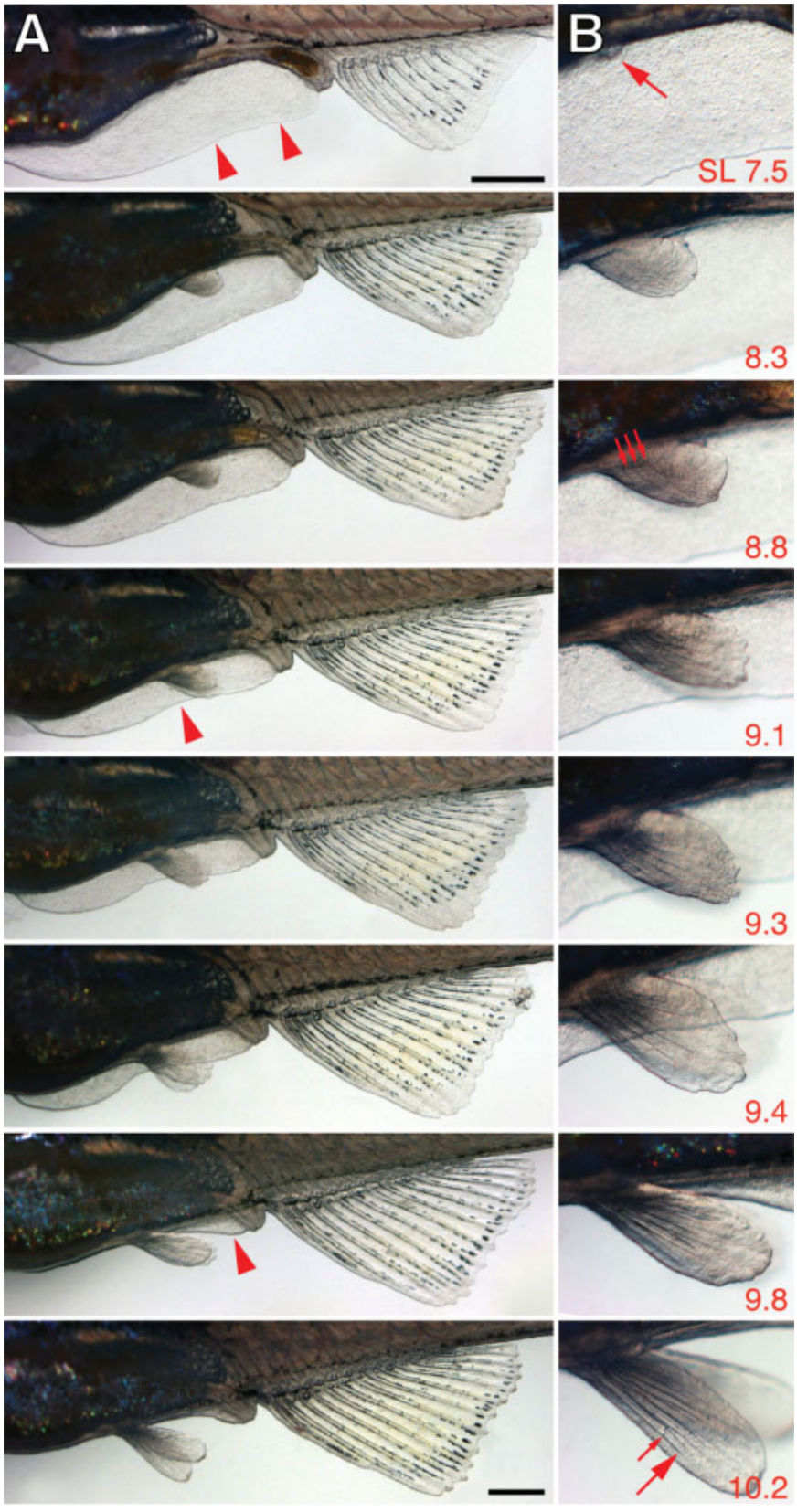

Lateral Line Sensory System

The lateral line sensory system undergoes several changes during postembryonic development (Ledent, 2002). This includes addition of new neuromasts and migration of existing neuromasts both to elaborate existing lateral lines and to form additional lateral lines (Fig. 28). During juvenile and

Fig. 22. Pelvic fin development and fin fold minor lobe regression. Shown is a single individual (standard length [SL] at lower right). **A**: Low magnification views showing minor fin fold (arrowheads), vent, and anal fin. Subtle resorption of the minor fin fold is first apparent in this individual at ~9.1 mm SL (arrowhead), and is clearly underway by 9.3 mm SL, when distal tips of the pelvic fins eclipse the edge of the fin fold; only small remnants of fin fold are present anterior to the vent at 9.8 mm SL (arrowhead) and 10.2 mm SL. **B**: Details of developing pelvic fin bud, first apparent in this individual at 7.5 mm SL (arrow). The bud extends from the body wall (8.3 mm SL), and three fin rays each comprising single developing segments are apparent by 8.8 mm SL (arrows). Second segments (large arrow) and the first joint between segments (small arrow) are clearly visible by 10.2 mm SL. Images shown are at decreasing magnifications. Scale bars = 7.5 and 10.2, 0.5 mm.

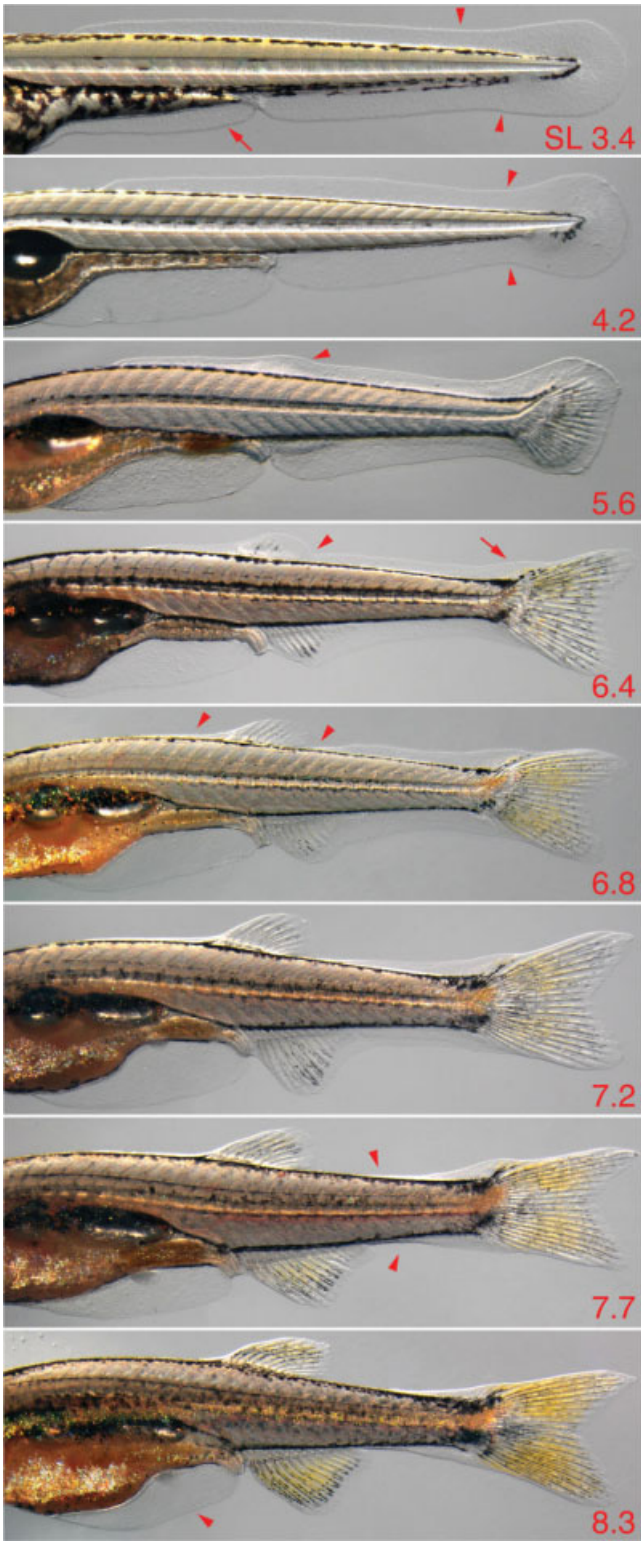

Fig. 23. Larval fin fold and fin fold resorption. Multiple individuals are shown (standard length [SL] at lower right). 3.4, Initial shapes of fin fold major lobe (arrowheads) and minor lobe (arrow); 4.2, a constriction is evident at the posterior tail (arrowhead); 5.6, a bulge is evident in the dorsal fin fold above the dorsal fin mesenchymal condensation (arrowhead); 6.4, a notch posterior to the dorsal fin indicates early fin fold resorption (arrowhead) and a bulge is evident over the developing supranotochordal fin rays (arrow); 6.8, resorption continues both anterior and posterior to the dorsal fin (arrowheads); 7.7, resorption occurs in an increasingly posterior zone along the tail (arrowheads); 8.3, early resorption of the minor lobe is revealed by flattening of its ventral posterior margin (arrowhead; also see Fig. 22).

adult development, clusters of neuromasts arise to form stitches.

DEVELOPMENTAL MILESTONES RELATED TO SIZE

The preceding review of several traits suggests milestones for indicating developmental progress. To relate these milestones to size, we used two complementary approaches.

First, we used larvae reared individually and imaged throughout development to determine, retrospectively, the average size of individuals immediately before and immediately after the milestone in question: we determined SL and HAA the day before the developmental transition, and then also on the first day after the transition was observed. These "longitudinal" measurements, therefore, bracket the sizes at which developmental milestones occurred.

Second, we imaged individuals from groups of fish reared at a range of densities and food availabilities and determined both size and whether or not specific milestones had been reached. To determine when milestones occurred, we treated each developmental transition as an ordinal variable in multiple logistic regression analyses. We used the resulting regression coefficients to estimate the sizes at which 50% of individuals were either "above" or "below" the milestone in question. These "cross-sectional" measurements, therefore, provide estimates of the sizes at which milestones occurred in groups of fish under a range of conditions.

Major developmental milestones are presented in Table 4, which provides sizes in SL as well as HAA (for values of HAA $>$ 0.5 mm, where this measure is linear; Fig. 4). Example images of fish that have recently achieved these milestones are provided below (see section: **REFERENCE INDIVIDUALS**). Milestones are based on traits that are readily discernible in living fish under brightfield or transmitted illumination. Size estimates for developmental transitions are in close agreement between longitudinal and cross-sectional datasets.

The milestones in Table 4 span a wide range of development. The first milestone, inflation of the posterior

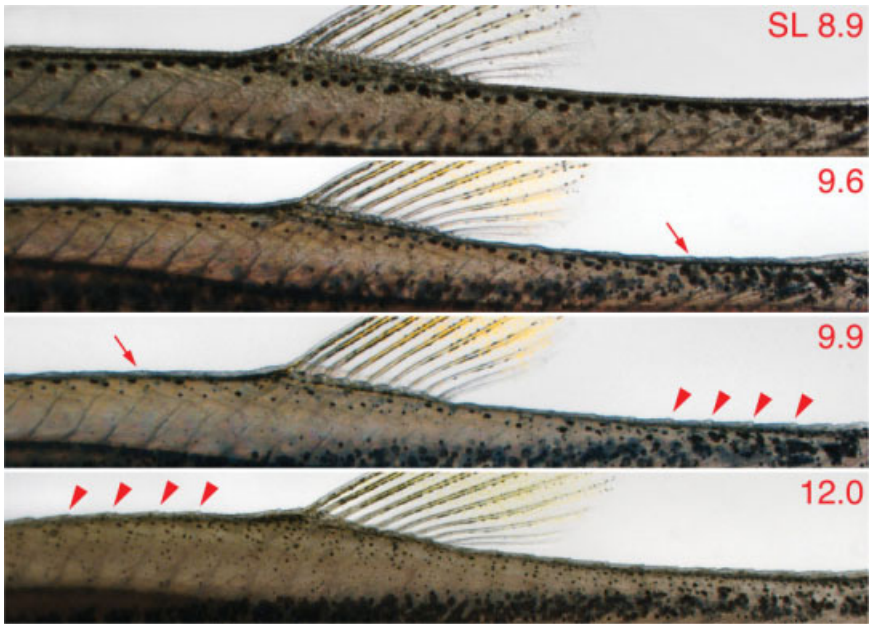

Fig. 24. Scale development revealed by transmitted illumination. A single individual is shown (standard length [SL] at upper right). 8.9, An initially smooth dorsum. 9.6, onset of posterior squamation is indicated by the appearance of raised ridges (arrow); 9.9, scales are well-formed posteriorly (arrowheads) and are starting to develop anteriorly (arrow); 12.0, scales are completed anteriorly (arrowheads).

swim bladder (pSB), occurs shortly after hatching and results in "float-up." The last milestone, completion of squamation, is used here to define onset of the juvenile period. These milestones represent a starting point for staging of postembryonic zebrafish (below).

A limitation to these milestones is their uneven distribution across sizes, suggesting they may not provide sufficient indication of developmental progress for some studies. For example, we were able to identify four readily discernible transitions between 5–6 mm SL, although some of these occur so close to simultaneously that they may not offer additional resolution and in some individuals reversals of order can be observed (e.g., aSB vs. MMA). We also identified two milestones each between 4 and 5 mm SL and 6 and 7 mm SL, but only one each for other 1-mm intervals of SL. Further analyses will be needed to reveal

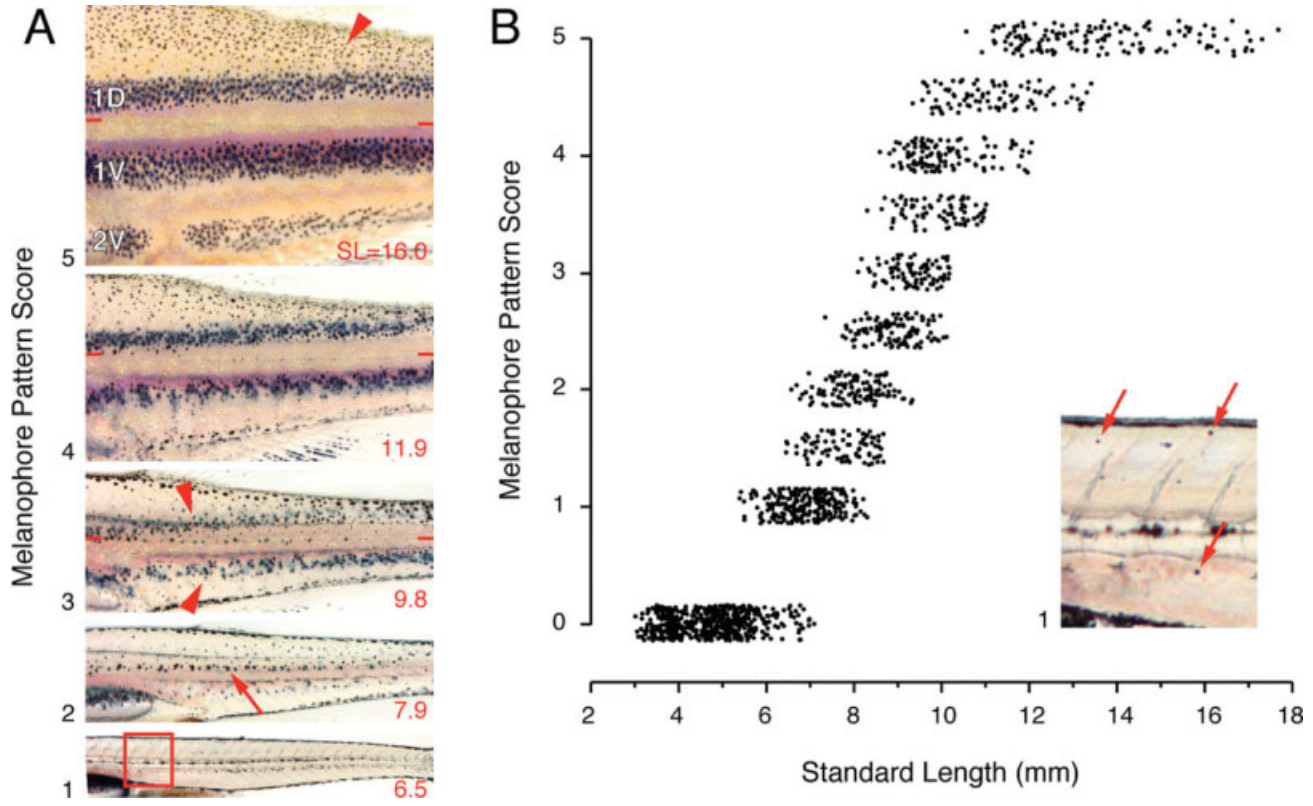

Fig. 25. Body melanophore pattern. **A**: Pigment pattern metamorphosis in a single individual (standard length [SL] at lower right) with qualitative scores assigned to each melanophore pattern state adjacent at lower left. Development is bottom-to-top, matching the plot in B. 1, At the onset of pigment pattern metamorphosis, a few metamorphic melanophores are scattered over the myotomes (boxed region shown at higher magnification in panel B, with metamorphic melanophores marked by arrows). 2, metamorphic melanophores are widely scattered over the flank, with residual embryonic/early larval melanophores at the horizontal myoseptum (arrow). 3, Adult melanophore stripes begin to be apparent (arrowheads) bordering an increasingly melanophore-free interstripe. Horizontal bars indicate the horizontal myoseptum. 4, Stripes are increasingly distinct as gaps are filled. 5, A juvenile pigment pattern comprising the first two primary adult stripes (1D, 1V) and a first secondary stripe (2V), as well as melanophores covering the dorsum and scales (arrowhead). **B**: Relationship between melanophore pattern and SL. Fish were placed into the classes represented by panels in A, or intermediate to these classes. Points are jittered vertically for clarity.

discrete, externally visible transitions that occur within these latter size ranges, if they exist.

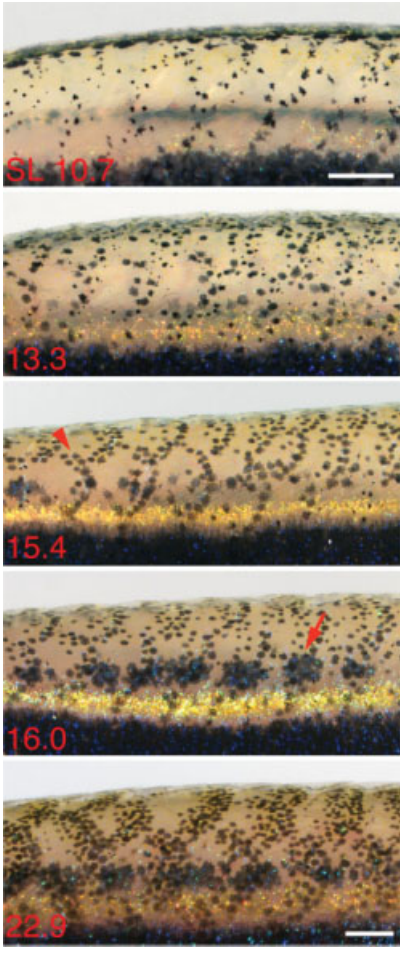

The major milestone following the juvenile period is attainment of sexual maturity, at which point fish can be considered adults. Sexual maturity is marked by the production of viable gametes as well as secondary sexual characteristics in fish that are in breeding condition, including a ventral yellowish tinge in males and a distended abdomen in gravid females. For males, these characteristics were apparent as early as 17.5 ± 0.6 mm SL, 3.64 ± 0.21 mm HAA; and for females: 18.3 ± 0.7 mm SL, 3.95 ± 0.12 mm HAA (means ± 95% confidence intervals).

GROWTH AND ENVIRONMENTAL EFFECTS

The paucity of discrete staging criteria during postembryonic development as compared with embryogenesis has prompted the use of size-based measures for indicating developmental progress in other fishes (Fuiman et al., 1998). If quantitative measures of size are to be used, relationships between size and development of other traits should be constant across temperatures and growth rates.

To test the constancy of size-based developmental relationships with temperatures and growth rates, we reared larvae in all combinations of three temperatures (24°C, 28.5°C, 33°C) and three growth conditions, constituting different larval densities (low, medium, high) with a single food level across conditions, thereby resulting in different food availabilities per capita. As intended, these different rearing conditions resulted in significantly different growth rates. For example, fish reared at 24°C grew more slowly than fish reared at 33°C (SL mm per day, mean ± SE: 0.45 ± 0.009, 0.54 ± 0.011, respectively; $F_{2,762} = 53.6$; $P < 0.0001$). Likewise fish reared at high density grew more slowly than fish reared at low density (SL mm per day, mean ± SE: 0.48 ± 0.006, 0.55 ± 0.006; $F_{2,762} = 40.9$; $P < 0.0001$). We then examined relationships between size and developmental states of several traits (swim bladder lobes; fin bud and fin ray appearance; scale development; melanophore pattern score). This allowed us to test if the likelihood of fish exhibiting particular states of each trait depended not only on size, but also temperature, density, or interactions among these variables.

Fig. 26. Development of melanophore pattern on scales. Shown are multiple individuals (standard length [SL] at lower left). Melanophores are organized along the outlines of scales initially (10.7) and are subsequently found along the distal edge of each scale (15.4, arrowhead). The body melanophore stripe 2D (16.0, arrow) appears beneath the scales. Images shown are at decreasing magnifications. Scale bars = 10.7 and 22.9, 0.5 mm.

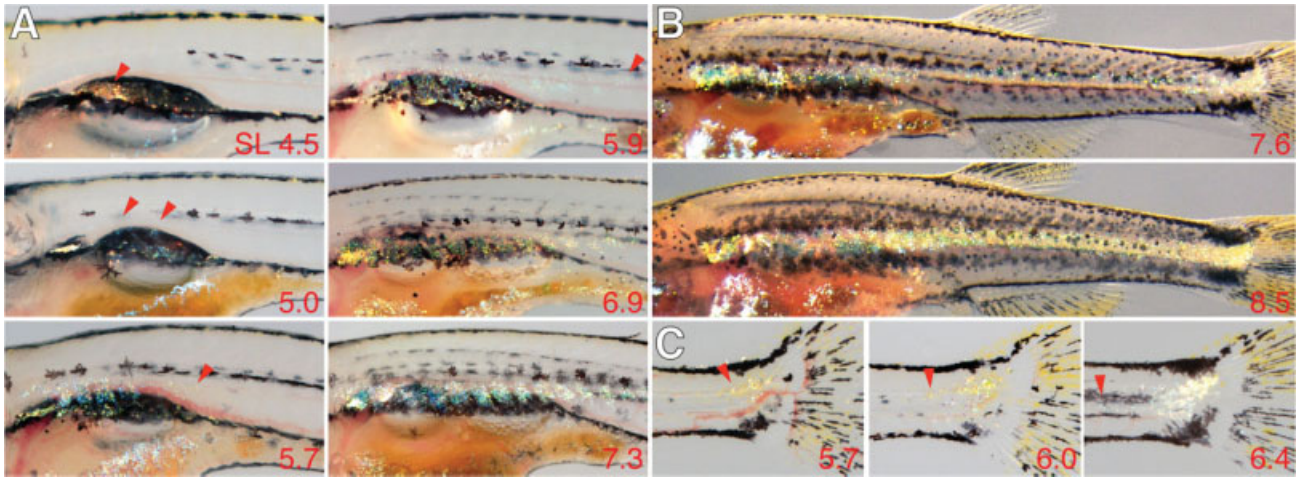

Fig. 27. Development of iridophore pattern. Shown are multiple individuals (standard length [SL] at lower right). **A**: Development of iridophores in the nascent interstripe of the anterior trunk. 4.5, iridophores are first present only internally, covering the swim bladder (arrowhead). 5.0, iridophores immediately under the skin first arise near the swim bladder, over the ventral–lateral surfaces of a few myotomes. 5.7–7.3, the initial patch spreads more posteriorly (arrowheads indicate posteriormost reflective cells). **B**: A continuous iridophore interstripe is formed as cells in the anterior become contiguous with a patch at the base of the tail. **C**: Development of iridophore patch near the site of notochord flexion (anteriormost reflecting cells indicated by arrowheads).

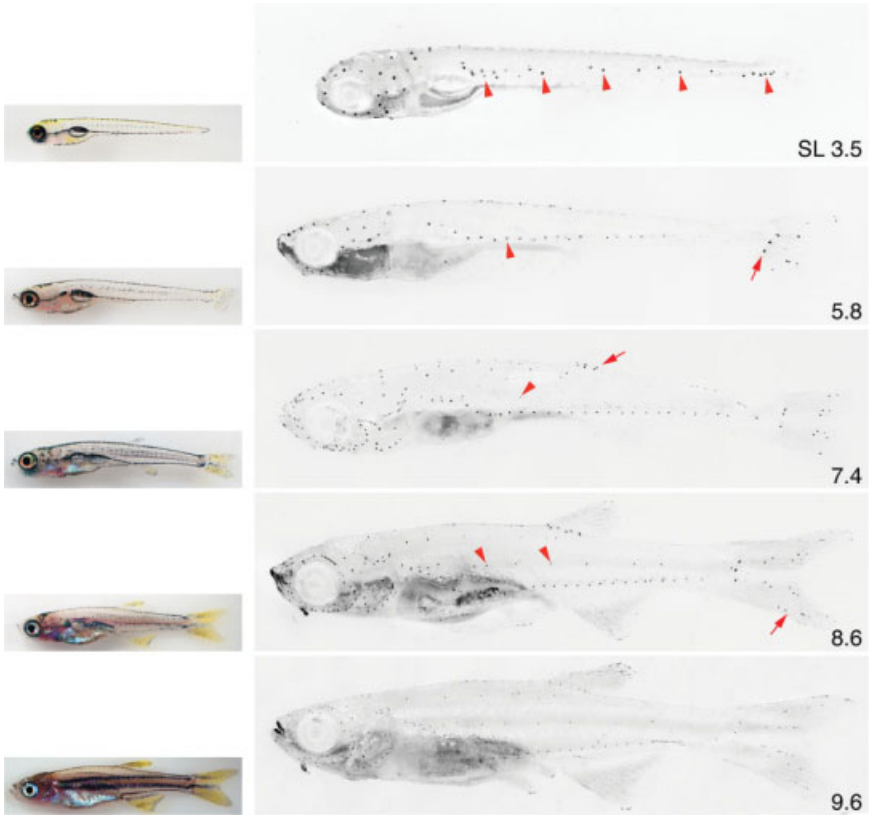

Fig. 28. Lateral line development revealed by labeling with vital fluorescent dye FM1-43. Shown are multiple individuals in brightfield (left) and inverted epifluorescence (right; standard length [SL] at lower right). 3.5, Neuromasts of the posterior lateral line (arrowheads), with a cluster near the base of the tail; additional neuromasts are visible on the contralateral side. 5.8, Additional neuromasts have arisen between pre-existing neuromasts of the main lateral (L) line (arrowhead) whereas caudal neuromasts are found in an increasingly vertical line at the base of the caudal fin (arrow). 7.4, Neuromasts are apparent within the secondary lateral (L′) line (arrowhead) and at the base of the dorsal fin (arrow). 8.6, Additional neuromasts are seen in the secondary lateral (L′) line (arrowheads) and on the caudal fin itself (arrow).

Multiple logistic regression analyses showed that, as expected, size (measured as SL or HAA) had the highest correlation with developmental progress for all traits examined (Table 5; all $R^2 > 0.5$). Additionally, even after controlling for size, we found significant effects of temperature (all traits: $0.001 < P < 0.05$) and in some instances effects of density as well as interactions between either size and temperature or size and density. These latter interactions are potentially important because they indicate that relationships between size and developmental progress vary among temperatures and growth rates (as modified by rearing densities). Such interactions are not unexpected and have been reported in other contexts for wild-type fish of other species (Klimogianni et al., 2004; Martell et al., 2005; Georgakopoulou et al., 2007), zebrafish mutants (Parichy and Turner, 2003), and amphibian larvae (Parichy and Kaplan, 1995).

Interactions between size and growth rate or rearing condition were most pronounced for late-arising traits. In pelvic fin transitions for example, as compared to larvae reared at 28.5°C, larvae reared at 24°C underwent transitions at slightly larger sizes, whereas larvae reared at 33°C underwent these transitions over a wider range of sizes (Fig. 29). Melanophore pattern transitions also differed between temperatures and densities (Fig. 30). Compared with larvae at 28.5°C, those reared at 24°C underwent transitions at slightly larger sizes. Moreover, compared with larvae at medium density, those at low density (that grew more rapidly) underwent transitions at larger sizes, whereas those at high density (that grew more slowly) underwent transitions at smaller sizes.

Many effects of temperature, density, and interactions with size were highly statistically significant, likely reflecting the large sample sizes that we used ($N = 782$). To assess the biological significance of these effects, we calculated coefficients of determination to estimate the proportions of variance explained by different factors. This showed that temperature, density, and their interactions with size explained very little additional variance after controlling for the main effect of size (all $R^2 < 0.05$; Table 5). Relationships between SL and HAA also differed between conditions, but these effects were of similarly low magnitude (Table 5). These findings indicate that, for quantifying developmental progress in zebrafish, relationships between SL or HAA and other traits are relatively, although not completely, independent of temperature and growth rate (as modulated by rearing density). This result is evident as well in the close similarity of size estimates for developmental transitions shown in Table 4. The longitudinal dataset presents values for larvae reared individually, whereas the cross-sectional dataset presents values for larvae reared at the range of temperatures and densities described here and analyzed in Table 5. Even though individually reared larvae that were repeatedly anesthetized grew slowly (SL mm per day mean ± SE: 0.32 ± 0.004; Fig. 3) the size-based estimates of developmental milestones were remarkably similar between datasets, and typically within 5% of one another.

Together, these data suggest that for most purposes, size should be a relatively robust indicator of developmental progress. Nevertheless, precise effects of growth rate on particular traits and organ systems should be evaluated on a case-by-case basis, and the conclusions presented here assume that larvae are not growing so slowly as to be unhealthy or at greater risk of mortality, as occurs under particularly adverse conditions. In general, poor growth conditions will typically generate increased

TABLE 4. Milestones in Postembryonic Zebrafish Development[a]

Milestone				Longitudinal[b]				Cross-sectional[c]	
Abbrev.	Description	Figure	SSL	SL_{pre}	SL_{post}	HAA_{pre}	HAA_{post}	$SL_{P=0.5}$	$HAA_{P=0.5}$
pSB	Swim bladder (pSB) inflation	33	3.5	3.4 ± 0.1	3.7 ± 0.1	—	—	n.d.	—
FLe	Early flexion 0<25°	35	4.5	4.4 ± 0.2	4.7 ± 0.1	—	—	n.d.	—
CR	C fin ray appearance	36	4.9	4.9 ± 0.1	5.1 ± 0.1	—	—	4.9 ± 0.2	—
AC	A fin condensation	37	5.4	5.2 ± 0.2	5.5 ± 0.2	—	—	5.4 ± 0.1	—
DC	D fin condensation	38	5.7	5.5 ± 0.2	5.8 ± 0.1	—	—	5.8 ± 0.1	—
MMA	Metamorphic melanophore appearance	40	5.9	5.9 ± 0.2	6.3 ± 0.2	0.52 ± 0.03	0.58 ± 0.03	6.0 ± 0.1	0.51 ± 0.02
aSB	aSB appearance	41	6.0	5.9 ± 0.1	6.2 ± 0.1	—	—	6.0 ± 0.1	—
AR	A fin ray appearance	43	6.2	6.3 ± 0.1	6.4 ± 0.2	0.53 ± 0.02	0.56 ± 0.02	6.1 ± 0.1	0.51 ± 0.01
DR	D fin ray appearance	45	6.4	6.5 ± 0.1	6.6 ± 0.1	0.58 ± 0.02	0.62 ± 0.03	6.4 ± 0.1	0.58 ± 0.02
PB	P fin bud appearance	47	7.2	7.2 ± 0.1	7.5 ± 0.1	0.78 ± 0.02	0.85 ± 0.03	7.4 ± 0.1	0.83 ± 0.04
PR	P fin ray appearance	49	8.6	8.5 ± 0.1	8.7 ± 0.1	1.16 ± 0.03	1.22 ± 0.03	8.6 ± 0.2	1.18 ± 0.03
SP	Squamation onset posterior	51	9.6	9.5 ± 0.2	9.6 ± 0.2	1.43 ± 0.05	1.48 ± 0.05	n.d.	n.d.
SA	Squamation through anterior	52	10.4	10.1 ± 0.2	10.4 ± 0.2	1.67 ± 0.05	1.73 ± 0.06	n.d.	n.d.
J	Juvenile (squamation completed)	53	11.0	11.3 ± 0.4	11.7 ± 0.3	2.02 ± 0.11	2.11 ± 0.07	10.9 ± 0.3	1.77 ± 0.06

[a]SSL, standardized standard length (see text for details); SL, standard length; HAA, height at anterior of anal fin; n.d., Not determined in this dataset. Dashes indicate not estimated.

[b]Longitudinal measures indicate mean sizes (±95% confidence intervals) immediately before the developmental milestone was evident (pre), and immediately after it was first apparent (post). All sizes are given in mm.

[c]Cross-sectional measures indicate the mean sizes (±95% confidence intervals) at which 50% of individuals are predicted to have made the transition to the developmental milestone indicated.[d]SSL: standardized standard length. See text for details.

variation in the sizes of larvae within tanks, as small differences in initial growth are magnified by larger individuals increasingly monopolizing resources and interfering behaviorally with smaller individuals (Brown, 1957; Ricker, 1958; Eaton and Farley, 1974; Ward et al., 2006). This phenomenon occurs in wild-type stocks and is observed across a wide variety of species and conditions. Differential growth rates and abilities also can complicate the recovery and propagation of mutants having postembryonic phenotypes. Therefore, asymmetric size distributions within tanks of wild-type fish are likely to indicate poor growth conditions that should be further optimized, whereas stocks segregating postembryonic mutant phenotypes should be sorted regularly to isolate such mutants, so as to prevent their loss due to competition from wild-type siblings.

POST HOC SIZE ESTIMATION

A limitation to using size as a proxy for developmental states arises when it is difficult or impossible to measure size before performing an experiment. For example, postembryonic fish are prone to exhibiting size variability even within tanks, yet it can be tedious or impractical to measure fish before histological analyses. We, therefore, asked how larval size and shape are affected by two frequently used histological procedures: paraformaldehyde fixation and whole-mount in situ hybridization.

Figure 31 shows relationships between pre- and postprocessing values of SL and HAA, and the linear or near-linear shrinkage observed suggests that post hoc estimates of size should be a useful substitute for prior measurements, so long as appropriate calibrations have been determined. For example, a larva of ~6 mm SL postprocessing corresponds to a larva of ~9 mm SL preprocessing, for the in situ hybridization protocol used here. Table 3 provides relationships allowing the estimation of initial SL and HAA from measurements that have been taken after histological preparation.

TABLE 5. Developmental Correlates of Size and Effects of Temperature and Growth Rate as Modulated by Density (See Text for Details)[a]

	Independent variable[b]													
	Size (SL or HAA)			Temperature			Temp x Size			Density			Density x Size		
Dependent Variable	X^2	P	R^2	X^2	P	R^2	X^2	P	R^2	X^2	P	R^2	X^2	P	R^2
SL vs.															
Swim bladder	349	<0.0001	**0.77**	8	<0.05	0.02	11	<0.005	0.01	NS	NS	—	NS	NS	—
Caudal fin	223	<0.0001	**0.64**	9	<0.05	0.02	—	—	—	NS	NS	—	NS	NS	—
Anal fin	745	<0.0001	**0.78**	21	<0.0001	0.02	NS	NS	—	NS	NS	—	NS	NS	—
Dorsal fin	501	<0.0001	**0.69**	7	<0.05	0.02	14	<0.005	0.01	NS	NS	—	NS	NS	—
Pelvic fin	539	<0.0001	**0.62**	25	<0.0001	0.03	12	<0.005	0.01	24	<0.0001	0.02	NS	NS	—
Squamation	106	<0.0001	**0.74**	16	<0.0005	0.04	13	<0.005	0.03	7	<0.05	0.02	NS	NS	—
Melanophore pattern	568	<0.0001	**0.50**	68	<0.0001	0.02	7	<0.05	0.005	72	<0.0001	0.02	80	<0.0001	0.03
HAA vs.															
Swim bladder	339	<0.0001	**0.69**	7	<0.05	0.02	7	<0.05	0.01	NS	NS	—	NS	NS	—
Caudal fin	214	<0.0001	**0.60**	12	<0.005	0.03	—	—	—	NS	NS	—	NS	NS	—
Anal fin	700	<0.0001	**0.74**	18	<0.0005	0.02	NS	NS	—	NS	NS	—	NS	NS	—
Dorsal fin	195	<0.0001	**0.67**	13	<0.005	0.01	15	<0.001	0.01	7	<0.05	<0.01	8	<0.05	0.01
Pelvic fin	522	<0.0001	**0.59**	29	<0.0001	0.04	22	<0.0001	0.02	21	<0.001	0.01	NS	NS	—
Squamation	96	<0.0001	**0.73**	13	<0.005	0.03	11	<0.005	0.02	9	<0.01	0.02	NS	NS	—
Melanophore pattern	545	<0.0001	**0.50**	8	<0.0001	<0.01	501	0.07	<0.01	75	<0.0001	0.02	73	<0.0001	0.02
	SL			Temperature			Temp x Size			Density			Density x Size		
	$F_{1,771}$	P	R^2	$F_{2,771}$	P	R^2	$F_{2,771}$	P	R^2	$F_{2,771}$	P	R^2	$F_{2,771}$	P	R^2
HAA	4437	<0.0001	**0.98**	123	<0.0001	0.001	4.9	<0.01	<0.001	4.5	<0.05	<0.001	14	<0.0001	<0.001

[a]SL, standard length; HAA, height at anterior of anal fin; NS, Not significant, $P>0.05$; dashes indicate not determinable owing to insufficient replicates across treatment.
[b]Size, d.f. = 1; Temperature, d.f. = 2, Temperature x Size, d.f. = 2; Density, d.f. = 2; Density x Size, d.f. = 2. Total sample size, $N = 782$ larvae.

REFERENCE INDIVIDUALS FOR DEVELOPMENTAL MILESTONES IN RELATION TO SIZE

Here, we present a series of individual fish that have reached particular developmental milestones, or exhibit developmental states intermediate to named milestones. Different views and magnifications are provided to facilitate comparisons among traits. In each figure is provided abbreviations of milestones at the lower left and a "standardized standard length" (SSL; see STAGE REPORTING CONSIDERATIONS AND RECOMMENDED CONVENTIONS Section) at the lower right. We provide brief descriptions below; developmental states for additional traits can be inferred by referring to the preceding sections.

Pec-fin Stage (3.4 mm SL onset)

Figure 32: For comparison with postembryonic stages, we include here the *pec fin* stage, which begins ~60 hpf at 28.5°C and corresponds to the late embryonic period (Kimmel et al., 1995). The pectoral fin exhibits a flat blade distally and is held along the side of the body; the mouth is open ventrally (not shown). Melanophores are well melanized and form stripes at the dorsal and ventral myotomes, except ventroposteriorly where the caudal fin condensation will arise. Melanophores remain scattered over the yolk sac. Xanthophores are yellowish throughout the body.

pSB, Swim Bladder Inflation (3.4–3.7 mm SL onset)

Figures 33, 34: The posterior (first) lobe of the swim bladder inflates, resulting in "float-up". The open mouth protrudes anteriorly, and the gut is more clearly visible beneath the swim bladder. An embryonic/early larval pigment pattern is complete, with melanophores in stripes over the dorsal and ventral myotomes, over the dorsal and ventral surfaces of the yolk sac, and along the horizontal myoseptum; melanophores are no longer dispersed over the yolk sac. Patches of iridophores are visible internally over

the swim bladder. The fin fold lobes extend further from the body.

FLe, Early Flexion (4.4–4.7 mm SL onset)

Figure 35: Notochord flexion has begun (0 < 25°C). A condensation of mesenchyme is seen ventroposteriorly where the caudal fin will develop and a few melanophores lie over it. The gut lumen is increasingly visible. The mouth and anterior head protrude further anteriorly. Larvae begin to feed.

CR, Caudal Fin Ray Appearance (4.9–5.1 mm SL onset)

Figure 36: Caudal fin rays are apparent and melanophores are scattered amongst them. Xanthophore coloration on the body is faded. Subtle constrictions in the major lobe of the fin fold are apparent dorsally and it is less symmetrical posteriorly over the tail. The mouth is located terminally and larvae are feeding actively.

AC, Anal Fin Condensation (5.2–5.5 mm SL onset)

Figure 37: A mesenchymal condensation is visible posterior to the vent where the anal fin will develop. A slight bulge may be present in the dorsal fin fold where the dorsal fin condensation will arise. The distal end of the larval fin fold is relatively rounded over the developing caudal fin.

DC, Dorsal Fin Condensation (5.5–5.8 mm SL onset)

Figures 38, 39: Condensed mesenchyme is present dorsally where the dorsal fin will form; the dorsal major lobe of the fin fold rises up above this site. The anal fin condensation is more pronounced. The caudal fin is flattened posteriorly; the dorsal region extends further posteriorly than the ventral region. Caudal fin ray number changes rapidly at this time. Melanophores are dispersed through the caudal fin and the first xanthophores are apparent. A patch of iridophores is visible on the flank adjacent to the swim bladder. The head exhibits an indentation dorsally, just above the eye, at the level of the pineal gland.

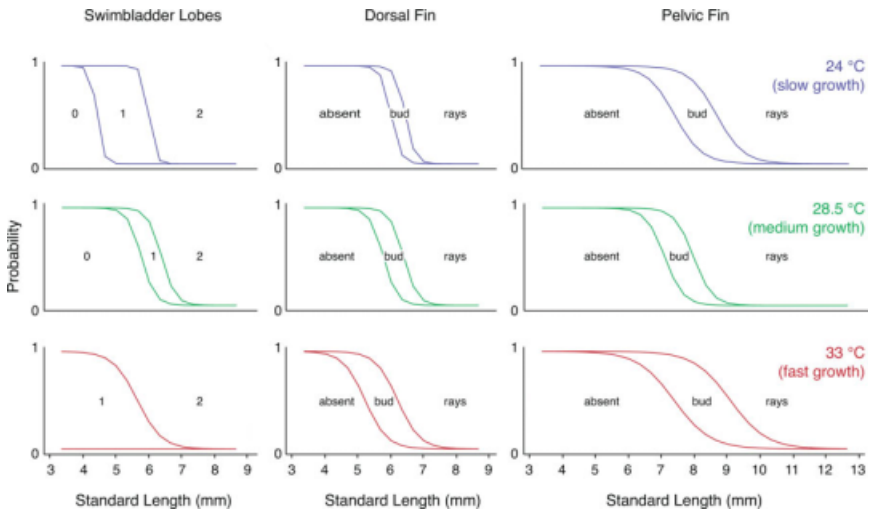

Fig. 29. Rearing temperature has subtle effects on the relationship between standard length (SL) and other traits. Shown are prediction plots from multiple logistic regressions for transitions in swim bladder, dorsal fin, and pelvic fin development. Probabilities indicate the likelihood that an individual of a particular SL will exhibit a particular developmental state, depending on rearing temperature. Trait-specific states are indicated within each plot.

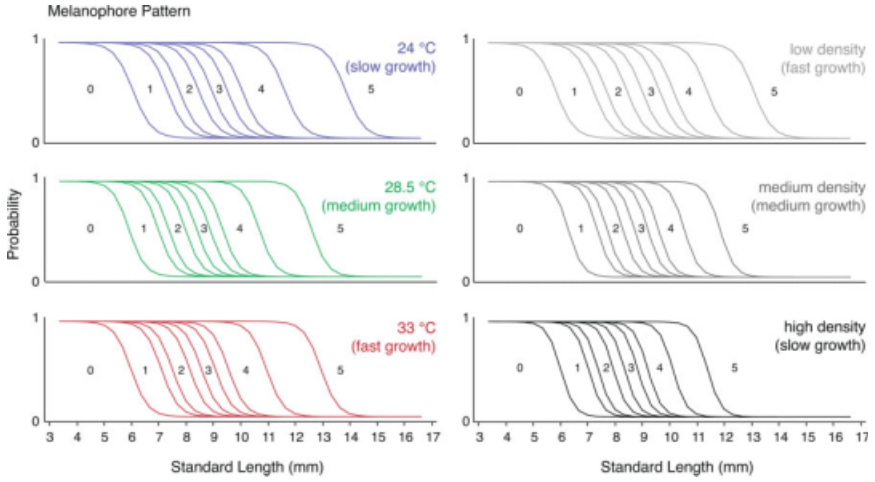

Fig. 30. Temperature and rearing density affect transitions in melanophore pattern. See Figure 29 legend and text for additional details.

MMA, Metamorphic Melanophore Appearance (5.9–6.3 mm SL onset)

Figure 40: The first metamorphic melanophores arise over the dorsolateral or ventrolateral myotomes, as single lightly melanized cells that are well separated from the embryonic/early larval melanophore stripes. The dorsal fin condensation is more pronounced and developing radials are visible in the ventral fin condensation.

aSB, Anterior Swim Bladder Appearance (5.9–6.2 mm SL onset)

Figures 41, 42: The anterior (second) swim bladder lobe appears. Timing and extent of inflation is rather variable; when very small, the lobe may be partially obscured by overlying pigment

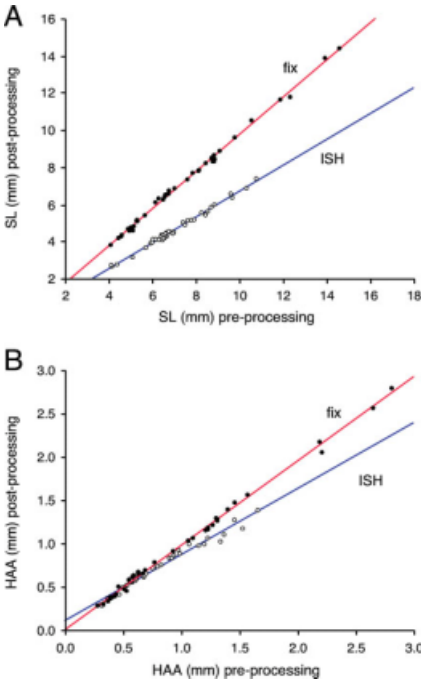

Fig. 31. Effect of histological processing on SL (standard length; upper plot) and height at anterior of anal fin (HAA; lower plot). Fish were either fixed or mock-processed for in situ hybridization (ISH). Regressions reported in Table 3.

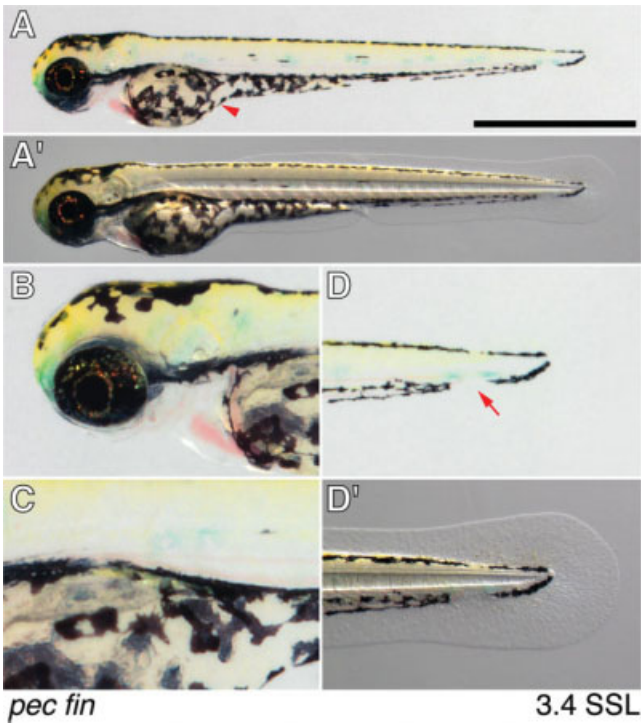

Fig. 32. Embryonic *pec fin* stage of Kimmel et al. (1995); 3.4 mm SL (standard length). **A,A′**: Whole body. Arrowhead, melanophores covering yolk ball. Scale bar = 1 mm. **B**: Head. **C**: Swim bladder, not yet inflated. **C′**: Tail. Arrow, gap in melanonophore pattern corresponding to region of caudal fin condensation.

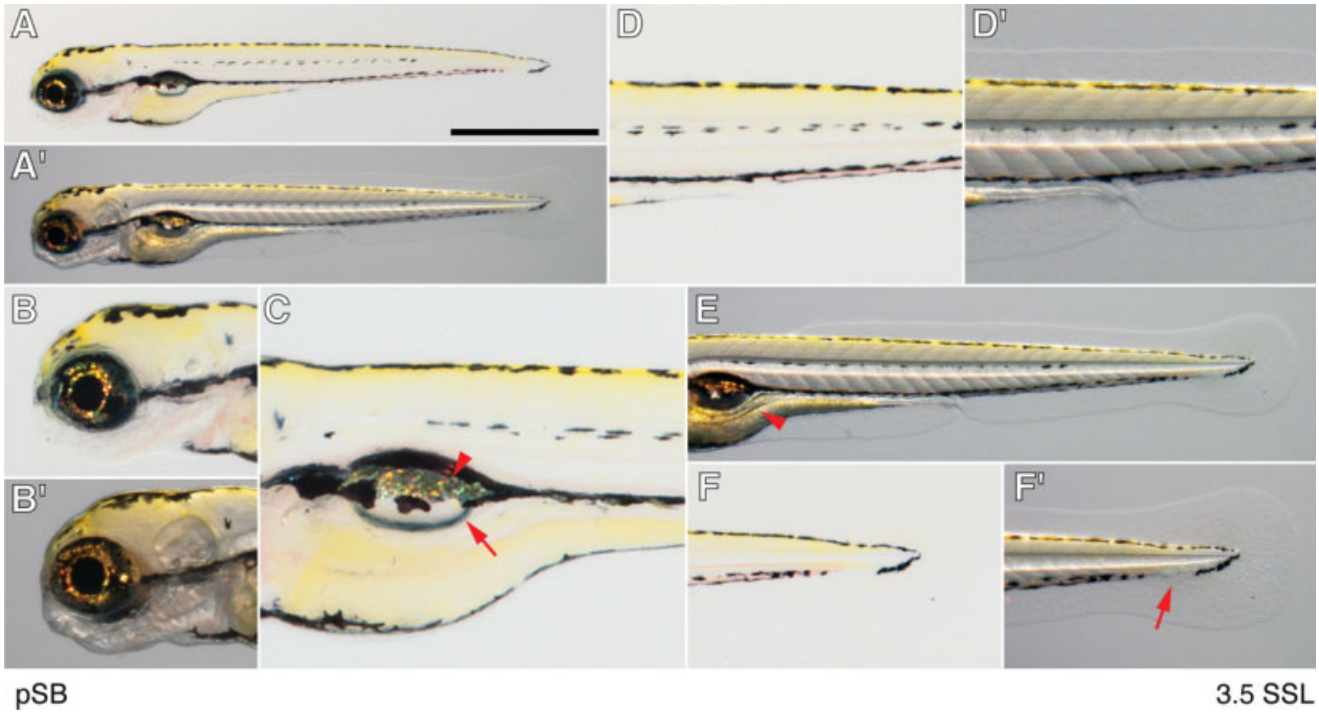

Fig. 33. Inflation of posterior swim bladder lobe; pSB, 3.5 mm SL (standard length). **A,A′**: Whole body. Scale bar = 1 mm. **B,B′**: Head. **C**: Anterior trunk showing inflated swim bladder (arrow) and covering iridophore patch (arrowhead). **D,D′**: Posterior trunk showing definitive early larval melanophore and xanthophore pattern. **E**: Caudal region, highlighting complete fin fold. Arrowhead, gut. **F,F′**: Posterior tail. Arrow, caudal fin condensation and gap in melanophore stripe.

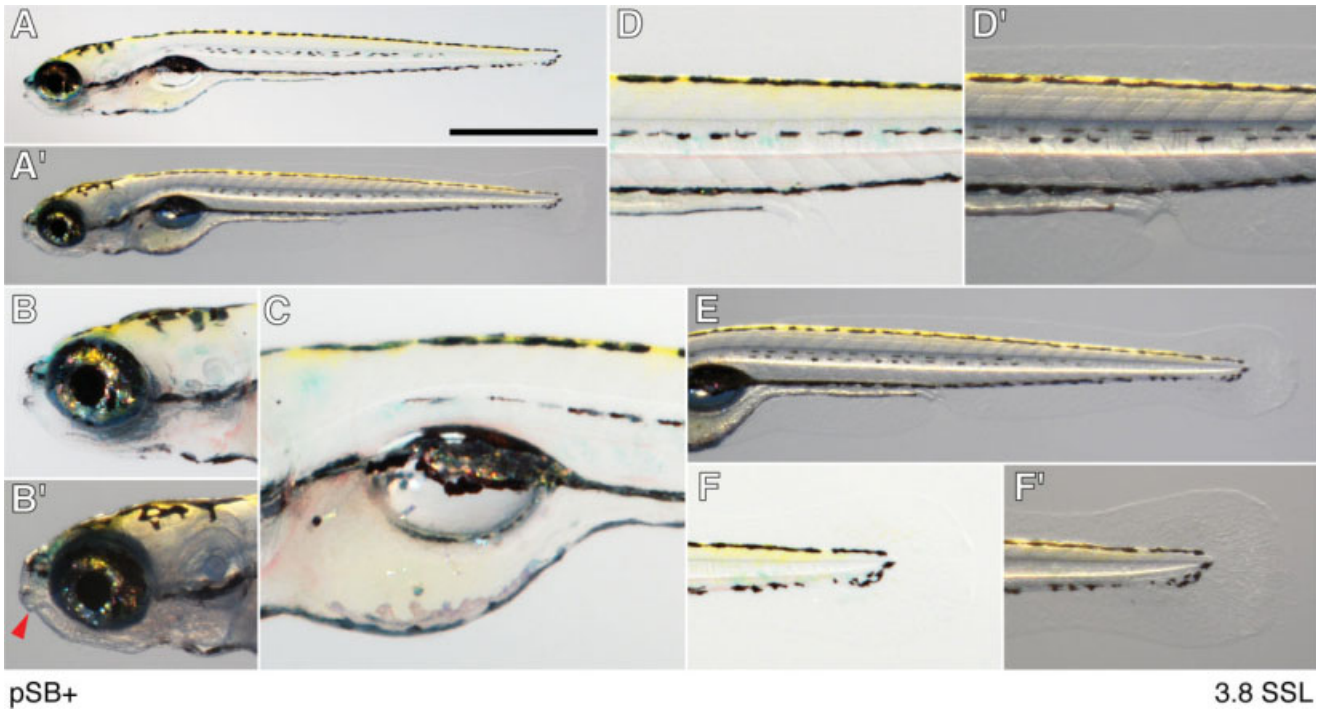

Fig. 34. Following inflation of posterior swim bladder lobe; pSB+, 3.8 mm SL (standard length). **A,A′**: Whole body. Scale bar = 1 mm. **B,B′**: Head showing more anterior mouth position (arrowhead). **C**: Anterior trunk. **D,D′**: Posterior trunk. **E**: Caudal region. **F,F′**: Posterior tail.

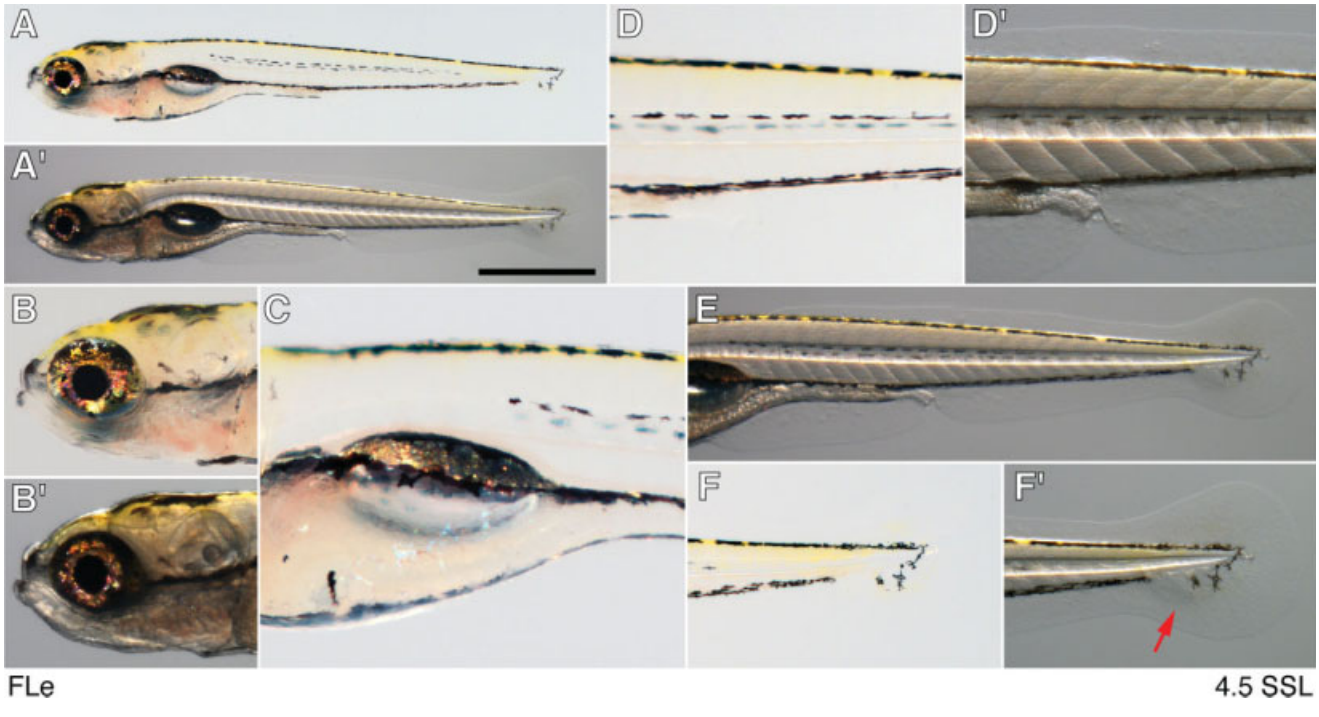

Fig. 35. Early flexion; FLe, 4.5 mm SL (standard length). **A,A′**: Whole body. Scale bar = 1 mm. **B,B′**: Head. **C**: Anterior trunk showing swim bladder. **D,D′**: Posterior trunk and pigment pattern. **E**: Caudal region. **F,F′**: Posterior tail. Arrow, caudal fin condensation is increasingly pronounced.

cells. The caudal fin has nearly the maximal number of rays (~20) and retains a mostly flat posterior region though the first indication of a cleft between dorsal and ventral lobes may be apparent. Xanthophores are now more distinct in the caudal fin. The outline of radials are becoming evident within the caudal fin condensation.

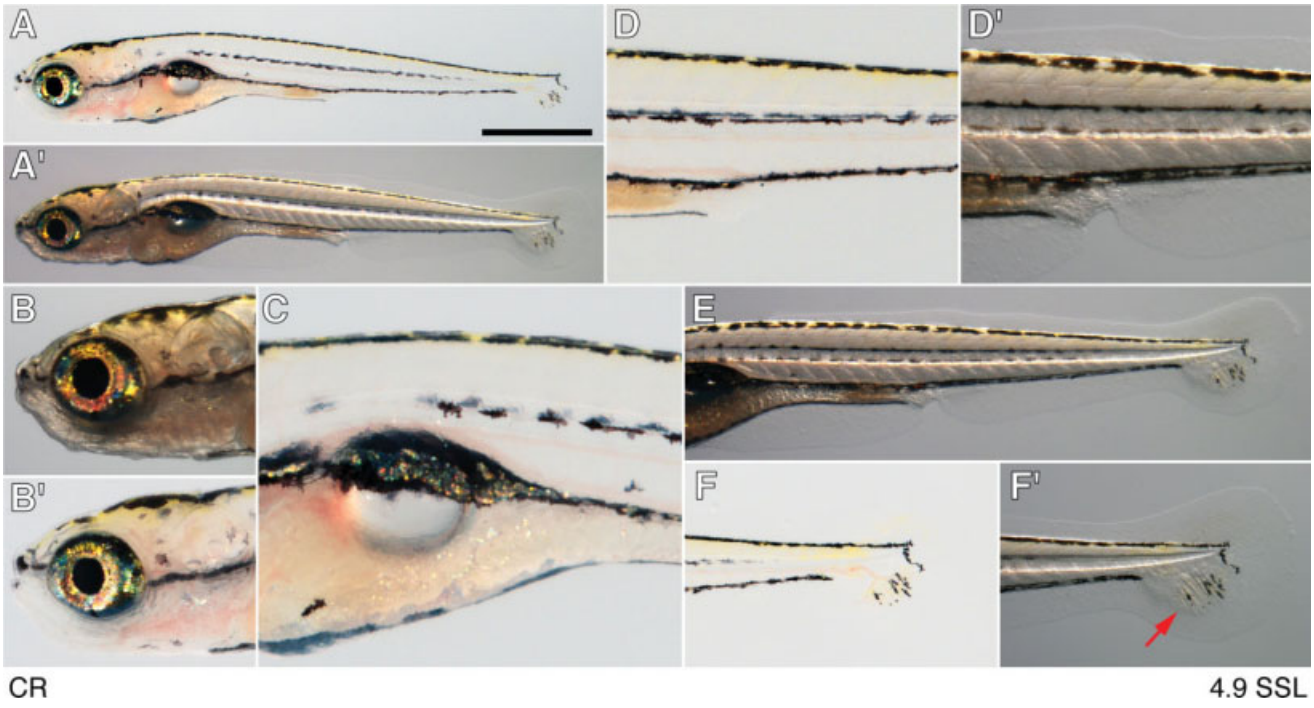

Fig. 36. Caudal fin ray appearance; CR, 4.9 mm SL (standard length). **A,A′**: Whole body. Scale bar = 1 mm. **B,B′**: Head. **C**: Anterior trunk. **D,D′**: Posterior trunk. Xanthophore pigment is now less pronounced. **E**: Caudal region. **F,F′**: Posterior tail. Arrow, first fin rays of caudal fin.

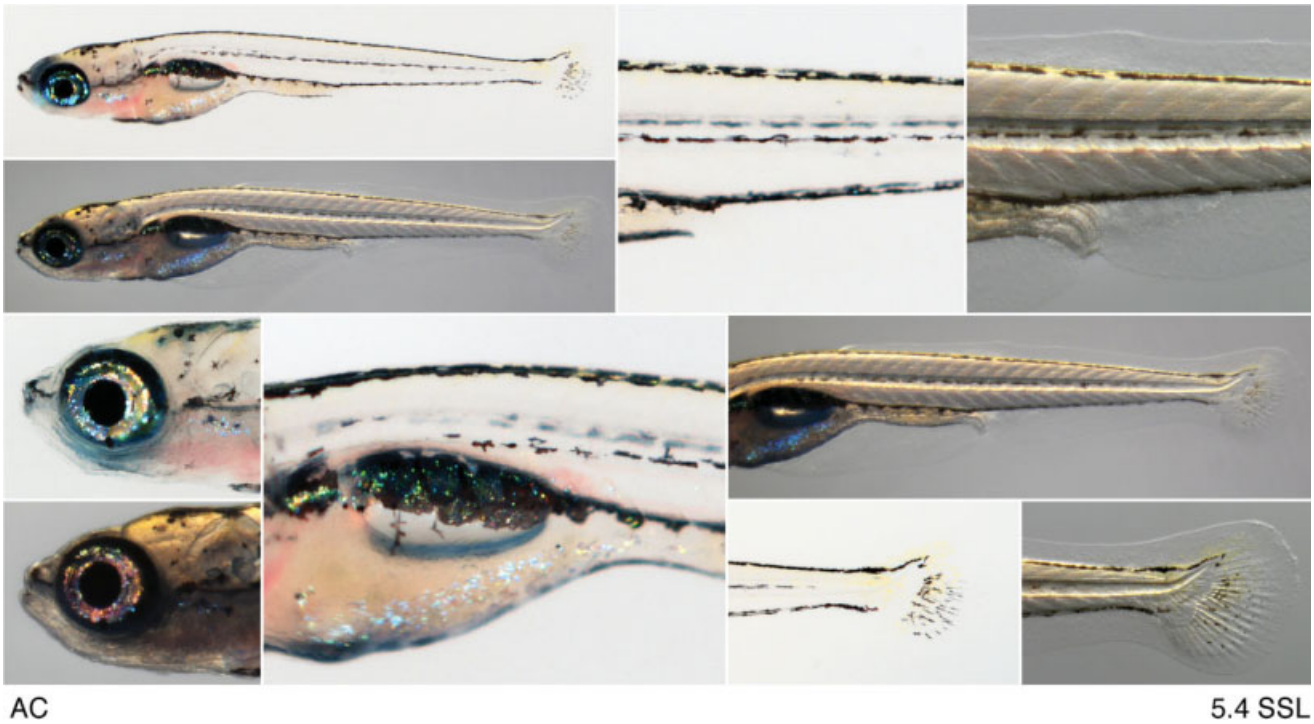

Fig. 37. Anal fin condensation; AC, 5.4 mm SL (standard length). **A,A′**: Whole body. Scale bar = 1 mm. **B,B′**: Head. **C**: Anterior trunk. **D,D′**: Posterior trunk showing condensed mesenchyme of prospective anal fin (arrow). **E**: Caudal region. **F,F′**: Posterior tail.

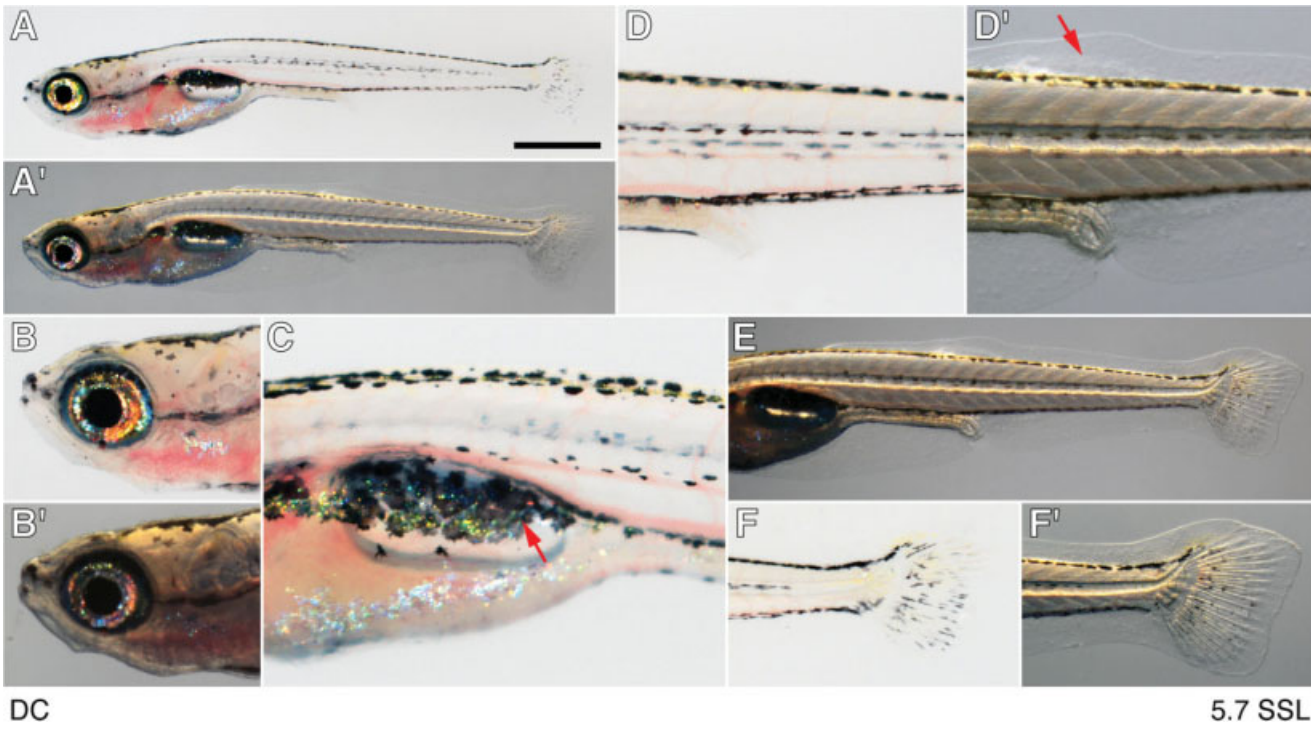

Fig. 38. Dorsal fin condensation; DC, 5.7 mm SL (standard length). **A,A′**: Whole body. Scale bar = 1 mm. **B,B′**: Head. **C**: Anterior. Arrowhead, iridophores cover ventral–lateral face of myotomes in anterior trunk. **D,D′**: Posterior trunk showing dorsal fin condensation (arrow). **E**: Caudal region. **F,F′**: Posterior tail. The fin is flattened at its end and melanophores are widely scattered amongst fin rays.

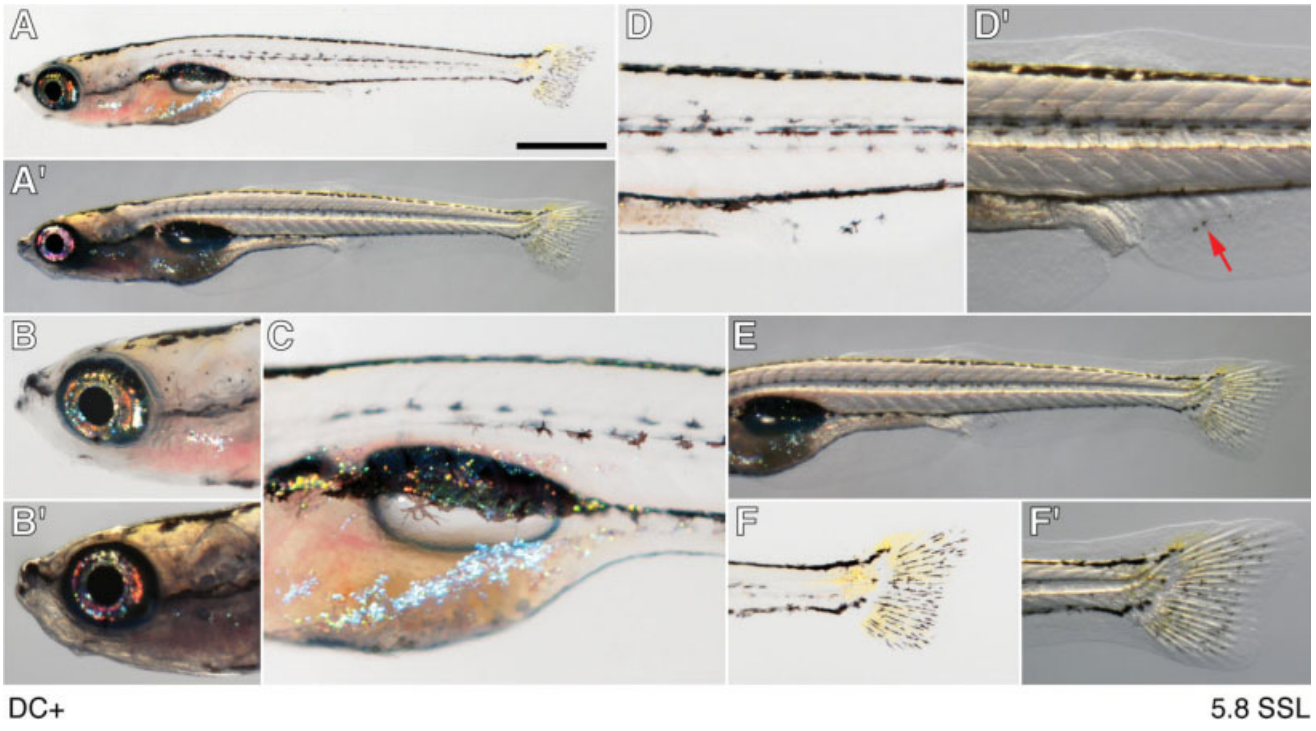

Fig. 39. Following dorsal fin condensation; DC+, 5.8 mm SL (standard length). **A,A′**: Whole body. Scale bar = 1 mm. **B,B′**: Head. **C**: Anterior. **D,D′**: Posterior trunk showing dorsal fin condensation and melanophores adjacent to the ventral fin condensation (arrow). **E**: Caudal region. **F,F′**: Posterior tail.

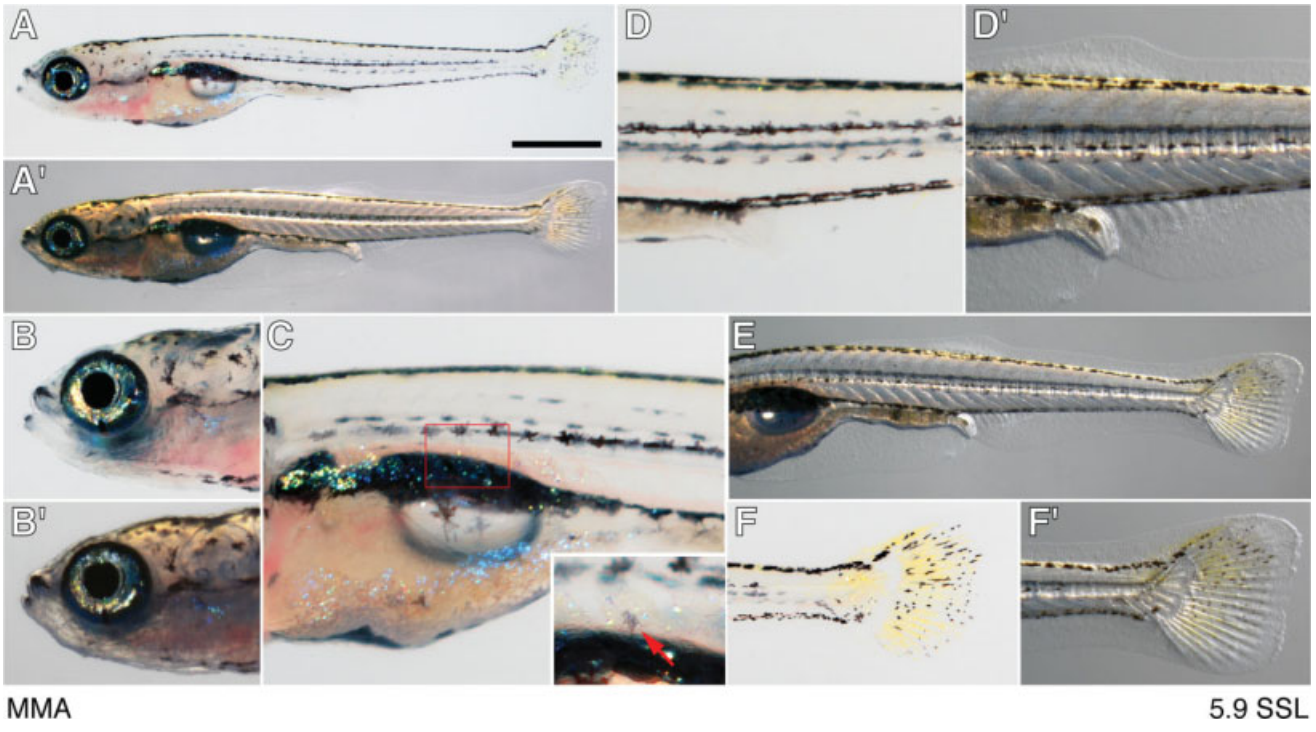

Fig. 40. Metamorphic melanophore appearance; MMA, 5.9 mm SL (standard length). **A,A′**: Whole body. Scale bar = 1 mm. **B,B′**: Head. **C**: Anterior, showing first metamorphic melanophore over ventrolateral myotome (arrow in inset). **D,D′**: Posterior trunk, where metamorphic melanophores have not yet arisen. **E**: Caudal region. **F,F′**: Posterior tail.

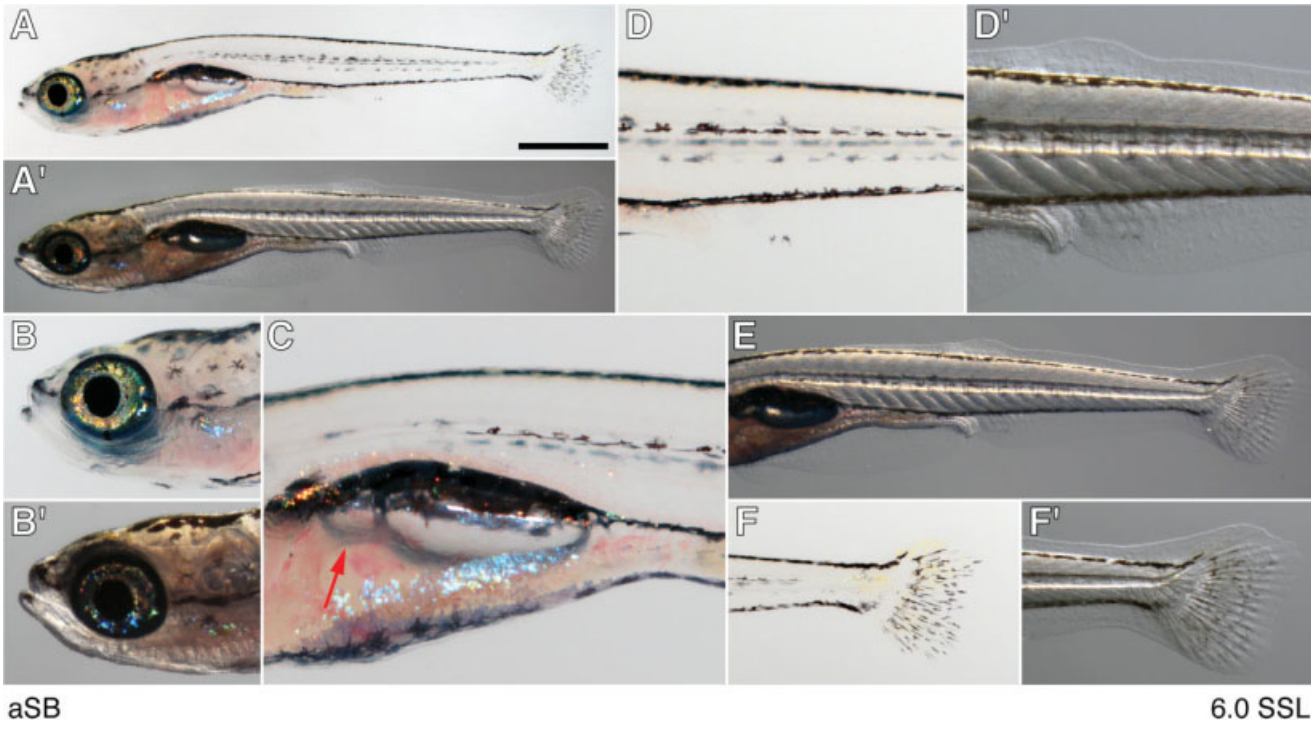

Fig. 41. Inflation of anterior swim bladder lobe; aSB, 6.0 mm SL (standard length). **A,A′**: Whole body. Scale bar = 1 mm. **B**: Head. **C,C′**: Anterior trunk showing newly inflated anterior lobe of swim bladder (arrow). **D,D′**: Posterior trunk. Arrow, developing radials of caudal fin. **E**: Caudal region. **F,F′**: Posterior tail.

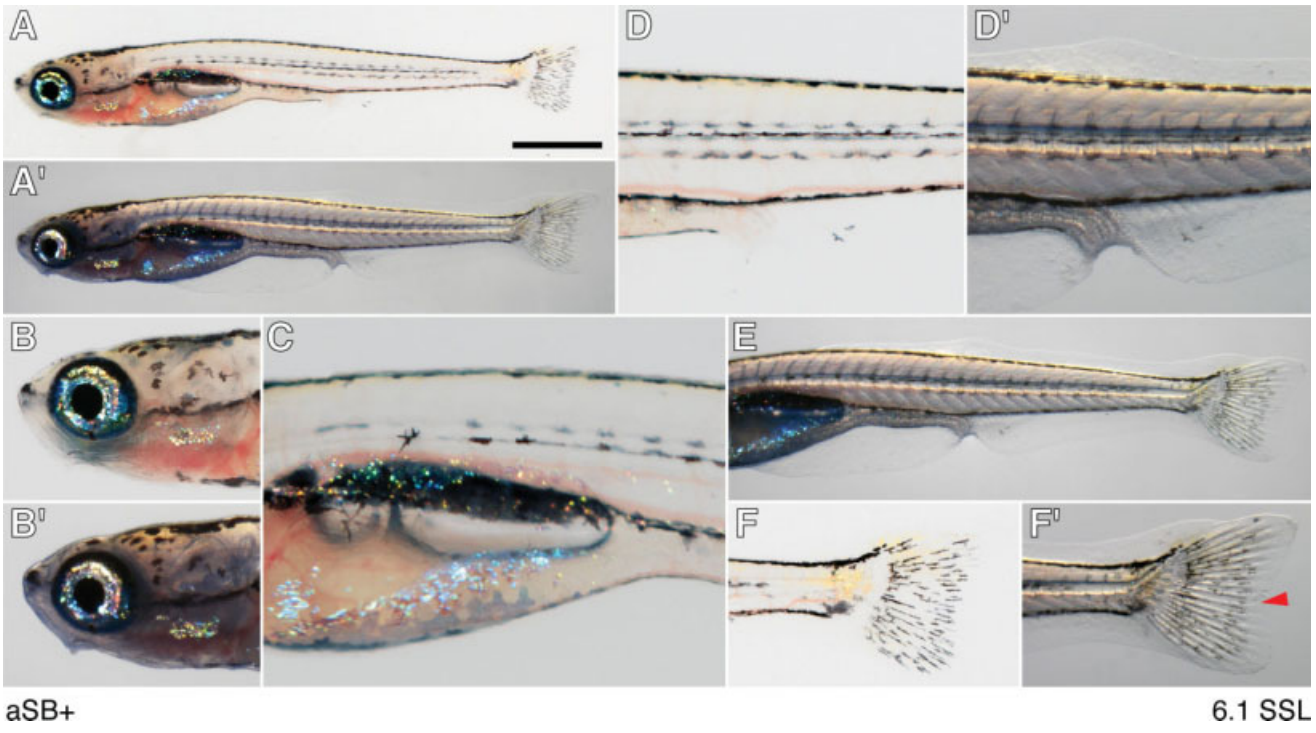

Fig. 42. Following inflation of anterior swim bladder lobe; aSB+, 6.1 mm SL (standard length). **A,A′**: Whole body. Scale bar = 1 mm. **B**: Head. **C,C′**: Anterior trunk showing newly inflated anterior lobe of swim bladder (arrow). **D,D′**: Posterior trunk. **E**: Caudal region. **F,F′**: Posterior tail showing developing cleft (arrowhead) between dorsal and ventral lobes of caudal fin.

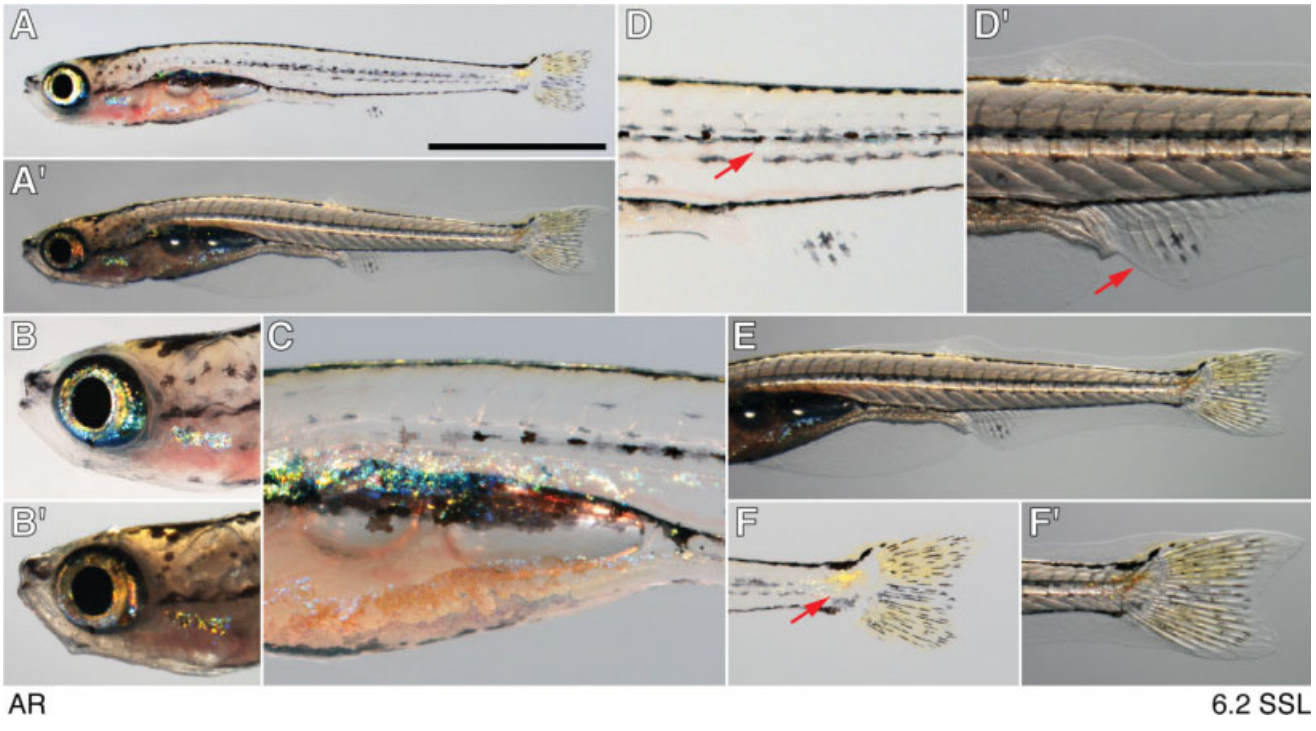

Fig. 43. Anal fin ray appearance; AR, 6.2 mm SL (standard length). **A,A′**: Whole body. Scale bar = 2 mm. **B,B′**: Head. **C**: Anterior showing distinct swim bladder lobes and overlying iridophores. **D,D′**: Posterior trunk. Iridophores form a thin line ventral to the myoseptum (arrow in D). First segments of anal fin rays are now evident distal to the radials (arrow in D′). **E**: Caudal region showing signs of fin fold resorption. **F,F′**: Posterior tail, showing iridophore patch at tip of tail (arrow).

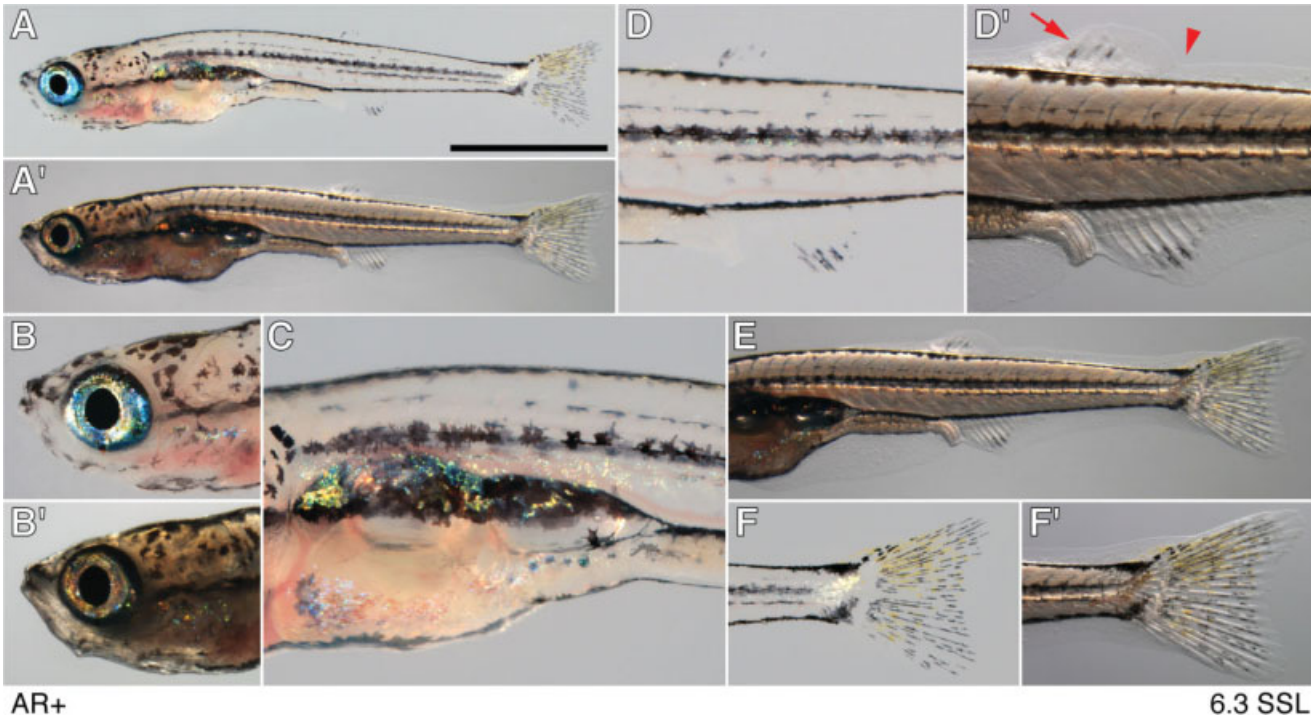

Fig. 44. Following anal fin ray appearance, AR+, 6.3 mm SL (standard length). **A,A′**: Whole body. Scale bar = 2 mm. **B,B′**: Head. **C**: Anterior trunk. Inset, metamorphic melanophores over middle trunk. **D,D′**: Middle trunk with dorsal and ventral fins. Arrow, condensing mesenchyme will form dorsal fin rays, which are not yet fully formed. Arrowhead, notch in fin fold. **E**: Posterior trunk. **F,F′**: Posterior tail.

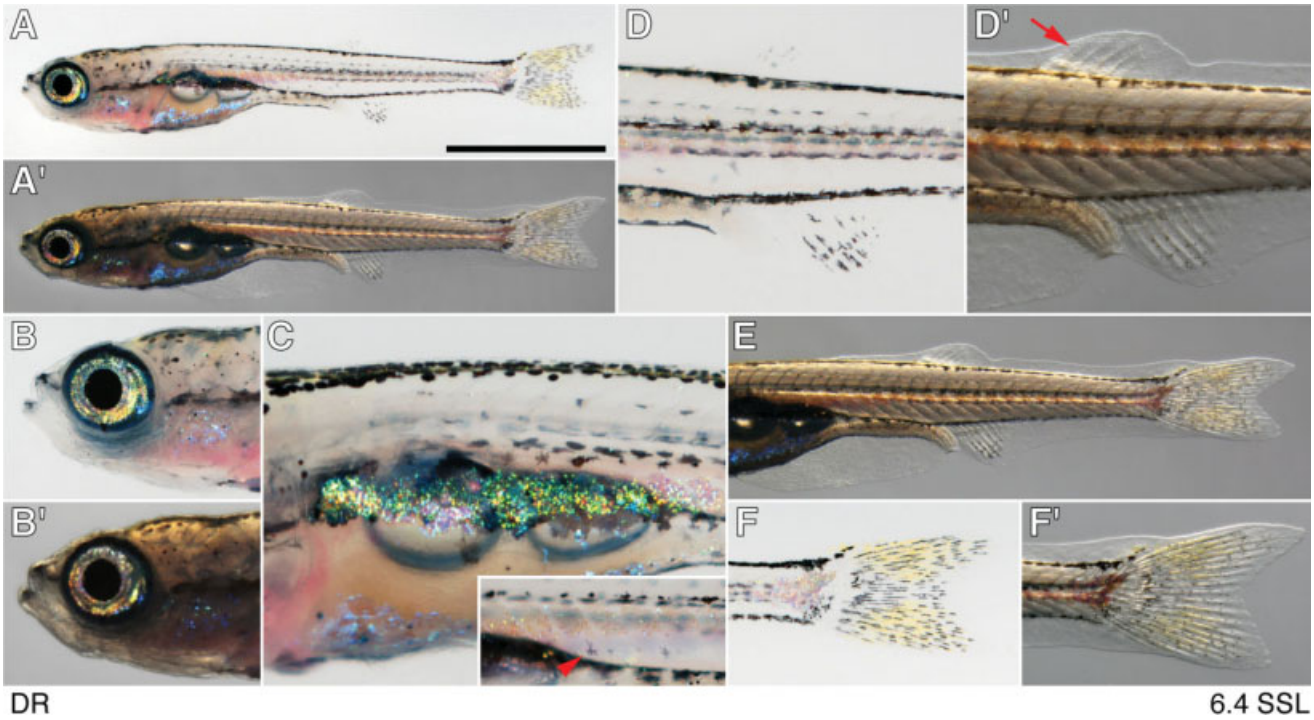

Fig. 45. Dorsal fin ray appearance; DR, 6.4 mm SL (standard length). **A,A′**: Whole body. Scale bar = 2 mm. **B,B′**: Head. **C**: Anterior trunk. Inset, individual metamorphic melanophores over ventrolateral myotomes just posterior to the posterior swim bladder lobe. **D,D′**: Middle trunk with dorsal and ventral fins. Arrow, dorsal fin rays. **E**: Posterior trunk. **F,F′**: Posterior tail.

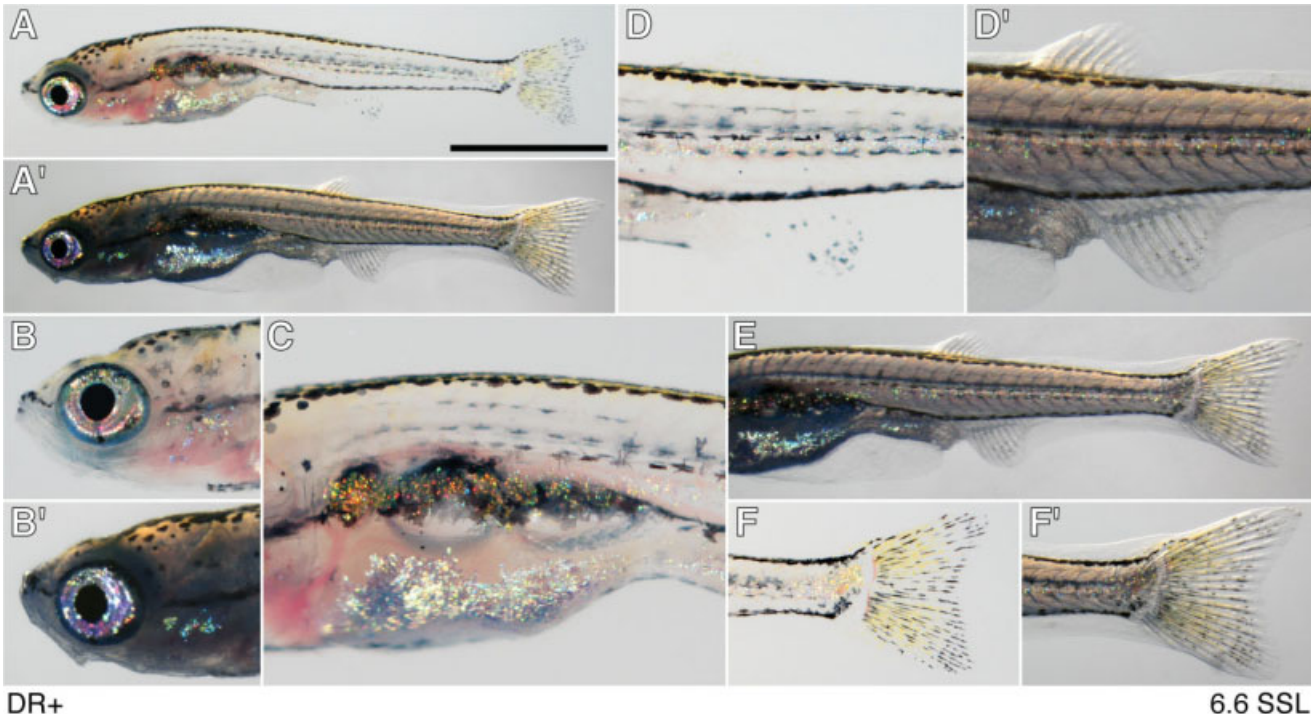

Fig. 46. Following dorsal fin ray appearance; DR+, 6.6 mm SL (standard length). **A,A′**: Whole body. Scale bar = 2 mm. **B,B′**: Head. **C**: Anterior trunk. **D,D′**: Middle trunk. **E**: Posterior trunk. **F,F′**: Posterior tail.

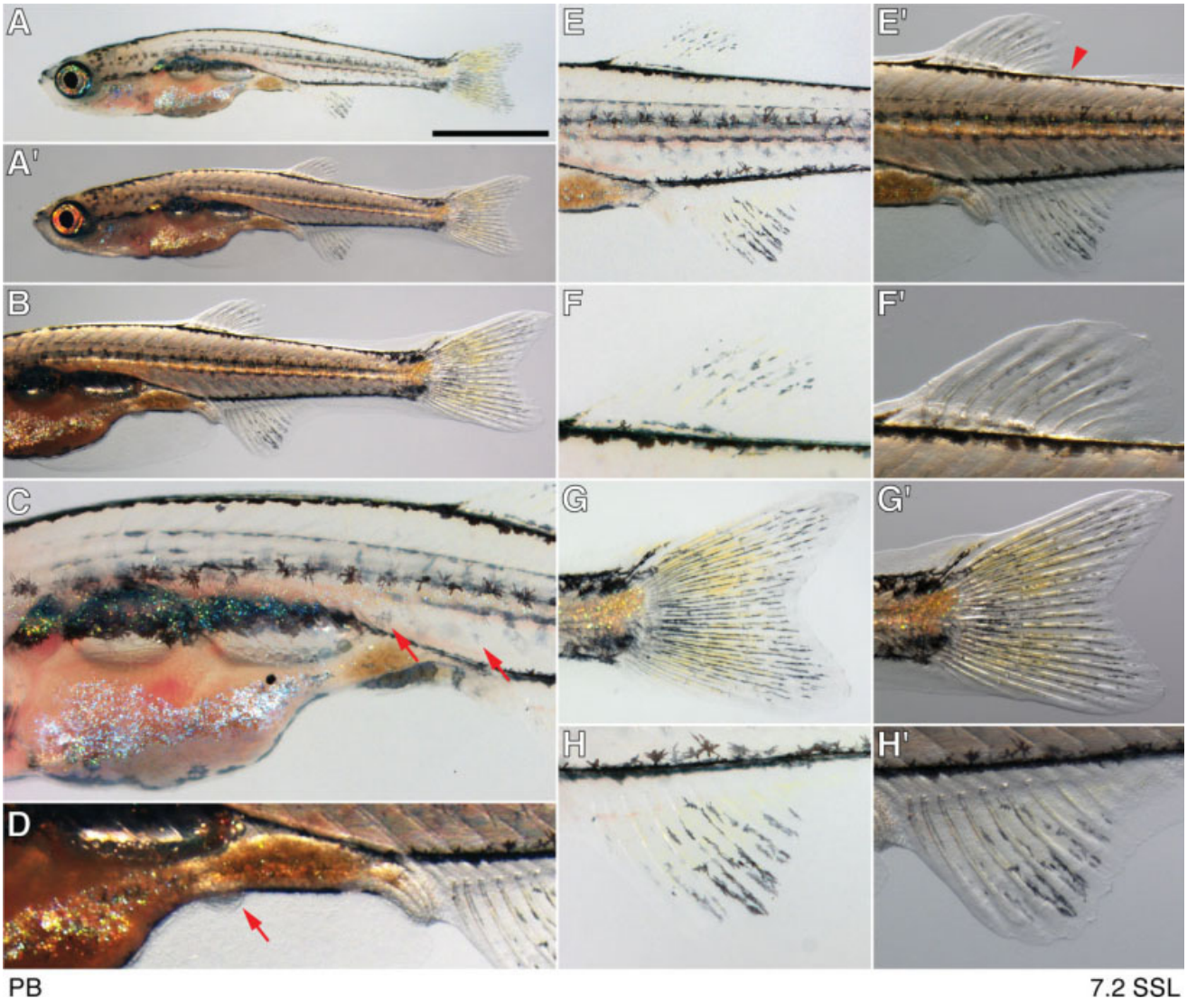

Fig. 47.

Fig. 48. Following pelvic fin bud appearance; PB+, 7.6 mm SL (standard length). **A,A′**: Whole body. Scale bar = 2 mm. **B,B′**: Head. **C,C′**: Anterior and middle trunk showing pelvic fin bud (arrow). **D**: Pelvic fin bud showing condensed mesenchyme without rays. **E,E′**: Middle trunk showing dorsal and anal fins as well as pigment pattern. Metamorphic melanophores are more fully melanozed and are scattered over the flank (e.g., arrow). **F**: Posterior trunk showing resorption of fin fold and extended line of iridophores (arrow) beneath the horizontal myoseptum. **G,G′**: Dorsal fin, showing xanthophores in addition to melanophores. **H,H′**: Caudal fin. **I,I′**: Detail of anal fin.

Fig. 47. Pelvic fin bud appearance; PB, 7.2 mm SL (standard length). **A,A′**: Whole body. Scale bar = 2 mm. **B**: Posterior trunk. **C**: Anterior trunk. Metamorphic melanophores are present but not fully melanized (e.g., arrows). **D,D′**: Ventral region showing pelvic fin bud (arrow). **E,E′**: Middle trunk showing dorsal and anal fins as well as pigment pattern. Arrowhead, region of fin fold resorption. **F,F′**: Detail of dorsal fin. **G,G′**: Detail of caudal fin. **H,H′**: Detail of anal fin.

AR, Anal Fin Ray Appearance (6.1–6.4 mm SL onset)

Figures 43, 44: Anal fin rays are distal to the developing anal fin radials. A few melanophores are interspersed with the developing rays. The dorsal fin condensation is becoming partitioned, but ossified (shiny) rays are not yet apparent; a few melanophores may be found in association with the mesenchyme. Later in this period, a notch becomes apparent in the major lobe of the fin fold, immediately posterior to the dorsal fin condensation. Iridophores on the flank extend posteriorly to the level of the yolk extension or past the anus; a posterior patch or iridophores is apparent at the base of the caudal fin. The caudal fin has now has a bilobate appearance with an

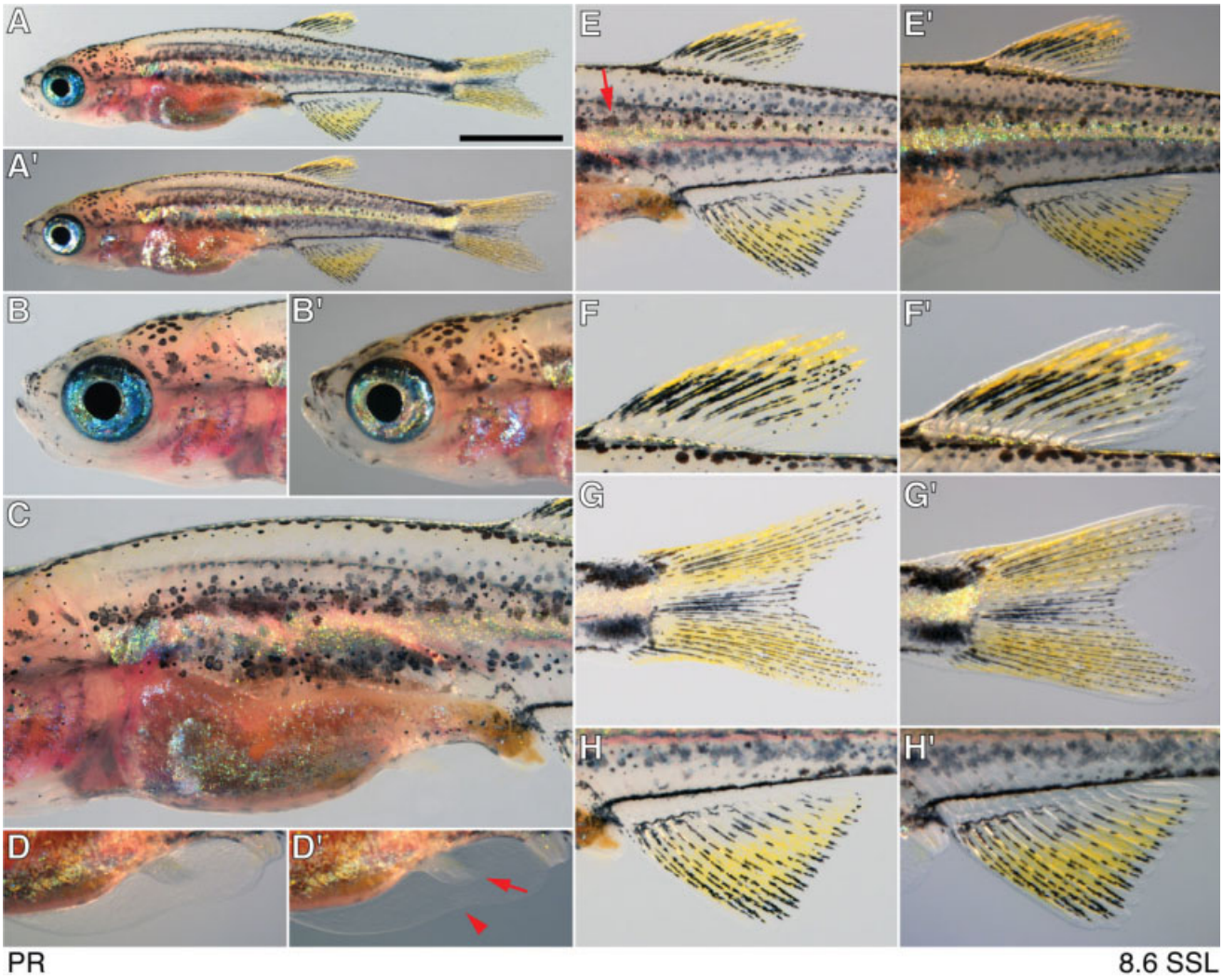

Fig. 49. Pelvic fin ray appearance; PR, 8.5 mm SL (standard length). **A,A′**: Whole body. Scale bar = 2 mm. **B,B′**: Head. **C**: Anterior and middle trunk. **D,D′**: Pelvic fin with first rays (arrow) as well as minor lobe of fin fold and site of resorption (arrowhead). **E,E′**: Middle trunk showing dorsal and anal fins and pigment pattern. Residual embryonic/early larval melanophores occur near the horizontal myoseptum (arrow). **F,F′**: Dorsal fin. **G,G′**: Caudal fin, showing emergence of first stripes. **H,H′**: Anal fin.

intervening cleft; melanophores and xanthophores are intermingled.

DR, Dorsal Fin Ray Appearance (6.4–6.6 mm SL onset)

Figures 45, 46: Rays are now visible within the developing dorsal fin. A few metamorphic melanophores are found singly over the dorsolateral and ventrolateral myotomes along the posterior trunk. Fin fold resorption is increasingly evident.

PB, Pelvic Fin Bud Appearance (7.2–7.5 mm SL onset)

Figures 47, 48: The pelvic fin buds appear as protuberances from the ventral body wall, below the posterior lobe of the swim bladder. The buds subsequently elongate until their length along the ventral edge is approximately half their height. Xanthophores are apparent in both dorsal and anal fins. Resorption of the primary lobe of the fin fold is increasingly evident, both anterior and posterior to the dorsal fin. Metamorphic melanophores are found dispersed over the flank in increasing numbers. Residual embryonic/early larval melanophores may be found over the lateral face of the myotomes and can contribute to adult primary stripe 1D (Parichy and Turner, 2003; Quigley et al., 2004), although a distinctive pattern of adult stripes has not yet emerged. The iridophore stripe is faint but continuous from anterior to posterior. Anal and dorsal fin ray numbers are reaching their maximum (~15 rays, ~10 rays, respectively). Anterior swim bladder lobe size is greater, whereas swim bladder angle has started to decrease.

PR, Pelvic Fin Ray Appearance (8.5–8.7 mm SL onset)

Figures 49, 50: Pelvic fin rays are first evident though pelvic fins remain relatively inconspicuous. An indentation is apparent in the minor lobe of the fin fold, adjacent to the pelvic fin. The adult primary melanophore stripes are now distinct as fewer metamorphic melanophores are found outside of stripes; nevertheless, some gaps in

Fig. 50. Following pelvic fin ray appearance; PR+, 9.2 mm SL (standard length). **A,A′**: Whole body. Scale bar = 2 mm. **B,B′**: Head. Arrowhead indicates developing barbel. **C**: Anterior and middle trunk. **D,D′**: Pelvic fin. **E,E′**: Middle trunk. **F,F′**: Dorsal fin. **G,G′**: Caudal fin. **H,H′**: Anal fin.

stripes are still apparent. Iridophores marking the first interstripe region are now more evident. A stripe pattern has started to emerge in the caudal fin as well as the anal fin. The posterior swim bladder lobe bends further ventrally.

SP, Squamation Onset Posterior (9.5–9.6 mm SL onset)

Figure 51: Scales are now apparent on the tail, posterior to the anal fin and caudal fin, as evidences by ridges, in the epidermis, especially ventrally. Pelvic fin ray numbers are now maximal (~6) and a few melanophores may be found associated with them. The primary melanophore stripes are more regular, although some melanophores remain outside of the stripes, including within the interstripe region.

SA, Squamation Through Anterior (10.1–10.4 mm SL onset)

Figure 52: Scales are apparent anterior to the dorsal fin, but may not extend to the head. Melanophores have started to organize along scale edges. Only a remnant of the minor lobe of the fin fold is present anterior to the vent.

J, Juvenile (10.9–11.7 mm SL onset)

Figures 53, 54, 55. Scales are fully formed and melanophores form ~2 rows along each scale edge. Fin fold resorption is complete. Melanophores are typically absent from the first interstripe region and the adult secondary melanophore stripe 2V is faintly apparent. Definitive stripe patterns are now evident in caudal and anal fins. Later in this period, secondary melanophore stripe 2V becomes distinct and 2D begins to form.

A, Adult

Figures 56, 57: Fish are sexually mature as evidenced by gamete production and secondary sexual

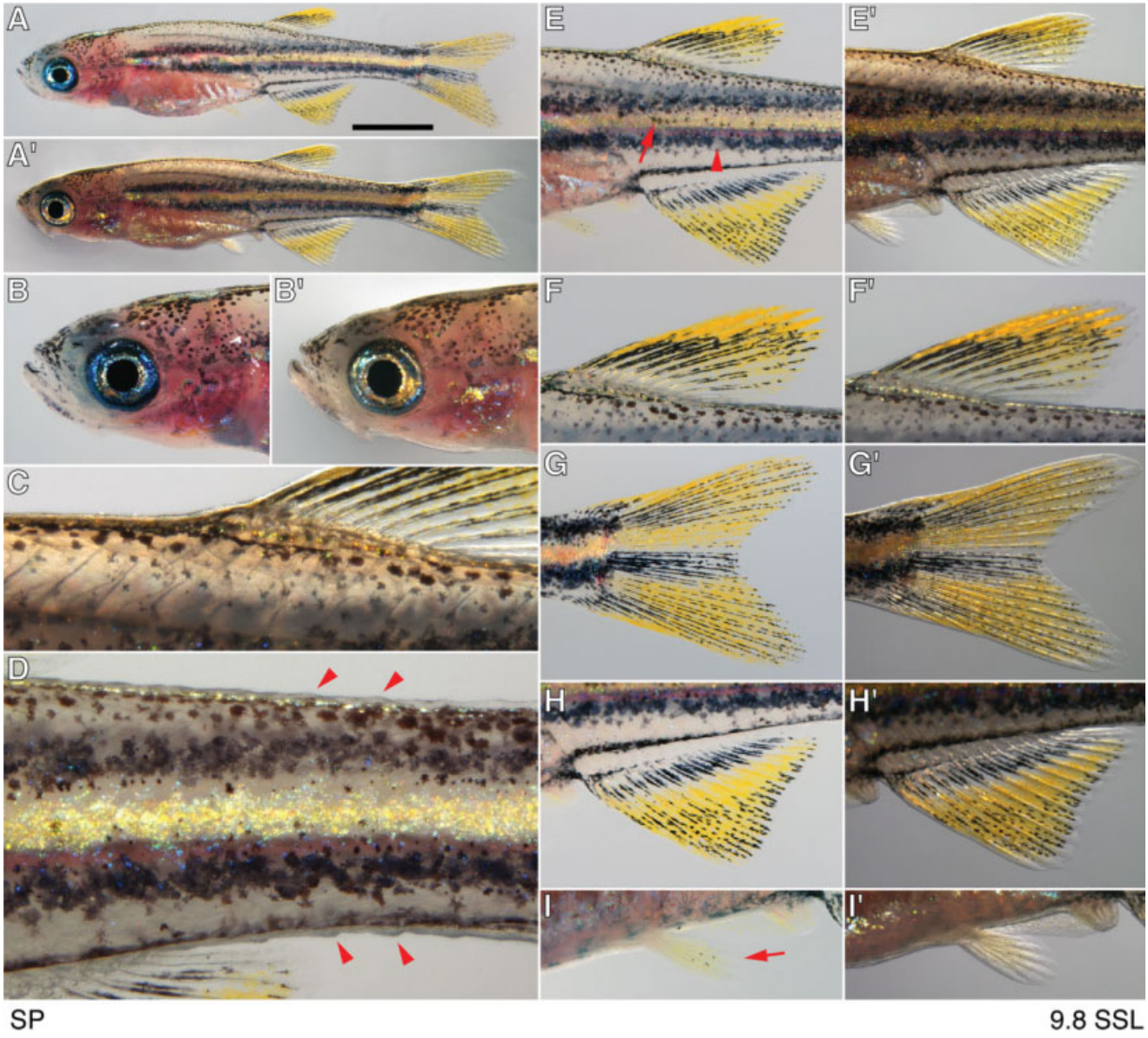

Fig. 51. Onset of posterior squamation; SP, 9.8 mm SL (standard length). **A,A′**: Whole body. Scale bar = 2 mm. **B,B′**: Detail of head. **C**: Dorsal flank showing absence of scales anterior to dorsal fin. **D**: Posterior tail, showing raised ridges of scales dorsally and ventrally (arrowheads). **E,E′**: Middle trunk showing dorsal and anal fins and pigment pattern. Stripes are increasingly distinct except for a few remaining gaps (arrowhead) and fewer embryonic/early larval melanophores are found in the interstripe region (arrow). **F,F′**: Dorsal fin. **G,G′**: Caudal fin, with increasingly distinct stripes. **H,H′**: Anal fin, with the first distinct melanophore stripe. **I,I′**: The pelvic fin (arrow) now has several distinct rays as well as a few melanophores amongst them.

characteristics when in condition. Gravid females have somewhat distended abdomens and a protruding vent. Males are more slender, lack a protruding vent, and often exhibit a yellowish tinge over the ventral flank.

STAGE REPORTING CONSIDERATIONS AND RECOMMENDED CONVENTIONS

The developmental milestones in Table 4 can be used to define the onset of postembryonic stages. Because these milestones are named, rather than numbered, additional milestones can be added easily, if and when they are found, and additional stages can be defined. Nevertheless, there are difficulties in using such milestones alone to define developmental stages. For example, several intervals between milestones include substantial growth and development. While these changes are continuous rather than discrete, they are real modifications that have relevance to the organism, and are likely to have relevance to studies of the organism. Moreover, if additional discrete changes are identified, strict adherence to the milestones in Table 4 could result in stages that are too coarse for describing a particular state of development. Finally, the milestones we have identified include changes in just a few traits, relying especially on the fins, and this will limit their utility for studies of strains or mutants having defects in these traits (Harris et al., 2008).

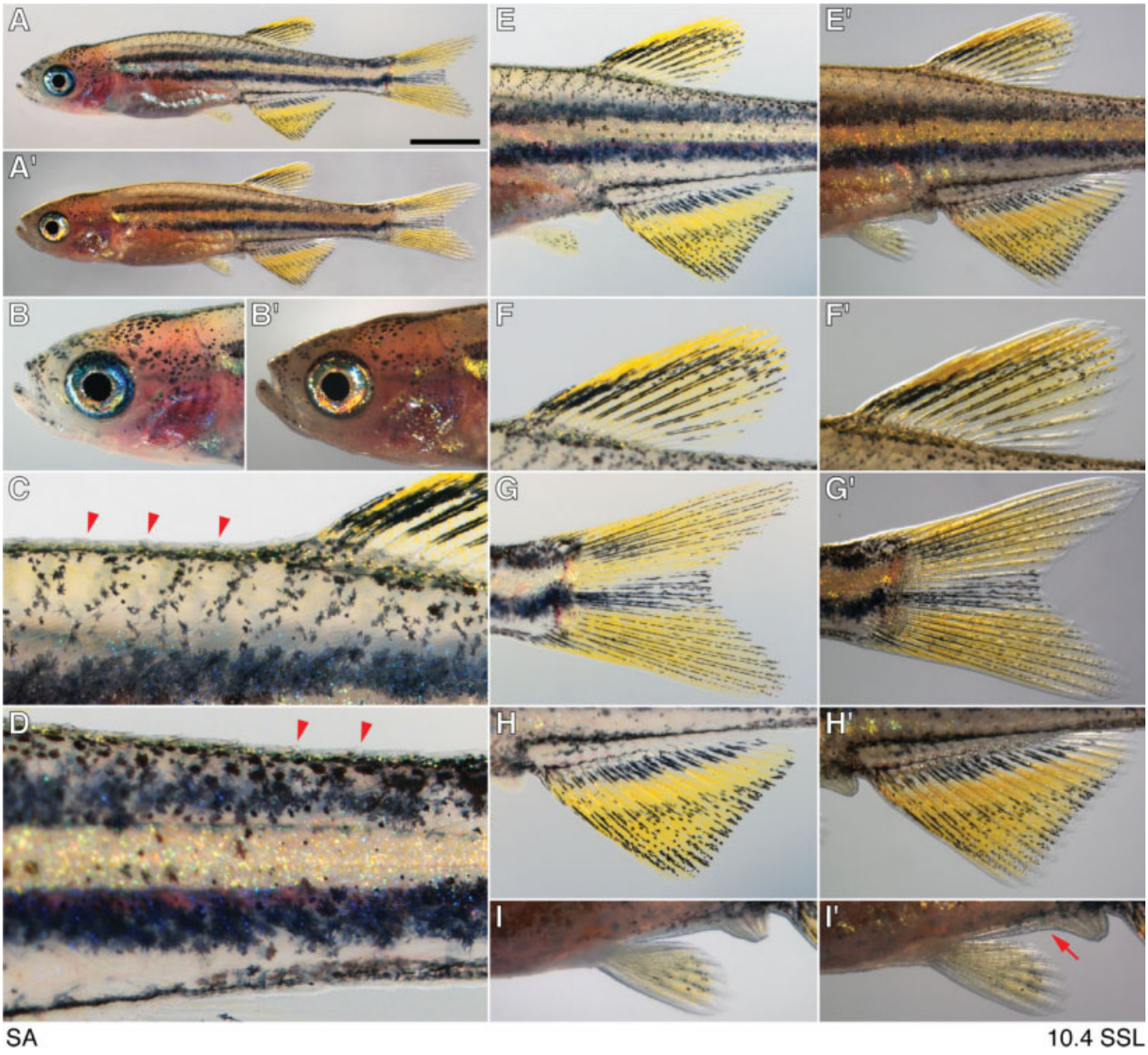

Fig. 52. Onset of anterior squamation; SA, 10.4 mm SL (standard length). **A,A′**: Whole body. Scale bar = 2 mm. **B,B′**: Head. **C**: Dorsal flank with ridges of scales (arrowheads) and early organization of scale melanophores. **D**: Posterior tail with scale ridges (arrowheads). **E,E′**: Middle trunk showing dorsal and anal fins and pigment pattern. **F,F′**: Dorsal fin. **G,G′**: Caudal fin. **H,H′**: Anal fin. **I,I′**: The pelvic fin and residual fin fold at vent (arrow).

The use of size, and especially SL, is one alternative to using discrete milestones for staging (Fuiman et al., 1998). In principle, the use of size has the advantage of allowing developmental progress to be parsed as finely as the resolution at which measurements can be made. Moreover, our analyses indicate very high correlations between size and developmental milestones; these correlations are relatively independent of rearing conditions, although not completely so (e.g., Fig. 30).

Nevertheless, size-based staging also has disadvantages. Despite high correlations with developmental progress overall, we still found substantial variation among individuals of a given size (e.g., Figs. 9, 12, 25B). Furthermore, strain differences may complicate the use of size alone. We have not observed differences between strain AB^{wp}, which has been inbred for ~10 years, and a wild-type stock, WT(WA), generated by intercrossing AB^{wp} and wik^{wp}. Yet, we cannot exclude the possibility that differences in the relationships between size and developmental progress exist among other strains currently in use, or zebrafish either in natural populations or recently derived from natural populations (Trevarrow and Robison, 2004; Engeszer et al., 2007). Finally, many postembryonic mutant

Fig. 53. Juvenile; J, 11.0 mm SL (standard length). **A,A′**: Whole body, showing newly completed squamation and scale melanophore pattern. Scale bar = 2 mm. **B,B′**: Head. **C**: Dorsum immediately posterior to head. **D**: Dorsal–anterior flank. **E,E′**: Middle trunk showing juvenile pigment pattern on body as well as dorsal and anal fins; a few residual embryonic/early larval melanophores still can be found in the interstripe at this stage. **F,F′**: Dorsal fin. **G,G′**: Caudal fin. **H,H′**: Anal fin. **I,I′**: Pelvic fin and vent, without residual fin fold.

phenotypes decouple growth and development (Mintzer et al., 2001; Elizondo et al., 2005), precluding the use of size alone for staging.

Given these considerations, and our desire to maximize the versatility of staging criteria for current and future analyses, and to maximize consistency across labs and stocks, we propose the use of either of two conventions for reporting stages of post-embryonic zebrafish development.

1. Composite Staging

In this convention, both developmental milestones and sizes of fish used are reported. We recommend the format "milestone:SL." For example, the individual shown in Figure 47 would be reported as "PB:7.2 mm SL" (or "PB:7.2" after its first use in a manuscript). Such composite stages have the advantage of providing both discrete criteria and any size-specific information unique to the particular strain or mutant being studied. If it is not possible or feasible to determine SL directly from the living fish, it may be estimable from another measure such as HAA, or based on sizes post-processing, using relationships such as those provided in Table 3. In these instances, we recommend that stages be reported in the format "milestone:eSL" (e.g., "PB:e7.2). If

Fig. 54. Following juvenile; J+, 13.0 mm SL (standard length). **A,A′**: Whole body. Scale bar = 2 mm. **B,B′**: Head. **C**: Dorsum anterior to dorsal fin, showing additional melanophores that have appeared on scales. **D**: Posterior tail. **E,E′**: Middle trunk showing completed juvenile pigment pattern on body as well as dorsal and anal fins. **F,F′**: Dorsal fin. **G,G′**: Caudal fin. **H,H′**: Anal fin. **I,I′**: Pelvic fin and vent, without residual fin fold.

it is not possible to estimate size than the format "milestone:—" (e.g., "PB:—") can serve to indicate this.

2. Standardized Standard Length (SSL) Staging

In this convention, we propose a streamlined format for reporting stages that relies on both discrete milestones and quantitative aspects of growth and development, while accommodating strain-specific variation. Specifically, we recommend the use of "standardized SL" (SSL) when developmental progress can be approximated by the reference fish illustrated in Figures 32–57. Thus, a larva that has already developed the pelvic fin buds and resembles the individual shown in Figure 47, could be described as "7.2 SSL," although actual SL might deviate slightly from 7.2 mm because of individual variation or strain differences. If actual SL differs substantially from that shown, owing to genetic background or rearing conditions, or if SL has been estimated from other measures of size, we recommend the value be reported as "e7.2 SSL."

An advantage of SSL-based staging is that intermediate stages can be described as interpolations between the reference individuals

shown, with intermediates parsed as finely as appropriate to the study and trait in question. Thus, a larva intermediate between the individuals shown in Figures 47 and 48, could be described as "7.4 SSL".

CONCLUSIONS

We have provided criteria for staging zebrafish in studies of postembryonic development. While no staging system is perfect, we propose two conventions for describing developmental progress that account for both discrete milestones and quantitative changes: composite staging and SSL staging. Our analyses suggest that both are preferable to using days postfertilization for indicating developmental progress. We anticipate that in many instances, SSL staging will provide the most expedient means of reporting stages, although analyses that explicitly focus on growth or inter-strain differences may be better accommodated by composite staging. The conventions and data provided here should assist with further studies into the important processes of postembryonic development.

Fig. 55. Following juvenile; J++, 16 mm SL (standard length). **A**: Whole body. Scale bar = 3 mm. **B**: Head. **C**: Dorsal flank anterior to dorsal fin, showing emergence of secondary dorsal melanophore stripe (2D). **D**: Middle trunk. **E,E′**: Caudal fin.

EXPERIMENTAL PROCEDURES

Fish Strains and Rearing Conditions

Fish were the inbred strain AB^{wp} or the outbred stock WT(WA) which is generated by intercrossing AB^{wp} and wik. Fish were reared at an average temperature of 28.5°C except for studies of temperature effects in which fish were reared at 24°C or 33°C as well. Fish were reared either individually or in groups at various densities. For analyzing the effects of density and food availability on growth and development, fish were reared at low density (3–5 individuals per 2.8-L tank), medium density (~30 individuals), or high density (~150 individuals). For following individuals through postembryonic development, fish were isolated in water-filled plastic cups changed daily. A light:dark cycle of 14:10 was used throughout these analyses. Fish were fed a standard diet, comprising marine rotifers shortly after hatching, transitioning to a blend of flake foods of increasing size as fish grew. Detailed protocols for fish rearing are available on-line at: http://protist.biology.washington.edu/dparichy/

Imaging and Microscopy

Fish images were acquired after brief anesthetization with MS222 using an Olympus SZX12 epifluorescence stereomicroscope or a Zeiss Discovery epifluorescence stereomicroscope, interfaced to Axiocam HR and MR3 cameras and Axiovision software. Most fish were imaged either immersed in 1% methylcellulose or after placement on an agarose-lined dish. Juvenile and adult fish were euthanized with MS222, then immediately placed on a plastic dish, gradually covered with warm agarose and, after agarose had hardened, dishes were inverted and fish imaged through the flat bottom. For thick specimens, z-stacks were acquired in brightfield or epifluorescence modes and projections generated with the Axiovision Extended Focus module. Images were further processed for color balance or to remove background defects in Adobe Photoshop CS4.

Statistical Analyses

All statistical analyses were performed with JMP 8.0 for Macintosh (SAS Institute, Cary NC). In general, continuous traits were examined using standard linear models or

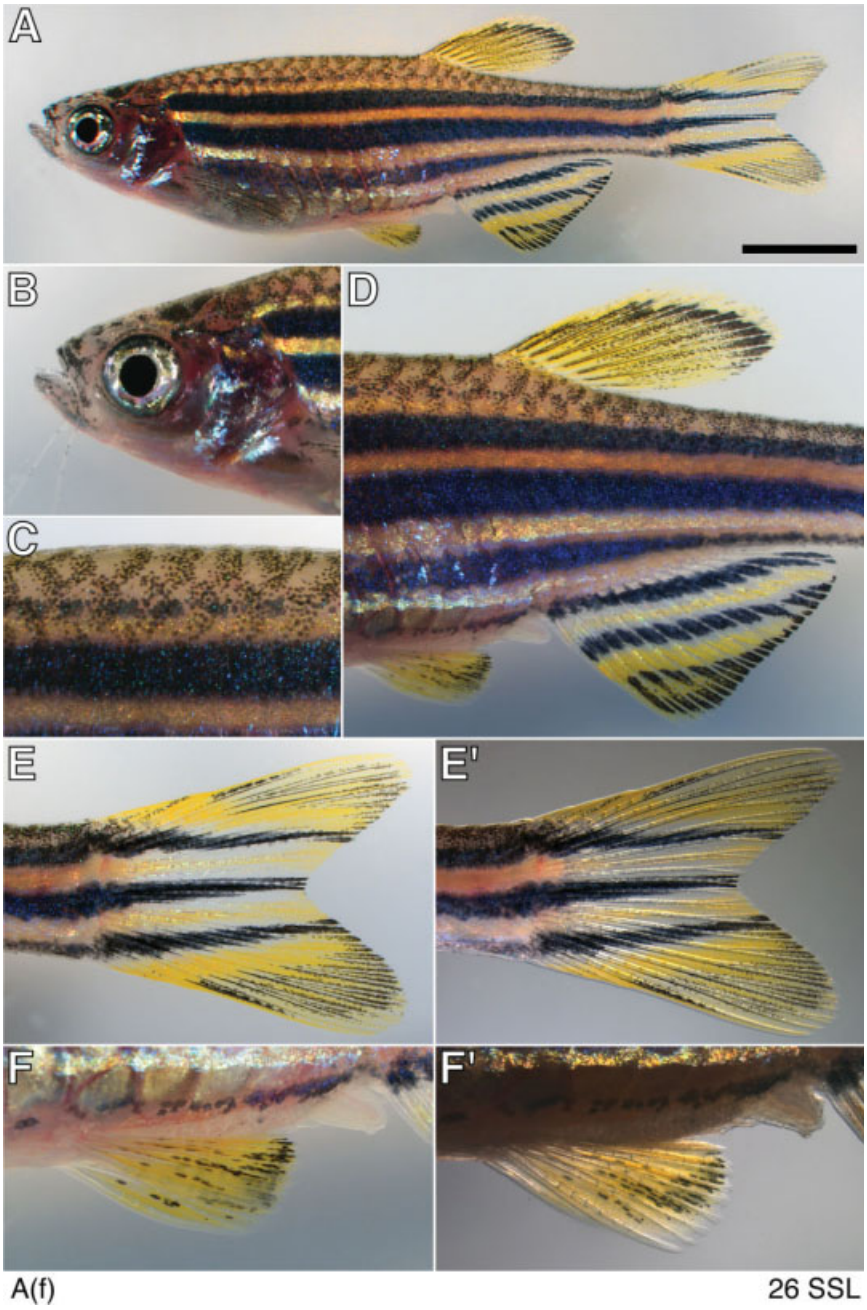

Fig. 56. Adult female; A(f), 23 mm SL. **A**: Whole body. This female is gravid as evidenced by distended abdomen. Scale bar = 4 mm. **B**: Head. **C**: Dorsal flank anterior to dorsal fin. **D**: Middle trunk. **E,E′**: Caudal fin. F,F′: Pelvic fin and vent, showing protrusion of cloaca from body wall typical of gravid females.

splines, whereas ordinal or nominal variables were examined with logistic regression. Detailed statistical methods are available on request.

Histological Procedures

Calcein and FM1-43 staining followed published methods (Elizondo et al., 2005; Ma et al., 2008). For determining the effects of histological processing on size, fish were measured then placed for 2 nights in 4% paraformaldeyde in phosphate buffered saline, then rinsed and remeasured. Additional fish were processed individually for in situ hybridization using standard methods for whole-mount zebrafish larvae (available at: http://protist.biology.washington.edu/dparichy/), and then remeasured after incubation in staining solution.

ACKNOWLEDGMENTS

Thanks to members of the Parichy lab for help with fish rearing and to C. Kimmel for helpful comments on the manuscript. Author contributions: D.M.P., data analyses, figure composition, stage definitions, manuscript writing, grant support; M.R.E., imaging and scoring of skeletogenesis; M.G.M., imaging and post hoc sizing; T.N.G., trait scoring and verification; R.E.E., image series of individual fish and trait scoring.

REFERENCES

Balon EK. 1999. Alternative ways to become a juvenile or a definitive phenotype (and on some persisting linguistic offenses). Environ Biol Fish 56:17–38.

Bird NC, Mabee PM. 2003. Developmental morphology of the axial skeleton of the zebrafish, Danio rerio (Ostariophysi: Cyprinidae). Dev Dyn 228: 337–357.

Brown ME. 1957. Experimental studies on growth. In: Brown ME, editor. The physiology of fishes. New York: Academic Press. p 361–400.

Brown DD, Cai L. 2007. Amphibian metamorphosis. Dev Biol 306:20–33.

Campinho MA, Moutou KA, Power DM. 2004. Temperature sensitivity of skeletal ontogeny in Oreochromis mossambicus. J Fish Biol 65:1003–1025.

Cubbage CC, Mabee PM. 1996. Development of the cranium and paired fins in the zebrafish Danio rerio (ostariophysi, Cyprinidae). J Morphol 229:121–160.

Du SJ, Frenkel V, Kindschi G, Zohar Y. 2001. Visualizing normal and defective bone development in zebrafish embryos using the fluorescent chromophore calcein. Dev Biol 238:239–246.

Eaton RC, Farley RD. 1974. Growth and the reduction of depensation of zebrafish, Brachydanio rerio, reared in the laboratory. Copeia 1974:204–209.

Elizondo MR, Arduini BL, Paulsen J, MacDonald EL, Sabel JL, Henion PD, Cornell RA, Parichy DM. 2005. Defective skeletogenesis with kidney stone formation in dwarf zebrafish mutant for trpm7. Curr Biol 15:667–671.

Engeszer RE, Patterson LB, Rao AA, Parichy DM. 2007. Zebrafish in the wild: a review of natural history and new notes from the field. Zebrafish 4: 21–40.

Fuiman LA, Poling KR, Higgs DM. 1998. Quantifying developmental progress for comparative studies of larval fishes. Copeia 1998:602–611.

Fig. 57. Adult female; A(f), 26 mm SL (standard length). **A**: Whole body. Scale bar = 4 mm. **B**: Head. **C**: Dorsal flank anterior to dorsal fin. **D**: Middle trunk. **E,E′**: Caudal fin. **F,F′**: Pelvic fin and vent; cloaca is flush with body wall, typical of males.

Georgakopoulou E, Sfakianakis DG, Koutouki S, Divanach P, Kentouri M, Koumoundouros G. 2007. The influence of temperature during early life on phenotypic expression at later ontogenetic stages in sea bass. J Fish Biol 70:278–291.

Goldsmith MI, Iovine MK, O'Reilly-Pol T, Johnson SL. 2006. A developmental transition in growth control during zebrafish caudal fin development. Dev Biol 296:450–457.

Harris MP, Rohner N, Schwarz H, Perathoner S, Konstantinidis P, Nusslein-Volhard C. 2008. Zebrafish eda and edar mutants reveal conserved and ancestral roles of ectodysplasin signaling in vertebrates. PLoS Genet 4:e1000206.

Hensel K. 1999. To be a juvenile and not to be a larva: an attempt to synthesize. Environ Biol Fish 56:277–280.

Hisaoka KK, Battle HI. 1958. The normal developmental stages of the zebrafish, Brachydanio rerio (Hamilton-Buchanan). J Morphol 1958:311–327.

Hopwood N. 2007. A history of normal plates, tables and stages in vertebrate embryology. Int J Dev Biol 51:1–26.

Iovine MK, Johnson SL. 2000. Genetic analysis of isometric growth control mechanisms in the zebrafish caudal Fin. Genetics 155:1321–1329.

Johnson SL, Africa D, Walker C, Weston JA. 1995. Genetic control of adult pigment stripe development in zebrafish. Dev Biol 167:27–33.

Kelsh RN, Parichy DM. 2008. Pigmentation. In: Finn RN, Kapoor BG, editors. Fish larval physiology. Enfield, NH: Science Publishers. p 27–49.

Kelsh RN, Harris ML, Colanesi S, Erickson CA. 2009. Stripes and belly-spots: a review of pigment cell morphogenesis in vertebrates. Semin Cell Dev Biol 20: 90–104.

Kimmel CB, Ballard WW, Kimmel SR, Ullmann B, Schilling TF. 1995. Stages of embryonic development of the zebrafish. Dev Dyn 203:253–310.

Kirschbaum F. 1975. Untersuchungen über das Farbmuster der Zebrabarbe Brachydanio rerio (Cyprinidae, Teleostei). Wilhelm Rouxs Arch 177:129–152.

Klimogianni A, Koumoundouros G, Kaspiris P, Kentouri M. 2004. Effect of temperature on the egg and yolk-sac larval development of common pandora, Pagellus erythrinus. Mar Biol 145: 1015–1022.

Kovac V, Copp GH. 1999. Prelude: looking at early development in fishes. Environ Biol Fish 56:7–14.

Ledent V. 2002. Postembryonic development of the posterior lateral line in zebrafish. Development 129:597–604.

Ma EY, Rubel EW, Raible DW. 2008. Notch signaling regulates the extent of hair cell regeneration in the zebrafish lateral line. J Neurosci 28:2261–2273.

Maderspacher F, Nusslein-Volhard C. 2003. Formation of the adult pigment pattern in zebrafish requires leopard and obelix dependent cell interactions. Development 130:3447–3457.

Martell DJ, Kieffer JD, Trippel EA. 2005. Effects of temperature during early life history on embryonic and larval development and growth in haddock. J Fish Biol 66:1558–1575.

Milos N, Dingle AD. 1978. Dynamics of pigment pattern formation in the zebrafish, Brachydanio rerio. I. Establishment and regulation of the lateral line melanophore stripe during the first eight days of development. J Exp Zool 205:205–216.

Mintzer KA, Lee MA, Runke G, Trout J, Whitman M, Mullins MC. 2001. Lost-a-fin encodes a type I BMP receptor, Alk8, acting maternally and zygotically in dorsoventral pattern formation. Development 128:859–869.

Parichy DM, Kaplan RH. 1995. maternal investment and developmental plasticity - functional consequences for locomotor performance of hatchling frog larvae. Funct Ecol 9:606–617.

Parichy DM, Turner JM. 2003. Zebrafish puma mutant decouples pigment pattern and somatic metamorphosis. Dev Biol 256:242–257.

Patterson SE, Mook LB, Devoto SH. 2008. Growth in the larval zebrafish pectoral fin and trunk musculature. Dev Dyn 237:307–315.

Power DM, Silva N, Campinho MA. 2008. Metamorphosis. In: Finn RN, Kapoor BG, editors. Fish larval physiology. Enfield, NH: Science Publishers. p 607–638.

Quigley AK, Turner JM, Nuckels RJ, Manuel JL, Budi EH, MacDonald EL, Parichy DM. 2004. Pigment pattern evolution by differential deployment of neural crest and postembryonic melanophore lineages in Danio fishes. Development 131:6053–6069.

Quigley IK, Manuel JL, Roberts RA, Nuckels RJ, Herrington ER, Macdonald EL, Parichy DM. 2005. Evolutionary diversification of pigment pattern in Danio fishes: differential fms dependence and stripe loss in D. albolineatus. Development 132:89–104.

Ricker WE. 1958. Handbook of computations for biological statistics of fish populations. Ottawa: Fisheries Research Board of Canada.

Robertson GN, McGee CA, Dumbarton TC, Croll RP, Smith FM. 2007. Development of the swimbladder and its innervation in the zebrafish, Danio rerio. J Morphol 268:967–985.

Sapede D, Gompel N, Dambly-Chaudiere C, Ghysen A. 2002. Cell migration in the postembryonic development of the fish lateral line. Development 129:605–615.

Schilling TF. 2002. The morphology of larval and adult zebrafish. In: Nüssslein-Volhard C, Dahm R, editors. Zebrafish: a practical approach. New York: Oxford University Press.

Schilling TF, Kimmel CB. 1997. Musculoskeletal patterning in the pharyngeal segments of the zebrafish embryo. Development 124:2945–2960.

Sire JY, Akimenko MA. 2004. Scale development in fish: a review, with description of sonic hedgehog (shh) expression in the zebrafish (Danio rerio). Int J Dev Biol 48:233–247.

Sire JY, Allizard F, Babiar O, Bourguignon J, Quilhac A. 1997. Scale development in zebrafish (Danio rerio). J Anat 190(pt 4):545–561.

Snyder DE, Muth RT, Bjork CL. 2004. Catastomid fish larvae and early juveniles of the Upper Colorado River basin—morphological descriptions, comparisons, and computer-interactive key. Denver: Colorado Division of Wildlife.

Trevarrow B, Robison B. 2004. Genetic backgrounds, standard lines, and husbandry of zebrafish. Methods Cell Biol 77:599–616.

Urho L. 2002. Characters of larvae - what are they? Folia Zool 51:161–186.

Ward AJW, Webster MM, Hart PJB. 2006. Intraspecific food competition in fishes. Fish Fisheries 7:231–261.

Webb JF. 1999a. Larvae in fish development and evolution. In: Hall BK, Wake MH, editors. New York: Academic Press. p 109–158.

Webb JF. 1999b. Larvae in fish development and evolution. In: Hall BK, Wake MH, editors. The origin and evolution of larval forms. New York: Academic Press. p 109–158.

Webb JF, Shirey JE. 2003. Postembryonic development of the cranial lateral line canals and neuromasts in zebrafish. Dev Dyn 228:370–385.

Developmental Dynamics